NTNU – Trondheim
Norwegian University of
Science and Technology

System Design and Configuration of a Stand-Alone PV-Biomass Micro Grid

An Application for Wawashang, Nicaragua

Marte Wiig Løtveit

Master of Energy and Environmental Engineering
Submission date: July 2014
Supervisor: Marta Molinas, ELKRAFT

Norwegian University of Science and Technology
Department of Electric Power Engineering

Problem Description

The focus of this thesis will be on developing an alternative micro grid in the Wawashang Agroforestal Complex, Nicaragua, that can satisfy the specific needs of the community also in the long term when expansion is considered. During a specialization project in the fall of 2013, the best mix of energy sources was evaluated using the simulation tools PVsyst and HOMER.

The objectives of the thesis will be to find the optimal configuration of the micro grid including a distribution system design. The specific task will be on evaluating two different scenarios to identify the most efficient operation of the system. A field trip to the complex in Wawashang may be carried out in order to maximize the outcome of the project by collecting data from the field and to feed in the simulation model. This will possibly be partially sponsored by Engineers without Borders NORWAY.

Start Date: 6^{th} of February, 2014

Supervisor: Marta Molinas

Preface

This master's thesis has been written at the Department of Electric Power Engineering at the Norwegian University of Science and Technology (NTNU), spring 2014. The title is System Design and Configuration of a Stand-Alone PV-Biomass Micro Grid - an Application for Wawashang, Nicaragua.

First, I would like to thank my supervisor, Professor Marta Molinas at NTNU and my advisers Post.Doc. Jon Are Suul and Professor Elisabetta Tedeschi at NTNU for their support and guidance during the last year. My travel companion during the field trip to Wawashang, Thomas Victor Fernandes, IUG Norway, deserves a big thanks for giving me a new perspective on the task in hand, for asking the questions I couldn't think of myself and for being an invaluable source of knowledge. A would also like to extend my gratitude to Susanne Thienhaus, although we regrettably never met, for her help in planning the field trip. A heartfelt thanks to the wonderful people we met at the Wawashang Complex, Silver Borge Guitiérrez, Luiz Guillén Luna and Pascal Herrera are mentioned amongst many others, and in Kahka Creek. The enthusiasm with which they do their work, whether it is educating young students in carpentry, agriculture or preserving the forest, is inspirational. The interest they showed in the project and their desire to help and to make us feel welcome was truly amazing. Remi Maupas and Gilles Charlier from blueEnergy, deserve my sincere thanks for their time, invaluable advice and experience. I would also like to thank Inger Johanne Rasmussen, IUG NTNU for her efforts in making the field trip happen and for help and advice in the planning stage. To IUG I want to give a my appreciation for allowing me the opportunity of working on this project that I have been so passionate about, and for financially supporting the field trip to Wawashang.

I would also like to thank all of my friends from my years in Trondheim for all the good memories. Finally, my parents deserve my deepest appreciation for always supporting and encouraging me.

Marte Wiig Løtveit

Trondheim, 24^{th} of July, 2014

Abstract

In this thesis, an evaluation of a stand-alone hybrid micro grid for the Wawashang Complex in rural Nicaragua is presented. A solution for a new electricity supply and distribution system for the complex is proposed with a focus on optimal configuration of the system. A field trip to Wawashang was conducted in April 2014 in order to collect data regarding biomass potential for electricity production and information for a possible distribution system design. The demand to be covered is divided into two systems; the micro grid, which denotes all buildings excluding the carpentry workshop and is the system for which the distribution system is designed, and the carpentry workshop. A single-phase/three-wire (split-phase) solution is suggested for the distribution system configuration, presenting the advantage of considerably smaller conductor size requirements than single-phase/two-wire systems for the same voltage drop and power loss. The total power loss of the distribution system is 896 kWh/year or 2.4 % of the demand.

The production system for the micro grid consists of a PV array and a battery bank, and for the carpentry workshop a diesel generator. Additionally, a biomass based generator is available for both systems according to a defined schedule. The simulation software HOMER is used to run simulations for the two systems simultaneously, with the intention of obtaining optimal operation of the biomass generator. Two cases are evaluated on both technical and economical aspects. In Case I, the high frequency AC power output from the biomass generator is rectified to DC power and then connected to the single-phase AC bus of the micro grid through a DC-AC converter and similarly to the three-phase AC loads of the carpentry workshop. In Case II, the output from the biomass generator is connected to the DC bus of the micro grid after rectification. The simulation results show that the optimal solution for the carpentry workshop in both cases is to operate the biomass generator as much as possible, with the diesel generator available to cover peak loads. In the micro grid in Case I, the biomass generator is operated with a load following strategy, while in Case II a cycle charging strategy is applied, resulting in a higher exploitation of the available biomass resource in the latter. Both cases present advantages and disadvantages and are similar in reliability and cost. Case II is evaluated as the optimal solution for the Wawashang Complex, as it is the overall least expensive and most reliable system, and the least unbalanced system when it comes to seasonal variations. The system consists of a 9 kW converter, a PV array with a global power of 30 kWp, producing a total of 37 254 kWh/year and a battery bank with a nominal capacity of 294 kWh (for the micro grid), a 15 kW biomass generator producing a total of 38 477 kWh/year divided between the micro grid (19.4 %) and the carpentry workshop (80.6 %) and a 15 kW diesel generator producing 5 400 kWh/year for the carpentry workshop. Total excess electricity is 6.3 % and unmet load is 0.21 %. Total net present cost is US$ 311 224 and levelized cost of electricity is US$ 0.285/kWh.

Sammendrag

I denne avhandlingen evalueres et frittstående microgrid for det avsidesliggende Wawashang-komplekset på øst-kysten av Nicaragua. En løsning for et nytt energiforsynings- og distribusjonssystem for komplekset er foreslått med fokus på optimal konfigurasjon av systemet. Et feltarbeid i Wawashang ble utført i April 2014 med den hensikt å samle inn data om potensialet for å utnytte biomasse til produksjon av elektrisitet i tillegg til informasjon angående et mulig design av et distribusjonssystem for komplekset. Etterspørselen som skal dekkes er delt inn i to systemer; microgridet, som betegner alle bygninger utenom verkstedet og som distribusjonssystemet er utformet for, og verkstedet. Et enfasesystem med tre ledere er foreslått for konfigurasjonen av distribusjonssystemet, da dette setter betraktelig lavere krav til størrelse på lederene for å oppnå samme spenningsfall og tap i linjen enn et enfasesystem med to ledere. Distribusjonstapene i linjen utgjør 896 kWh/år eller 2.4 % av den totale etterspørselen.

Produksjonssystemet for microgridet består av solcellepanel og en batteribank, og for verkstedet en dieselgenerator. I tillegg er en generator basert på biomasse tilgjengelig for begge systemene i henhold til en definert timeplan. Simuleringsprogrammet HOMER er brukt til kjøre simuleringer av de to systemene samtidig, med den hensikt oppnå optimal drift av biomassegeneratoren. To alternative konfigurasjoner av microgridsystemet er vurdert med hensyn på både tekniske og økonomiske faktorer. Biomassegeneratoren er en dampdreven turbogenerator, og den høyfrekvente AC kraften som produseres må først omformes til DC før den kan enten omformes tilbake til AC og kobles direkte til AC-busen i microgridsystemet (Alternativ I), eller kobles til den felles DC-busen med solcellepanelene og batteriet (Alternativ II). I begge alternativene kobles produksjonen fra generatoren til trefaselastene i verkstedet etter AC-DC/DC-AC omforming. Simuleringsresultatene viser at optimal løsning for verkstedet for begge alternativene er å kjøre biomassegeneratoren så mye som mulig med dieselgeneratoren tilgjengelig for å dekke topplast. I Alternativ I blir biomasseproduksjonen i microgridet kun brukt til å dekke lasten, mens i alternativ II kjøres generatoren alltid ved så høy effekt som mulig for å lade batteriene dersom den må settes i gang for å dekke lasten. Resultatet er at mer biomasse utnyttes i alternativ II. Begge alternativene har fordeler og ulemper ved seg og er relativt like i både pålitelighet og kostnad. Alternativ II vurderes som den optimale løsningen for Wawashang-komplekset ettersom det er det minst kostbare og mest pålitelige systemet, og det mest balanserte systemet når det gjelder variasjon med årstidene. Systemet består av en 9 kW omformer, 30 kWp solcellepanel som produserer 37 254 kWh/år og en batteribank med nominell kapasitet på 294 kWh (for mikrogridet), en 15 kW biomassegenerator som produserer totalt 38 477 kWh/år fordelt mellom microgridet (19.4 %) og verkstedet (80.6%) og en 15 kW dieselgenerator som produserer 5 400 kWh/år for verkstedet. Overflødig elektrisitetsproduksjon er 6.3 % og udekket last er 0.21 %. Total kostnad (nåverdi) er US$ 311 224, eller US$ 0.285 /kWh.

Table of Contents

List of Tables

List of Figures

Abbreviations

AC	Alternating Current
AM	Air Mass
AWG	American Wire Gauge
BESS	Battery Energy Storage System
CC	Cycle Charging
DC	Direct Current
ESS	Energy Storage System
FADCANIC	Fundación para la Autonomía y el Desarollo de la Costa Atlántica
HDI	Human Development Index
HOMER	Hybrid Optimization Modeling software for Electric Renewable and fossil energy
IDB	Interamerican Development Bank
LF	Load Following
NASA-SSE	National Aeronautics and Space Administration - Surface meteorology and Solar Energy
NGO	Non-Govermental Organization
NREL	US National Renwable Energy Laboratory
PF	Power Factor
PV	Photovoltaic
RAAN	Región Autónoma del Atlántico Norte
RAAS	Región Autónoma del Atlántico Sur
RES	Renewable Energy Sources
SAIH	Norwegian Students' and Academics' International Assistance Fund
SOC	State of Charge
STC	Standard Test Conditions
US$	United State Dollar
USAID	U.S Agency for International Development

Chapter 1

Introduction

1.1 Motivation

In a world struggling with climate change due to an excessive use of fossil fuels to cover our energy need, about 1.3 billion people still lack access to electricity. More than 99 % of these live in developing countries, mostly in rural areas. For a sustainable future in a world with a growing population and increasing demand for electricity, energy services can and should be provided in ways that are cost-effective, with the goal to decrease rural poverty while transitioning away from fossil fuel dependence [1]. Biomass is the largest single renewable energy source today, accounting for 10 % of the total primary energy supply. Most of this is consumed in inefficient, traditional ways in developing countries for cooking and heating, with negative impacts such as local pollution and deforestation. Although the numbers are steadily increasing, modern use of biomass is small in comparison. About 1.5 % of the total electricity generation in 2010 came from biomass. However, to be able to cover an increasing energy demand while achieving significant reductions in emissions, electricity from biomass will play an increasing role. Off-grid biomass electricity supply in developing countries will be an important measure in achieving universal access to clean energy [2].

Latin America is closer to achieving full energy access compared to other developing regions of the world. Only 6 % of the population in Latin America lack access to electricity. Also here, lack of electricity is primarily a rural issue. Nicaragua, being the second poorest country in the region, has a higher rate than the region as a whole. About 75 % of the rural population on the Atlantic Coast of Nicaragua remains without electricity access [3]. This is an example of an area that can benefit from electricity supply regarding health, education and economic development. Rural electrification has increased over the last years also in Nicaragua. Between 2007 and 2011, five new mini hydro plants and 20 new micro turbines were added, and more than 6 900 individual household solar panels were installed

in isolated areas, which shows that there is initiative and will to improve the situation of the rural population.

The Foundation for the Autonomy and Development of the Atlantic Coast of Nicaragua, FADCANIC, is an organization that works for improving the quality of life of the peoples of the Caribbean Coast of Nicaragua. One of their projects is the Environmental and Agroforestry Education Center and Agroforestry Innovation Center in Wawashang. The Wawashang Complex is not connected to the main power grid in Nicaragua, but is one of the few villages in the area with local electricity production in the form of PV panels on rooftops and gasoline and diesel generators. The current system is unreliable and inefficient and education is limited to hours with daylight. Additionally, an expansion of the complex is expected to increase the demand. FADCANIC is therefore looking for new energy solutions for the complex that can assure a sustainable and reliable electricity supply in the future. As a measure to achieve this, FADCANIC established contact with Engineers without Borders, Norway, who contribute by enabling students to write a "Meaningful Master's Thesis", a program of which this thesis is a part. This thesis is based on a specialization written by the author during the fall 2013, which itself was a continuation of the work done by Marco Boninella and Linn Solheim in their theses during the spring 2013. It proposes a solution for a new electricity supply system for the Wawashang Complex based the locally available energy sources, solar photovoltaic power and electricity production from biomass with a focus on system configuration.

1.2 Outline of the Thesis

The work contains 9 chapters. In this chapter, the motivation behind the work has been presented, and the next chapters are organized as follows:

Chapter 2 gives a short introduction to the concept of rural electrification and stand-alone micro grids. It also provides background information on Nicaragua, the electricity situation in Nicaragua and the current situation on the Atlantic Coast. The projects partner organizations are presented and the previous work is described.

Chapter 3 presents the Wawashang Complex. Current and future energy demand is described and information about the field trip to Wawashang is provided. The potential of the available energy sources at the Complex is described.

Chapter 4 proposes a distribution system design and distribution loss is calculated based on chosen conductor size.

Chapter 5 comprises information on the production system, presenting the system components and the simulation cases that are evaluated. Inverter losses are also calculated.

Chapter 6 gives an introduction to the simulation tool HOMER that is used to evaluate different cases for the production system configuration. An explanation on the simulation methods and settings for the simulations are provided.

Chapter 7 presents the results from the simulations in HOMER.

Chapter 8 starts with a discussion of the simulation systems that have been evaluated. A comparison to previous work is also included.

Chapter 9 gives the conclusion of the thesis and suggestions for further work.

Appendix A is a publication by the author based on the work in her specialization project during the fall 2013.

Appendix B provides the detailed current and future load profiles for the demand, including distribution and inverter losses.

Appendix C consists of the equations used for calculating conductor size, voltage drop and power loss in the distribution system.

Appendix D-G provides the full system reports from the simulations in HOMER.

Chapter 2

Background and Theory

2.1 Rural Electrification

Rural electrification is the process of supplying electricity to remote and rural areas. About 70 % of the world's rural population still lack access to electricity [4]. Improving their economical and social situation depends on increasing their access to goods, services and information, all of which are linked with a reliable access to energy [5]. Many areas are too remote located for grid connection to be an economically viable option and stand-alone micro grids have emerged as a suitable alternative. In this thesis, the focus will be on planning a hybrid stand-alone micro grid for a rural area in Nicaragua.

2.1.1 Stand-Alone Micro Grids

Stand-alone micro grids are energy supply systems that are not connected to the main electricity grid. Stand-alone systems are most common as electrification of areas that are not in proximity to the main grid and where grid extension is too expensive. The most common way of ensuring electrification to such areas has been through installation of diesel generators, although micro grids provide good opportunities to utilize locally available energy resources. As renewable energy technologies, particularly photovoltaic (PV) power, have developed regarding price, efficiency and reliability, these are becoming increasingly popular and affordable for rural areas. At the same time, diesel generators suffer from increasing fuel prices, with the added costs of to transportation to remote locations, and low efficiency at low loads. However, its output can be regulated as opposed to solar power, an intermittent resource which varies both on a daily and seasonal basis. Combining a PV system with a generator in a hybrid micro grid makes it possible to limit some of the disadvantages in both technologies [6]. Depending on the requirements of the energy supply, a micro grid might include an energy storage system (ESS). A typical

configuration of a hybrid micro grid with a PV array, generator, battery bank, converters and control components is shown in **Figure 2.1**.

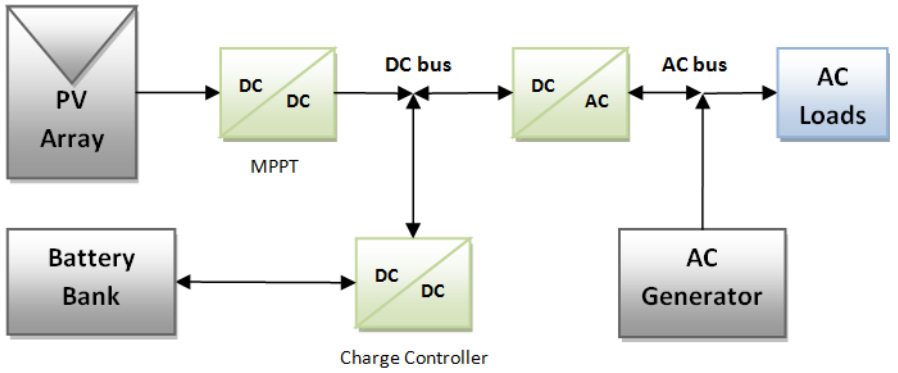

Figure 2.1: Typical Configuration of a Hybrid Micro Grid

The generator in such hybrid micro grids is normally working on diesel fuel. In areas with access to biomass waste that can be utilized in a sustainable manner, the diesel generator can be replaced by a biomass based generator. Compared to renewable energy sources like PV and wind power, a significant advantage of biomass is that it can be stored, and thereby allows easy regulation and dispatch [7]. Consequently, both the environmental impact and the generation costs connected to using fossil fuels can be reduced, while limiting the impact of the intermittent properties of solar power.

2.2 Study Area

The Environmental and Agroforestry Educational Center and Agroforestry Innovation Center Wawashang is located on the Atlantic Coast of the Republic of Nicaragua. In this section, a short introduction to Nicaragua is provided with a focus on current electricity situation and the Atlantic Coast.

Nicaragua has a population of 5.85 million, of which 52.5 % is under the age of 25. The country is the second poorest in the Western Hemisphere, succeeded only by Haiti. 42.8 % of the population lives below the poverty line. Unemployment, high infant mortality and low access to drinking water are some of the problems the country struggles with. With a Human Development Index (HDI) of 0.599, the country is ranked as number 129 in the world, and scores below average [8].

2.2.1 Geography

Nicaragua is the largest country in Central America, with 130 370 km^2 [9]. The country boarders to Honduras in the north, Costa Rica in the south, and stretches from coast to coast, touching the North Pacific ocean in the west and the Caribbean Sea in the east. **Figure 2.2** shows a map of Nicaragua.

Figure 2.2: Map of Nicaragua [10]

2.2.2 Climate

Although the climate is cooler in the highlands, the general climate of Nicaragua is tropical with one dry and one rainy season. As can be seen **Figure 2.3**, dry and rainy season coincide on the west coast and east coast. Amount of rainfall is, however, much higher on the east coast (represented by Bluefields) than on the west coast (represented by Managua). The temperatures are high year-around [11].

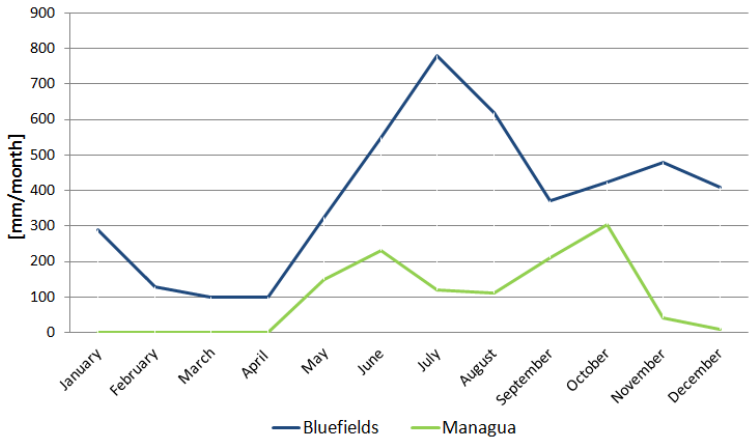

Figure 2.3: Average Rainfall in Nicaragua [11]

2.2.3 History and Background

The growth and development of Nicaragua has faced challenges from both natural disasters such as earthquakes, volcanic eruptions, cyclones and floods, and political unrest. After achieving its independence from Spain in 1821, Nicaragua was heavily influenced by military interventions from the U.S, dictatorships and fiscal crisis. This political turmoil led to the revolution in 1979, followed by a civil was that lasted throughout the 80s [12]. Today, Nicaragua is a presidential representative democratic republic. The president, Daniel Ortega, from the Sandinista National Liberation Front (FSLN), was reconfirmed in 2011, although his election was accused of several irregularities [13].

2.2.4 The Atlantic Coast

The Atlantic Coast of Nicaragua has been under several different forms of foreign control, independent from the rest of the country. The last one, The British Protectorate, lasted until the mid 19^{th} century. The process of integrating the Atlantic Coast to the rest of the country began in the late 20^{th} century. Since then, the inhabitants of the Atlantic Coast fought for juridical autonomy, which they gained in 1987 when the North Atlantic Autonomous Region (RAAN) and the South Atlantic Autonomous Region (RAAS) were created (the yellow and green area to the east in **Figure 2.2** [14]. RAAN and RAAS are characterized by a large rural population(two thirds), high dispersion (about 6 people per km^2) and poor road and electricity access. 67.9 % of the people on the Atlantic coast live in poverty or extreme poverty. Illiteracy is 55 %, whereas for the whole country this number is only 24.5 %. 75 % of the population in this area still has no access to electricity, and those who do mainly rely on diesel generators [15]. The Wawashang Complex is one of the few areas in rural RAAS with electricity access. Its location is indicated on the map

in **Figure 2.4**. **Chapter 3** is dedicated to the Wawashang Complex.

Figure 2.4: Map of the South Atlantic Coast, Nicaragua

2.2.5 Current Electricity Situation

Production and Consumption

In 2013, installed electricity capacity in Nicaragua was 1.725 GW, of which 49 % is fossil fuels, mainly imported from Venezuela, and 59 % renewable energy sources (RES) [9, 16]. Production potential from RES in the country exceeds ten times the current national demand, with large geothermic resources, good exposure to wind and sun and several water sources [17]. Only 5 % of this potential is currently exploited. A long term dependency on fossil fuel imports combined with limited power lines led to one of the highest electricity rates in the region, US$ 0.24/kWh, in 2006. This energy crisis led the government to address the issue and start changing the electricity sector, and while electricity generation from fossil fuel is still high, it has been reduced by 35 % only since 2011. Nicaragua has an aggressive renewable energy goal, intending to produce 90 % of its electricity from RES in 2027, primarily from hydro, geothermal and wind. **Figure 2.5** shows the current and future electricity matrix for Nicaragua. Reaching this goal would be a great success both environmentally and economically [16].

28 % of the Nicaraguan people currently lack access to electricity, and consumption per

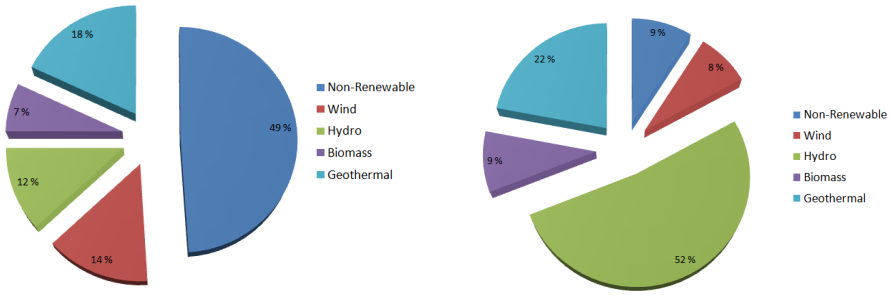

(a) 2013 (b) 2027

Figure 2.5: Electricity Production Matrix for Nicaragua [16]

capita is lower than in the neighboring countries, as can be seen in **Figure 2.6**.

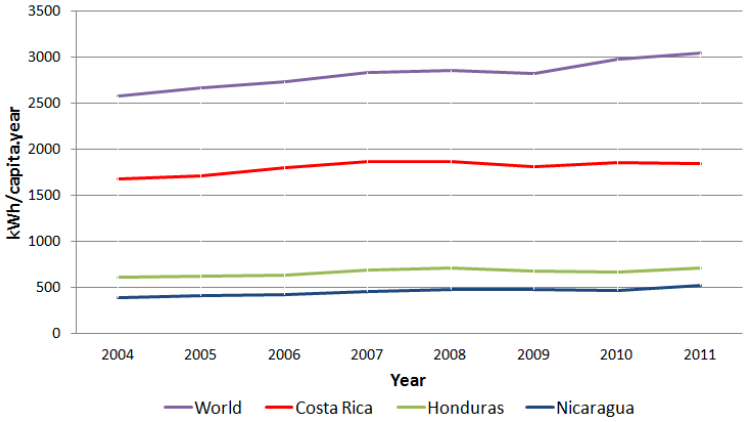

Figure 2.6: Electricity Consumption per Captia per Year

Transmission and Distribution

In 1999, ENEL, the state monopoly that previously controlled both production and distribution of power, was privatized and divided into what initally were three production companies and two distribution companies. Transmisson was kept state owned, and ENATREL is in charge of 100 % of the electricity transmission in Nicaragua. DISNORTE-DISSUR provide electricity distribution to national clients in the north (52.3 %) and south (46.3 %), respectively. Smaller companies such as Bluefields, Wiwil and ATDER-BL provide electricity distribution to smaller areas. The transmission and distribution network suffer from the highest losses in Central America due to technical losses and theft of electricity.

While technical losses from transmission and distribution in Europe are normally around 8-10 %, they are estimated to be as high as 15 % in Nicaragua [18]. Total losses were 24.2 % in 2010 [4]. As mentioned, large areas in RAAS and RAAN are not reached by the distribution network. Some villages are supplied by local grids and production, mostly from mini grids supplied by diesel generators. In some cases individual PV and hydro power installations are used. The electricity tariff is based on a cross-subsidy system, divided into categories based on size and type of consumption. This system impose a higher rate for high usage customers and a subsidized rate for low usage customers and rural inhabitants. Although it might seem like an advantage for rural customers, this system has made it unprofitable for the distribution companies to increase rural electrical connections, encourages theft by larger customers and causes inefficient consumption by smaller customers. An analysis of a rural electrification subsidy program performed by the Interamerican Development Bank (IDB) in 2005 indicated that they would have to pay more than 100 % of the interconnection cost to compensate the distribution company for connecting the rural customers [19].

2.3 Partner Organizations

2.3.1 Engineers without Borders, NTNU

Engineers without Borders, NTNU (IUG NTNU) is a student organization that enables engineer students to write a "Meaningful Master's Thesis". The intention of the program is to facilitate master theses that can benefit developing countries in an ethical and sustainable manner, and allowing engineer students use their knowledge to do developing work [20]. IUG NTNU cooperates with local organizations in various developing countries, such as FADCANINC in Nicaragua. This thesis is a part of IUGs meaningful master thesis program and IUG has been involved with advice, planning and financial support to make it possible to visit Wawashang during a field trip in April 2014.

2.3.2 FADCANIC

The Foundation for the Autonomy and Development of the Atlantic Coast of Nicaragua, FADCANIC, is a non-profit and non-partisan civil society organization based in the Autonomous Regions of Nicaragua. Their work is supported by several partners, amongst them the Norwegian Government, Norwegian Students' and Academics' International Assistance Fund (SAIH) and the U.S Agency for International Development (USAID). The organization works for improving the quality of life of the peoples of the Caribbean Coast. It ensures funding for innovative projects and helps with efficient execution of these projects. One of the projects the foundation is involved in, and one of its most important achievements, was constructing the boarding school and Agroforestry Development Center in Wawashang [14].

2.3.3 blueEnergy

Although an official cooperation is not established with IUG NTNU, the NGO blueEnergy has been involved in projects at the Wawashang Complex and other projects of FADCANIC, and is a great source of information. blueEnergy delivers energy, water and sanitation to some of the world's most isolated communities. Their goal is to provide a foundation for health, education and economic opportunity. Their Nicaraguan offices are located in Bluefields [21]. Contact with representatives from blueEnergy was established during a field trip to Wawashang in 2013, and was continued during the field trip in 2014.

2.4 Previous Work

In 2013, Linn Solheim and Marco Boninella wrote their master's theses "Scaling an Optimized PV-cluster as part of a Microgrid in Wawashang, Nicaragua" and "Hybrid Off Grid Energy System for the Wawashang Area, East Nicaragua", respectively [22, 23]. Their work, and the work of the author in her specialization project from the fall 2013 "Introducing Biomass as Part of a PV Micro Grid in the Village of Wawashang, Nicaragua" [24], constitutes the base for this thesis. In her thesis, Linn Solheim investigated the possibilities for exploiting solar power to provide electricity with or without a diesel backup generator, and the optimal solution for the system regarding economic, technical, cultural, social and environmental aspects were evaluated. Marco Boninella investigated the possibilities of exploiting hydro power. During their work, a field trip to Wawashang was performed, during which the current electricity consumption at the complex was measured. The hydro power potential was also investigated. While Marco Boninella concluded that there is little potential for hydro power at the Wawashang Complex, Linn Solheim concluded that solar power is a viable and sustainable way to ensure electricity supply to the complex. Although the system with a diesel backup generator was the most reliable, it was also the most expensive, and it was decided that the optimal solution for the complex was the system without backup. However, due to great seasonal variations in irradiation, a system based solely on solar power is bound to be either over-dimensioned for the dry season with high irradiation resulting in high amounts of excess electricity, or under-dimensioned for the rainy season with high amount of unmet load in this period. This is to a certain degree avoided by including a backup generator. One of the arguments for choosing the system without backup, was the possibility of including a biomass based generator in the system. This possibility was investigated by the author in her specialization project, where it was concluded that including a biomass generator in a hybrid micro grid compared to increasing the PV-battery system in order to achieve a higher reliability in the rainy season is the optimal solution regarding both technical and economical aspects. These results are also presented in [25], which is a publication by the author and is enclosed in **Appendix A**.

Chapter 3

The Wawashang Complex

3.1 Location

The Environmental and Agroforestry Educational Center and the Agroforestry Development Center, or the Wawashang Complex, is a boarding school and an agricultural center consisting of the school, a carpentry workshop and a large plantation. The complex is located in the Wawashang Natural Reserve in the municipality Pearl Lagoon in RAAS. The only way to reach the complex is by boat. Bluefields, the capital of the Atlantic Coast of Nicaragua, is the closest city and can be reached by road and boat or plane from Managua. A map of the South Atlantic Coast indicating the location of Wawashang is presented in **Figure 2.4** on **Page 9**. The proximity to Bluefields can also be seen in this map. This area is characterized by a tropical climate with high humidity. Temperatures stay between 24.7-27 ° year-round [26]. The area has high precipitation and is exposed to regular hurricanes in varying magnitude, some causing great damages.

3.1.1 Activities at the Complex

The boarding school in Wawashang is a secondary school acknowledged by the Nicaraguan Ministry of Education and seeks students from all over the region, especially students from poor backgrounds and with a mix of ethnicity [27]. The school combines practical and theoretical education with a focus on learning by doing. Currently, there are two study-programs; agro-forestry and cabinetmaking/carpentry. The carpentry workshop is both a center for education, and used to produce furniture that are either sold or used in the different offices of FADCANIC. The 260 Ha large plantation is divided between the school and the agricultural center and is composed of native trees and agricultural crops. The school utilizes the plantation both for harvesting and for educational purposes. The main objective of the agricultural center is to conserve the genetic diversity of plants and crops

(a) Meeting with Members of FADCANIC and blueEnergy

(b) Presenting the Project for FADCANIC

Figure 3.1: Field Work, Wawashang 2014

such as coconut, sugar cane, heart of palm, ginger, cacao, lemon and vegetables. Products such as chocolate, spices and coconut oil are produced at the complex and sold to nearby villages or in Bluefields, although lack of machinery to relieve the need for manual labor makes the production at the moment quite low. The center also has a nursery with pigs, chicken and African goats. Today, about 96 students, 10 professors, 5 carpenters and 5 members of the technical team of the innovation program live or work at the Wawashang complex. Additionaly, a total of 20 guest can stay in the complex.

3.2 Field Trip

In cooperation with IUG NTNU, a field trip to Wawashang was conducted in April 2014. The participants on the trip were Thomas Victor Fernandes, representative from Engineers without Borders Norway, and the author. The motivation for the field trip to Wawashang was the following:

- to collect data regarding available biomass for electricity production at the complex
- to perform a thorough mapping of the complex in order to make a layout of the distribution system
- to investigate possible locations of the components of the system
- to evaluate the recent and future development of the complex
- to strengthen and create new relationship with FADCANIC and blueEnergy

In **Figures 3.1-3.2** some of the work performed during the field trip, including meetings, presentations and visits to various locations, is shown.

Making an estimation of the available biomass at the complex was a difficult task and consisted in conversations with the teachers and staff in charge of the plantations and the carpentry workshop, and visits to the different locations. Inquiries about what type

(a) Maize Cobs (b) Coconut Shells

Figure 3.2: Investigating Biomass Potential at the Wawashang Complex

of crops they are growing, how much is harvested each year and the current purpose of the biomass waste were made. Asking the right questions was essential, as the people that were interviewed did not necessarily know what kind of information was needed. The different types of biomass waste that can be used for electricity production were also weighed. The results are presented in **Section 3.4.1**.

While the initial plan was to perform a detailed mapping of the complex, it was discovered that this was already done recently in the process of extending the water supply system. Hence, a map of the area, including correct scaling and locations of the different buildings already existed and was provided for the use in this thesis. This map is used to design the distribution system, and is displayed in **Figure 3.3**.

The locations for the components of the system were also evaluated through conversations with the Wawashang staff, and by visiting the relevant locations. It was desired to be able to place the PV-battery system close to the biomass generator, and also close to the carpentry workshop. This is further explained in **Chapter 4**.

The field trip was indispensable for the work on this project, not only because of the data that was collected, but because it was realized how important it is to understand the needs of the consumers - the people in Wawashang - their thoughts and positions regarding the project and how things are not always as straight forward when working on a project in an isolated, rural area. The field trip changed the work of this thesis in ways that exceed the concrete results of the data collected, and it has been attempted to stay true to the experiences and knowledge that was acquired during the trip.

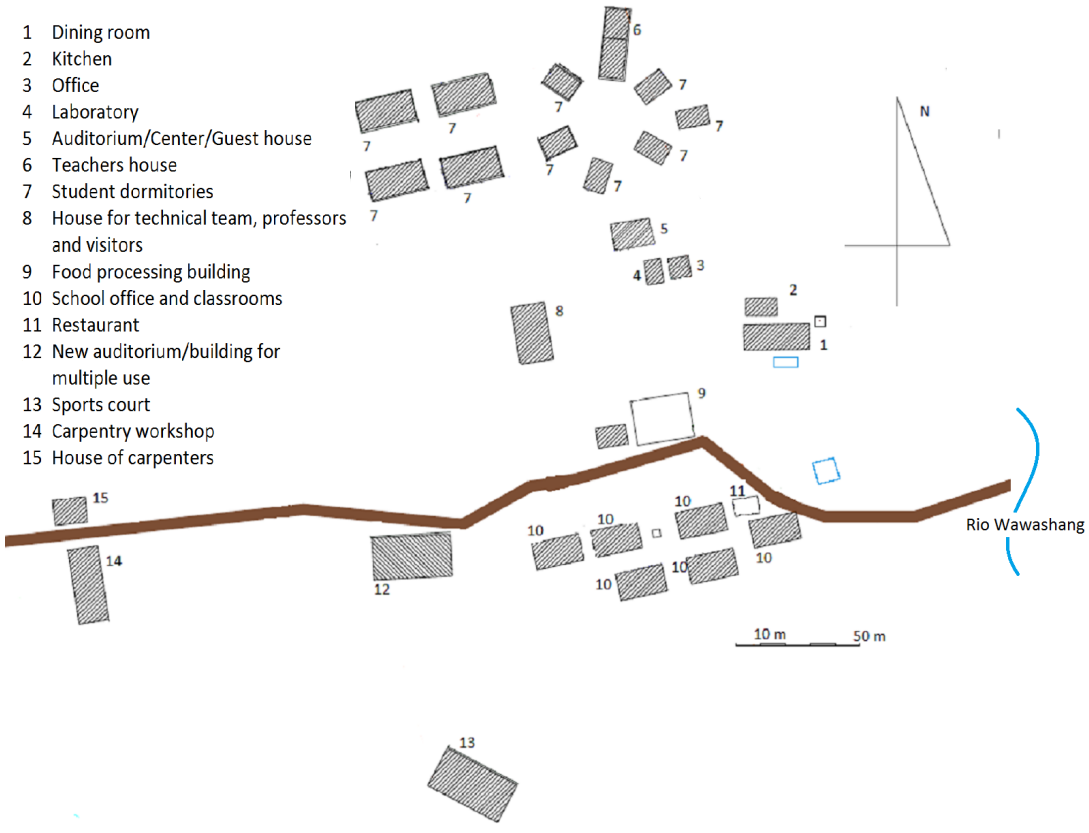

Figure 3.3: Map of the Wawashang Complex

3.3 Electricity Supply and Demand

3.3.1 Current System

In this section, the current electrical supply and demand for the Wawashang Complex is presented. The information presented is mainly a summary of the findings from the field trip to Wawashang in 2013 conducted by Linn Solheim and Marco Boninella, and more detailed information can be found in their master's theses [22, 23].

The current electrical system in Wawashang consists of:

- individual rooftop PV panels and storage for each building
- diesel generators
- gasoline generators

A full overview of the current electricity supply inventory can be found in [22].

Each building is equipped with individual PV-battery systems. Apart from the teachers house supplying the students dormitories and a gasoline generator in the food processing building that operates as a backup for the office and auditorium, there is no distribution system enabling electricity to be shared between the buildings. This reduces the efficiency of the system and might lead to electricity excess one place while there is electricity deficit somewhere else. Tilt and azimuth of the PV panels currently do not result in the highest possible yield and shading from trees nearby is also a factor that reduces efficiency of the system.

Load profiles for the current demand were made based on measurements at the different buildings during the field trip to Wawashang in 2013. Electricity consumption was measured over a time period of 10 days. The monitor stored data for every minute, and hourly load profiles were estimated for each building. A maximization approach was used by determining the peak minute from each hour from all 10 days and using this as the hourly value. This method is further explained in [22]. Although the resulting total demand is over-estimated, this method was chosen in order to obtain a system that is able to cover the peak demand.

The most power consuming activity at the complex is the carpentry workshop, using high power equipment from around 06:00 until 18:00 on weekdays. It is closed in the weekends and in Easter and Christmas vacations. The workshop is equipped with two diesel generators, one of 24 kW and one of 10 kW. The 10 kW generator has not been functioning for the last year, so the 24 kW generator is currently supplying the workshop at all times. This leads to inefficient operation of the generator, having to cover low loads at low efficiency. Diesel consumption is currently 53 liters per day.

Electricity in the remaining buildings is, depending on the purpose of the building, mainly used for lighting, fans, computer and cell-phone charging and a few higher power demanding equipment such as a fridge. Food is made using wood burning stoves. The food processing building does not have electricity supply, but a gasonline generator that is

used as backup for the auditorium and the main office is located here. The water pump is also driven by a gasoline generator, while the water purification process is driven by solar power. A full overview of the appliances that uses electricity can be found in [22].

The remaining buildings constitute:

- The dining room
- The kitchen
- The main office
- The laboratory
- The auditorium
- The teachers house
- The students dormitories
- The house for technical team, professors and visitors
- The food processing building
- The school offices and classrooms
- The restaurant
- The new auditorium
- The house of carpenter

In **Figure 3.4** the current load profiles for the Wawashang Complex are displayed. In this project, the complex is divided into two systems that will be referred to as the carpentry workshop (**Figure 3.4(c)**) and the micro grid (**Figures 3.4(a)-3.4(b)**. As can be seen, the demand from the carpentry workshop is significant compared to the rest of the complex. It constitutes almost 60 % of the total demand, and about 80-85 % in peak hours. When talking with the engineers from blueEnergy and the staff at Wawashang, it became clear that including the carpentry workshop in a PV-battery system had little support and is unlikely to happen due to the big differences in load. It was also considered that keeping a diesel generator present at the complex might be a good idea for extra security, should there be unexpected problems with the renewable energy sources.

3.3.2 Future Demand

The electricity consumption in Wawashang is expected to increase in the coming years. How much and when is, however, uncertain. New buildings are planned and the capacity of the school is intended to increase. As these plans are dependent on funding, it proved to be difficult to estimate a time-horizon for their implementation.

During the field trip to Wawashang in April 2014, it was decided that a new evaluation of the future demand was necessary. The ones used in [22–25] were considered as significantly over-estimated and resulting in a very large and expensive system that in reality

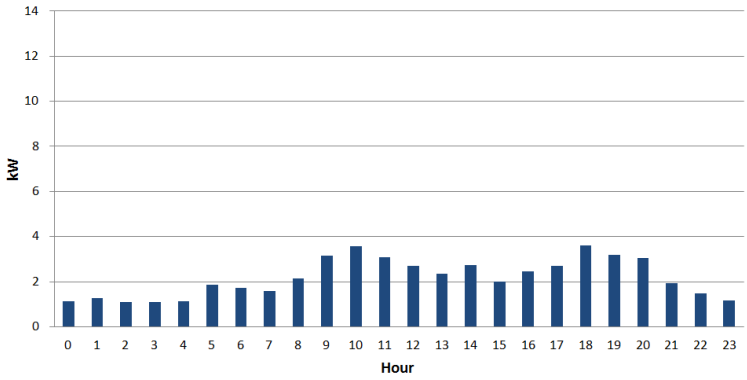

(a) Micro Grid, Weekdays

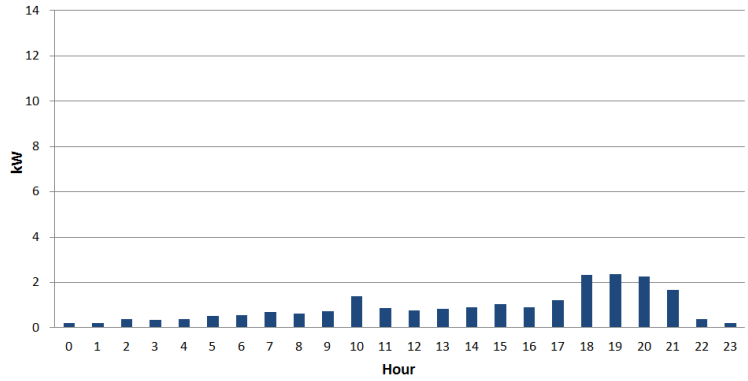

(b) Micro Grid, Weekends

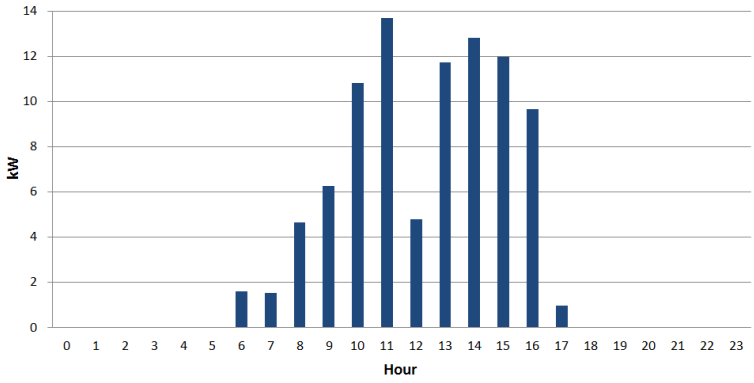

(c) Carpentry Workshop

Figure 3.4: Current Load Profiles

never would be installed in Wawashang. Additionally, it was revealed that the main electrical grid in Nicaragua is in expansion towards Wawashang and that the complex will probably be able to connect to the main grid within the next 3-5 years. This is information is uncertain as there has not been found any official plans from the Nicaraguan government or grid companies confirming this development. It is known that there has been activity on the Atlantic Coast recent years, reducing distance to the grid from about 70 km to only 28 km [23]. Even if grid connection in fact will be possible, the people in Wawashang still has a desire to have their own electricity supply. The main grid is unreliable and may suffer from outages that can last for days in remote areas such as Wawashang. Exploiting locally available renewable energy sources in a sustainable manner is also something the staff in Wawashang is passionate about. In this thesis, a possible grid connection has not been considered.

It was decided that using a 5 year horizon when talking about the future demand is more realistic than scaling for 2032. These decisions where made together with engineers from blueEnergy and the staff in Wawashang. It should be commented that from [22] it is clear that determining the multiplication factors was difficult process and that contact persons in Wawashang in fact initially desired even higher values. In retrospect, the consequence of over-estimating future demand appears in the magnitude and cost of the production system. The multiplication factors used to determine the future load profiles in previous work were 2 for the carpentry workshop and 5 for the rest of the complex. The same method, applying one multiplication factor for the carpentry workshop and one for the rest of the complex, is used in this project. A factor of 1.3 is chosen for the carpentry workshop and 2 for the rest of the complex. In **Figure 3.5**, the resulting future load profiles are presented. Although the multiplication factor is higher for the micro grid loads than for the carpentry workshop, it can be seen that the workshop still constitutes a large portion of the demand. 50 % of total demand and 75-80 % in peak hours.

3.4 Available Energy Sources

3.4.1 Biomass Potential

As mentioned, the locally available biomass potential was mapped by doing research at the complex during the field trip in 2014. The Wawashang complex has access to a vast amount of solid biomass that can be used for electricity production from the carpentry workshop and from the plantations. Currently, some of the biomass waste is destined for other purposes such as firewood for the kitchen and the food processing building, and for compost. During conversations with the teachers and the workers at the complex, it was revealed that the Agricultural Center is planning to cultivate energy crops for firewood purposes. It was also confirmed that the waste currently used for compost can be destined for electricity production if this solution is implemented. In this project it is therefore is therefore assumed that all of the biomass potential that was mapped can be used for electricity production. In the following section, the thermal potential of biomass at the Wawashang Complex is calculated.

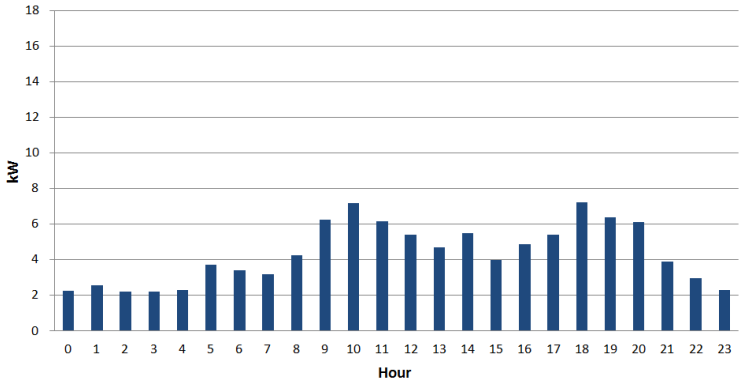

(a) Weekdays, Micro Grid

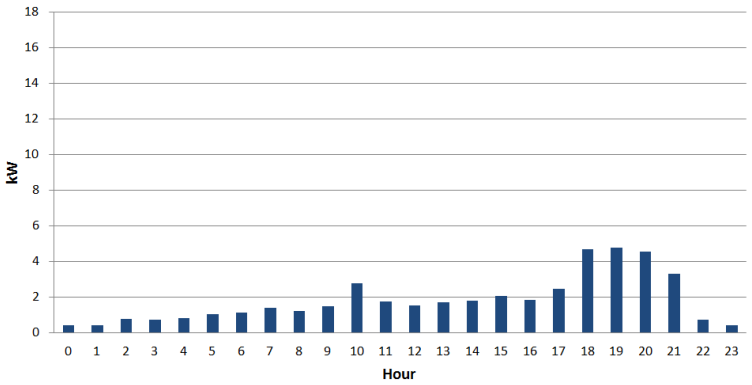

(b) Weekends, Micro Grid

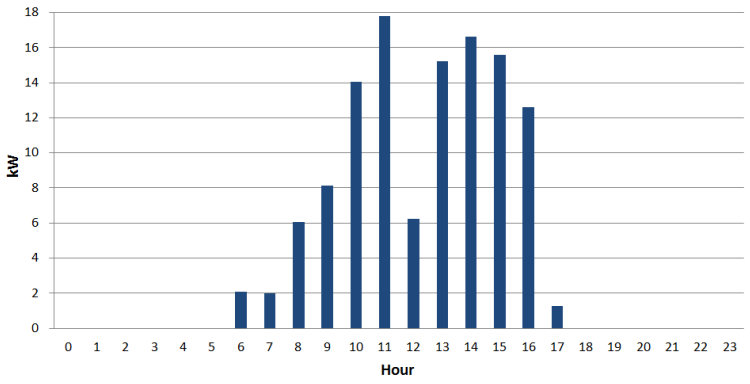

(c) Carpentry Workshop

Figure 3.5: Future Load Profiles

Biomass Resources from the Carpentry Workshop

The carpentry workshop serves as a place to educate the students in carpentry and cabinetmaking. It is also a furniture workshop were chairs, tables and other furniture are made in order to sell the products to the different offices of FADCANIC and other customers.

From the workshop, a considerably large amount of wood waste is available. This waste comes in two forms:

- Sawdust
- Small pieces of wood that cannot be used for other purposes

The main data for calculating energy potential from sawdust and wood is presented in **Table 3.1**.

Table 3.1: Density and Calorific Value of Sawdust and Wood

	Density $[kg/m^3]$	**Calorific Value** $[kWh/kg]$
Sawdust	210 [28]	2.25 [29]
Wood		
Santa María	660 [30]	
Caoba	560 [31]	
Coyote	680	
Pino Montero		
Average	633	3.5 [32]

Sawdust

The sawdust is gathered in bags of 0.6 m^2 and a well comprised bag weighs 126 kg. According to the teachers and workers at the workshop, 1.75 full bags of sawdust are packed on average every working day, 24 days per month considering 6 working days per week. Given this information, the thermal energy potential is calculated in **Equations 3.1-3.3**.

$$1.75 bags \times 24 days = 42 \frac{bags}{month} \tag{3.1}$$

$$42 \frac{bags}{month} \times 126 \frac{kg_{sawdust}}{bag} = 5292 \frac{kg_{sawdust}}{month} = 176.4 \frac{kg_{sawdust}}{day} \tag{3.2}$$

$$176.4 \frac{kg}{day} \times 2.25 \frac{kWh_{th}}{kg} = 397 \frac{kWh_{th}}{day} \tag{3.3}$$

Wood Pieces

The wood pieces from the carpentry that can not be used for other purposes originate from four different wood species with different densities. The average density is therefore calculated, as shown in **Table 3.1**. The density of Pino Montero was not found. The production of wood pieces is divided into short pieces of 1 inch (0.025 m) and long pieces of 2 inches (0.05 m). Both are considered to have a volume per inch of:

$$1in \times 12in \times 12in = 144in^3 = 0.0023\frac{m^3}{in} \tag{3.4}$$

With help from the workers at the carpentry, it was estimated that 7 short pieces are produced per working day (168 per month), and 50 long pieces per month. Thermal energy potential from wood pieces is calculated in **Equations 3.5-3.6**.

$$\begin{aligned}(168\frac{shortpieces}{month} \times 1\frac{in}{piece} + \frac{50\,long\,pieces}{month} \times 2\frac{in}{piece}) \times 0.0023\frac{m^3}{in} \times 633\frac{kg}{m^3} \\ = 390.2\frac{kg_{wood}}{month} = 13\frac{kg_{wood}}{day}\end{aligned} \tag{3.5}$$

$$13\frac{kg_{wood}}{day} \times 3.5\frac{kWh_{th}}{kg} = 45.5\frac{kWh_{th}}{day} \tag{3.6}$$

Biomass Potential from the Plantations

From the plantations, residues from coconut, sugar canes, maize and cacao are available for electricity production. Both the school and the agricultural center have control a of part of the plantation. In continuation, the available biomass from these plantations will be considered as a whole. **Table 3.2** shows the densities and calorific values of the different crops that are considered.

Table 3.2: Density and Calorific Value of Plantation Crops

	Density $[kg/unit]$	**Calorific Value** $[kWh_{th}/kg]$
Coconut shell	0.2	4.767 [33]
Sugar Cane Bagasse	038	2.52 [34]
Cacao Shell	0.09	3.864 [35]
Maize Cob	0.024	5.04 [33]

Coconut

At the center, dry coconut meat and coconut oil is made. The average weight of one dry coconut shell was obtained by weighing several shells in Wawashang. One shell weighs approximately 0.2 kg. According to the people responsible for the harvesting, approximately 17 000 coconut shells can be collected per month. This information gives the thermal energy potential shown in **Equations 3.7-3.8**.

$$0.2\frac{kg}{shell} \times 17000\frac{coconut\,shells}{month} = 3400\frac{kg_{coconut}}{month} = 113.3\frac{kg_{coconut}}{day} = \tag{3.7}$$

$$113.3\frac{kg_{coconut}}{day} \times 4.676\frac{kWh_{th}}{kg} = 529.8\frac{kWh_{th}}{day} \tag{3.8}$$

Sugar Cane

The Wawashang Complex has 2 hectares of sugar canes. The work to harvest and produce the sugar cane juice (guarapo), is currently done manually and is very time consuming. There is no equipment available for processing the sugar canes mechanically nor is there enough electricity to run the equipment. If a new micro grid were to be actualized, the production of sugar cane would probably increase. In this thesis, the potential from sugar cane will be based on the current production, which is estimated to about 670 sugar canes per month. Most of the sugar cane is used as food for the pigs in the nursery. The bagasse that remains after the feeding is currently gathered and used as compost. The weight of dry bagasse from one sugar cane was found by weighing the dry bagasse remains from several sugar canes. The bagasse from one sugar cane weighs approximately 0.38 kg. The thermal energy potential from sugar cane is calculated in **Equations 3.9-3.10**

$$0.38\frac{kg}{sugar\,cane} \times \frac{670\,sugar\,canes}{month} = 254.6\frac{kg_{bagasse}}{month} = 8.5\frac{kg_{bagasse}}{day} \tag{3.9}$$

$$8.5\frac{kg_{bagasse}}{day} \times 2.52\frac{kWh_{th}}{kg} = 21.4\frac{kWh_{th}}{day} \tag{3.10}$$

Cacao

Also the shells from the cacao plant can be used to produce electricity. The cacao is used to produce chocolate and cacao powder. During the field trip, it was approximated that 5 dry cacao shells is weighs 1 pound, or 0.09 kg per shell, and harvesting is estimated to 3833 shells per month. **Equations 3.11-3.12** show the calculation of the thermal energy potential from cacao.

$$0.09\frac{kg}{cacao\,shell} \times 3833\frac{cacao\,shells}{month} = 345\frac{kg_{cacao}}{day} = 11.5\frac{kg_{cacao}}{day} \tag{3.11}$$

$$11.5\frac{kg_{cacao}}{day} \times 3.864\frac{kWh_{th}}{kg} = 44.4\frac{kWh_{th}}{day} \tag{3.12}$$

Maize

The Wawashang Complex has a large production of maize, with 24 000 cobs harvested two times per year, resulting in an average of 4000 cobs per month. The waste is currently used as compost. The weight of one average sized shelled and dried maize cob was estimated to 0.024 kg. The thermal energy potential from the maize is calculated in **Equations 3.13-3.14**.

$$0.024\frac{kg}{maize\,cob} \times 4000\frac{maize\,cobs}{month} = 96\frac{kg_{maize}}{month} = 3.2\frac{kg_{maize}}{day} \tag{3.13}$$

$$3.2\frac{kg_{maize}}{day} \times 5.04\frac{kWh_{th}}{kg} = 16.128\frac{kWh_{th}}{day} \tag{3.14}$$

Total Biomass Potential

The total thermal energy potential from biomass is shown in **Table 3.3**. The average calorific value of the biomass is

$$\frac{1054\,kWh_{th}/day}{326\,kg/day} = 3.23\frac{kWh_{th}}{kg} = 11.5\frac{MJ}{kg} \tag{3.15}$$

Table 3.3: Total solid biomass potential

Biomass source	**Amount** $[kg/day]$	**Thermal Energy Potential** $[kWh_{th}/day]$
Sawdust	176.4	397
Wood pieces	13	45
Coconut shells	113.3	529.8
Bagasse	8.5	21.4
Cacao	11.5	44.4
Maize	3.2	16.13
Total	**326**	**1054**

3.4.2 Solar Power Potential

The solar radiation in Nicaragua is greatest on the west coast, where the global horizontal solar radiation lies between 5-6 kWh/m^2.day. In eastern Nicaragua, where Wawashang is

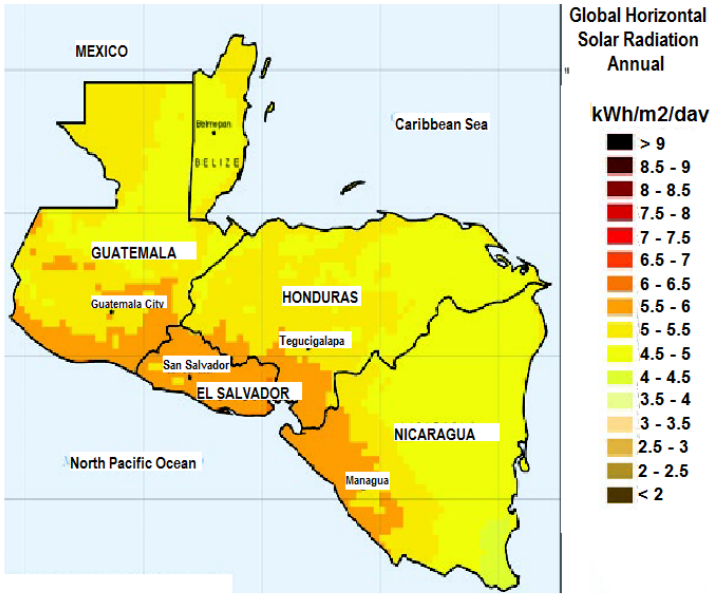

Figure 3.6: Solar Potential in Central America

located, the the radiation is between 4.5-5 kWh/m^2.day. This is not high, but sufficient in small-scale, off-grid installations like the one planned in Wawashang.

To find the average monthly irradiation data for Wawashang, both Meteonorm and the NASA-SSE database were considered. The two databases have different ways of obtaining meteorological data that can be accessed by implementing the latitude and longitude for the site in question (12.65 and -83.75 for Wawashang, respectively). Meteonorm uses an interpolating tool implementing the 3 nearest of 1 200 meteorological stations all over the world (1960-1990 or 1981-2000 averages) [36]. NASA-SSE contains monthly data of satellite measurements (1983-2005 averages) fro any cell of $1^\circ \times 1^\circ$. 1° latitude equals 111 km and 1° longitude is approximately 111.3 km, so the cells used by NASA-SSE are 12 354.3 km^2 [37]. There are three meteorological stations in Nicaragua, displayed in the map in **Figure 3.7**; one in Ocotal (north), one in Chinandega (west) and one in Rivas (south-west) [36]. There is no station in the eastern parts of Nicaragua. Therefore, it might be suspected that the data from Meteonorm actually corresponds better with the western part of the country, and, as shown in **Figure 2.3** on **Page 8**, although the dry and rainy season coincide, amount of rainfall is much higher on the east coast.

In **Figure 3.8** the monthly irradiation data from Meteonorm and the NASA-SSE database is compared to the average monthly rainfall for Managua and Bluefields, respectively. The figures reveal that the Meteonorm irradiation data corresponds very well with rainfall in Managua, while the data from NASA-SSE corresponds with rainfall in Bluefields. This

Figure 3.7: Map of MeteoNorms Meteorological Stations in Nicaragua (Red Dots) [36]

confirms the suspicion that Meteonorm actually provide data for the western Nicaragua, and not the actual site.

Figure 3.9 shows the temperature data provided by the two databases compared to temperature information from Bluefields. It can be seen that the NASA-SSE data for temperature corresponds much better with average temperature data for Bluefields than the data from Meteonorm.

Considering all these factors, using the meteorological stations from Meteonorm is an uncertain source for the site in question. Additionally, the distances between the stations used in Meteonorm and the location of Wawashang are actually larger than those within the cell used in the NASA-SSE database. Hence, the NASA-SSE database is chosen as the source for meteorological data in this thesis. The data is presented in **Table 3.4**. Monthly average irradiation is very influenced by seasonal changes, varying from 174 kWh/m^2.month in April (dry season) to 115 kWh/m^2.month in July (rainy season).

3.4.3 Hydro Power Potential

As mentioned in **Chapter 2**, hydro power potential in Nicaragua is high. The Atlantic Coast is no exception, with high precipitaion and large amounts of rivers. However, Marco Boninella evaluated the potential to be quite low in his thesis [23]. The main arguments for this were

- Very flat area
- Property issues

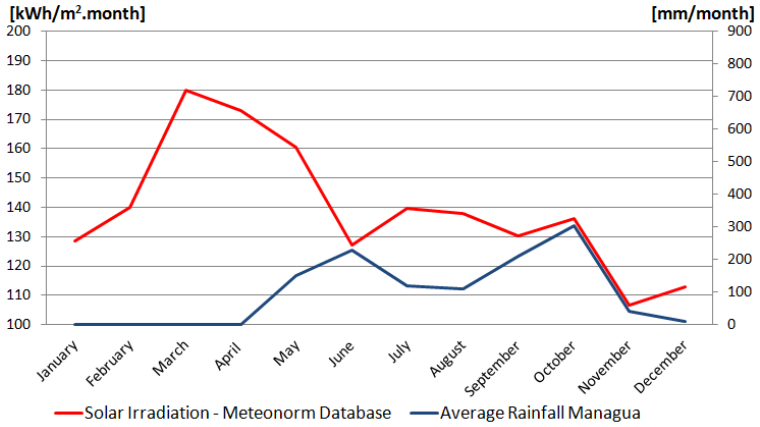

(a) Meteonorm and Managua

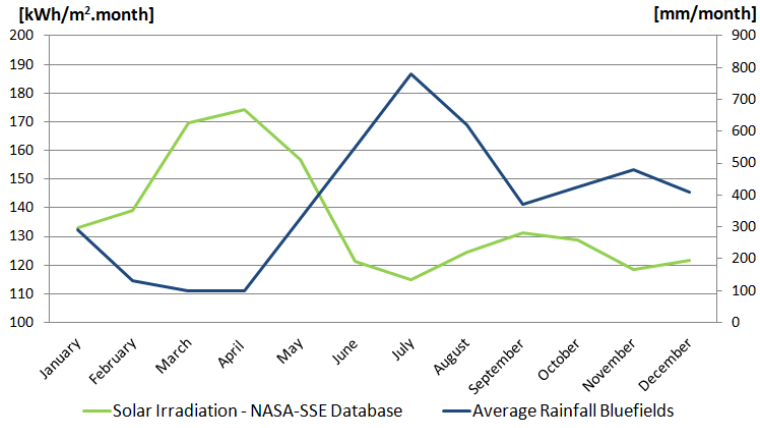

(b) NASA-SSE and Bluefields

Figure 3.8: Average Monthly Solar Irradiation Compared to Monthly Rainfall

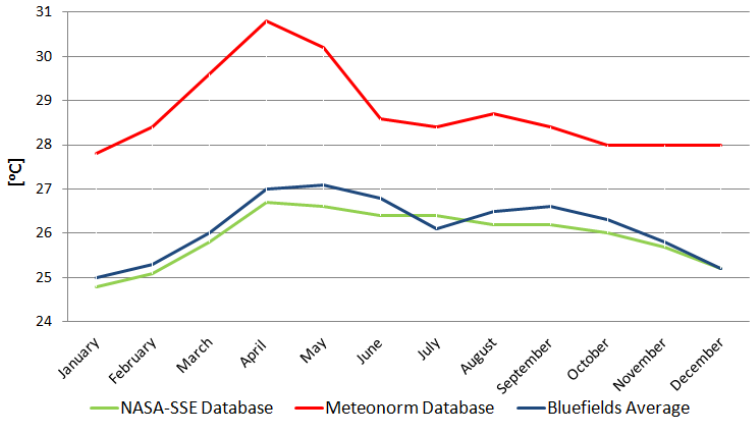

Figure 3.9: Average Temperatures from NASA-SSE and Meteonorm Compared to Average Temperatures in Bluefields

Table 3.4: Global Irradiation and Temperature for Wawashang from the NASA-SSE Database [26]

Month	**Global Irr.** $[kWh/m^2.mth]$	**Diffuse Irr.** $[kWh/m^2.mth]$	**Temp.** [° C]
Jan	133.0	53.0	24.8
Feb	138.9	52.1	25.1
Mar	169.6	64.2	25.8
Apr	174.3	66.3	26.7
May	156.9	71.3	26.6
Jun	121.2	67.5	26.4
Jul	115.0	68.8	26.4
Aug	124.6	66.3	26.2
Sep	131.4	66.3	26.2
Oct	128.7	62.6	26.0
Nov	118.5	54.0	25.7
Dec	121.8	51.8	25.2
Year	**1633.8**	**748.9**	**25.9**

- Forest surrounding the area could contrast civil work and made exploring the sites difficult
- Installing hydropower in Rio Wawashang would influence the habits of the local people as it is used for transportation

A study of one possible site for a micro hydropower installation in State Creek, a small river flowing through the Wawashang Complex, was still made, and the results can be found in the master's thesis of Marco Boninella.

3.4.4 Wind Power Potential

Wind power has good potential on the Pacific coast, and while blueEnergy has installed wind turbines on the Atlantic Coast, the area has proved to be a challenging place for wind power. Low to medium wind strenghts, frequent lightning strikes, humidity and heat makes the work difficult and technology import lack subsidizing from the government [23, 38]. **Figure 3.10** shows the wind power potential in Nicaragua.

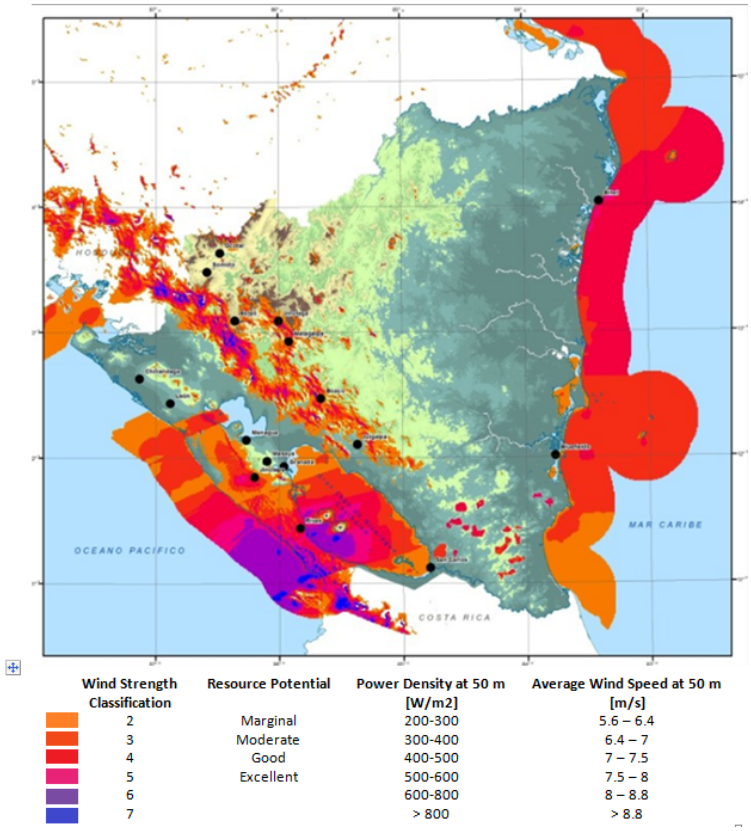

Figure 3.10: Wind Power Potential in Nicaragua

3.4.5 Energy Sources in this Project

As in [24], the renewable energy sources that will be used for the production system in this thesis are solar photovoltaic and biomass. The production system will be explained in **Chapter 5**.

Chapter 4

Distribution System Design

A distribution system is necessary to transmit the electricity from the power supply to the consumers. In this chapter, a suggested design for the distribution system of the micro grid in Wawashang Complex, excluding the carpentry workshop, is presented. This is done in order to get an idea of the layout of the distribution system and to calculate voltage drop and power loss along the line. The focus is therefore only on the main distribution lines, and design of poles and service drop are not evaluated.

The process of designing the distribution system for the Wawashang Complex requires five main decisions:

- Estimate expected load
- Estimation of the loads power factor (PF)
- Layout of the distribution system
- The type of line configuration
- The conductor type and size

Expected load profiles were estimated in **Chapter 3**, and this chapter will evaluate the possible solutions for the next four steps and present the decisions that are made.

4.1 Power Factor

PF is defined as the ratio of the real power flowing to the load (kW) to the apparent power (kVA). The loads in the micro grid in Wawashang are, as mentioned, mainly lighting, fans and computer and cell-phone charging. The PF is usually between 0.85-0.95 in an average household, and a value of 0.9 is used in this project.

4.2 Distribution System Layout

In the map in **Figure 4.1**, the layout of the distribution system for Wawashang in shown. The power supply is located close to the carpentry workshop, as it was desired to keep the biomass generator close to both the carpentry workshop and to the PV-battery system. This is also an area where there is enough free space for the PV-array and battery bank. The carpentry workshop lies at certain distance from the loads of the micro grid, but during the field trip to Wawashang it was not considered as possible to place the system any closer. Another possible location would be by the sports court, but this would not reduce the distance to the loads significantly while the distance between the generator (or the carpentry workshop) and the PV-battery system would increase. The total distance between the power supply and the end of the line (by the student dormitories) is 402 meters. The red dots represent the poles, placed at approximately 25-30 m distance from each other. The black line is the distribution line.

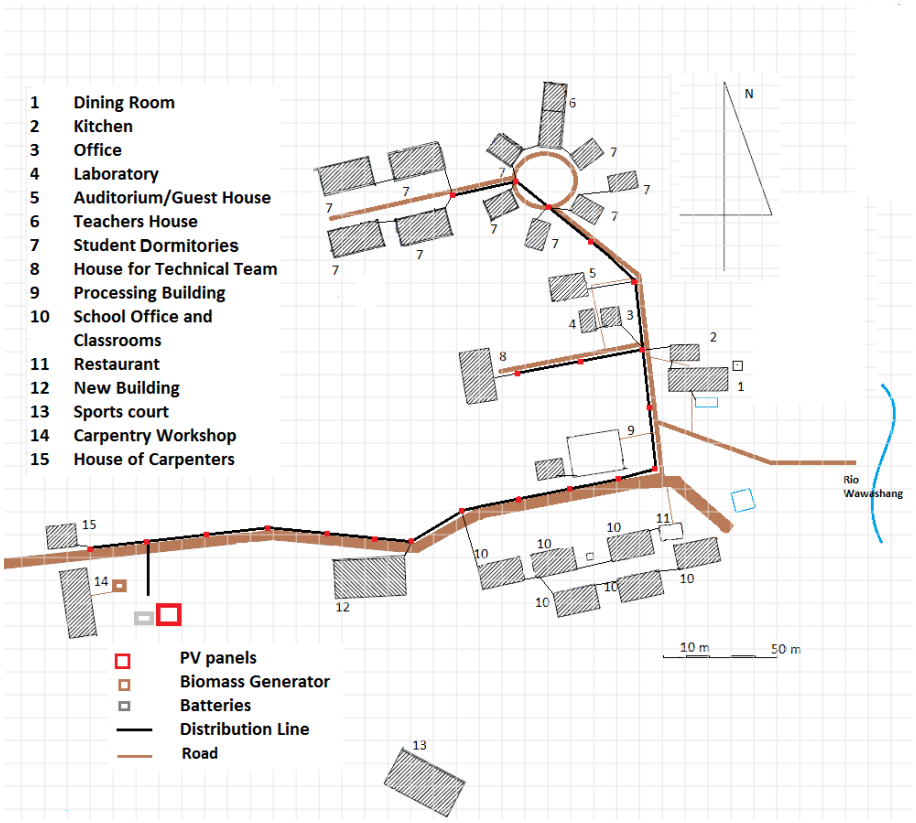

Figure 4.1: Layout of the Distribution System

4.3 Line Configuration

The voltage and frequency of AC power in Nicaragua is 120 V, 60 Hz, following the same standards as in North America. Most household appliances such as refrigerators, fans, lamps and computers operate at 120 V AC single-phase. In Wawashang, the loads of the micro grid require a 120 V AC single-phase supply, while the carpentry workshop loads are three-phase 240 V and 440 V AC. For the micro grid, there are two possible distribution line configurations:

- Single-phase/Two-wire
- Single-phase/Three-wire (split-phase)

4.3.1 Single-Phase/Two-Wire

A single-phase/two-wire configuration consists of two conductors leading from the power source, serving the loads at a voltage of 120 V (in this case) through a service drop that taps both lines as shown in **Figure 4.2(a)**. This is the simplest and most common design for rural micro grids, but not necessarily the most efficient nor the cheapest solution [39].

4.3.2 Single-Phase/Three-Wire

The split-phase or single-phase/three-wire configuration, emerged as a way of increasing the efficiency of low-voltage single-phase distribution in countries operating with 120 V (foremost the U.S.). With this configuration, two 120 V supplies (in phase with each other, 180 ° shifted so they counter-balance each other) are used in series to produce 240 V, with a third wire run to the connection point between the loads (grounded, neutral). The service drop for 120 V consumers connects to one of the phase-conductors and to the neutral wire, while to achieve a 240 V one can connect to the two phase-conductors, as shown in **Figure 4.2(b)**. If the loads are well balanced between the two phase-conductors this can lead to cost savings compared to a single-phase/two-wire configuration, even though three wires are required instead of two, because a smaller conductor can serve the same load. In the case of perfectly balanced loads, the neutral conductor will carry a zero current and the voltage drop along the return would be negligible. Consequently, each of the loads are only affected by the voltage drop along one conductor rather than two, and the conductors can optimally have a quarter of the cross-section area that would be necessary in a two-wire configuration to achieve the same voltage drop and power loss. If the loads are not perfectly balanced, the savings are reduced but, depending on the degree of unbalance, still present [39].

Considering these factors, and the fact that split-phase systems are common in countries with 120 V, such as Nicaragua, this is the configuration of choice for the micro grid in Wawashang. This was also the configuration suggested by Gilles Charlier from blueEnergy in [29].

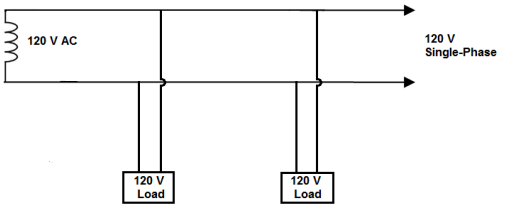

(a) Two-Wire

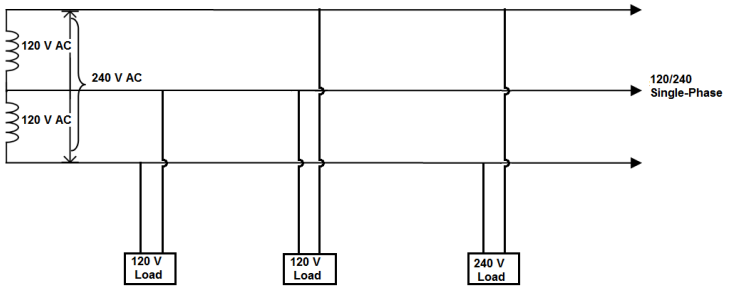

(b) Three-wire (Split-Phase)

Figure 4.2: Single-Phase Distribution Line Configurations

4.4 Conductors

4.4.1 Conductor Type

Copper and aluminum are the most common materials used in conductors for electricity distribution. Aluminum conductors have only two-thirds of the conductivity of copper and require 1.6 times the cross-sectional area of a copper conductors given the same resistance per length. Aluminum conductors also have a smaller weight-to-strength ratio that permits longer spans [39].

In this project, a THHN/THWN (Thermoplastic High Heat-resistant Nylon-coated / Thermoplastic Heat and Water-resistant Nylon-coated) insulation copper conductor is chosen, as this was suggested in [29]. Wires with THHN/THWN insulation are common for electrical distribution systems of all types and sizes, at voltage levels between 110-600 V, and are compatible in dry locations up to 90°C and wet location up to 75 °C [40].

4.4.2 Conductor Sizing

When choosing the size of the conductor, two important factors must be considered

- power loss along the line

- voltage drop along the line

High voltage drop will reduce the quality of power for the consumer, for example decreasing the light output of incandescent light bulbs. Loss of power along the line will increase the amount of power that must be generated in order to cover the users demand. Based on the information attained about the load, power factor, distribution system layout and conductor type, the required size of the conductor for a maximum percentage of voltage drop and the resulting power loss in the line can be estimated. The equations for calculating voltage drop and power loss along the line are presented in **Appendix C**.

Voltage Drop

The resistance of the conductor is determined by type and the cross-sectional area of the conductor, while the reactance is determined by its diameter and physical proximity to other conductors. Both affect the voltage drop in the line, as can be seen in **Appendix C**.

Figure 4.3 shows the resistance and reactance of a copper conductor as a function of its cross-sectional area. In **Figure 4.4**, the effect of conductor spacing on reactance is shown. As can be seen, the resistance is usually much larger than the reactance for common conductor sizes used in a micro grid. Consequently, the reactance has but a small significance for the resulting voltage drop of the line [39].

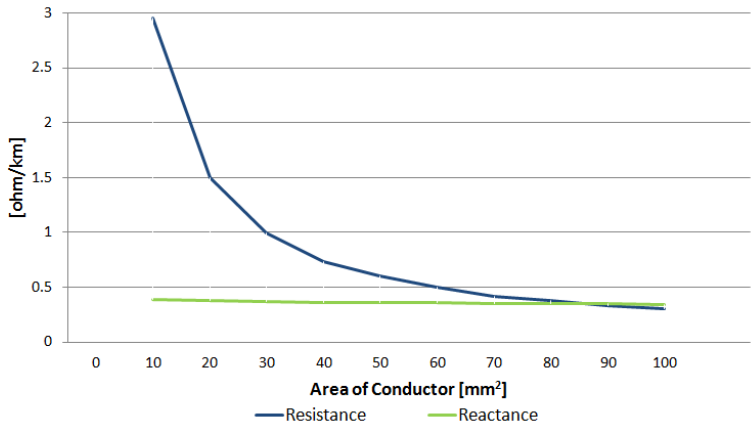

Figure 4.3: Resistance and Reactance for Copper Conductor, 0.6m conductor spacing/55 Hz

The voltage drop is also affected by the magnitude of the current that flows through the line, which is dependent on the real power of the load, the loads power factor (0.9 in this case) and the operating voltage (120 V in this case). This relationship is shown in **Appendix C**.

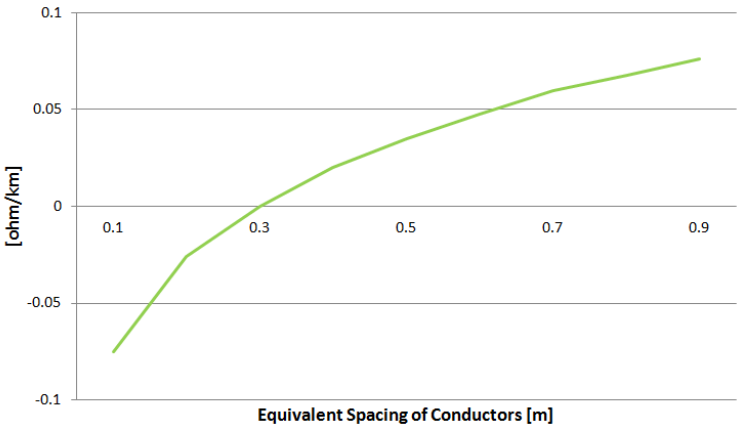

Figure 4.4: Additional Reactance Resulting from Changes in Conductor Spacing

Finally, the voltage drop is dependent on the length of the line between power supply and power consumption. A simple equation giving an estimation of the voltage drop in the case where the whole load is concentrated at the end of the line can be found in **Appendix C**. For the common situation where the loads are distributed at different distances along the line, an approximation of the voltage drop and power loss along the line can still be calculated quite easily. First, the product of power demand and distance from the supply is calculated for each point, and then these products for all *N* loads are summed. The voltage drop at the end of the line is then equal to that if a load P_T [kW] (the total sum divided by total distance from supply to end of line) is placed at the end of that line as shown in **Appendix C** [39]. The resulting equation for percentage of voltage drop with load distributed along the line is also presented the appendix.

4.4.3 Conductor Sizing for Wawashang

For simplicity, the loads that were measured in Wawashang have been divided into 6 accumulated loads at different locations on the line. It is assumed that the increase in demand will be evenly distributed, so that each load is increased by a multiplication factor of two, although in reality demand might increase more in some buildings and areas, and less in others.

The map in **Figure 4.5** shows how the area is divided into 6 loads. The peak load of the system is 7.24 kW and occurs at 18:00 on weekdays, as shown in **Figure 3.5** in **Chapter 3**. The conductor is to be dimensioned for a peak load of 7.5 kW, and maximum accepted voltage drop should be 6 %.

The loads at each location (P_n [kW]), their respective percentage of total load and distance from the power supply (L_n [km]) (shown in **Figure 4.5**), and $P_n \times L_n$ are presented in **Table 4.1**.

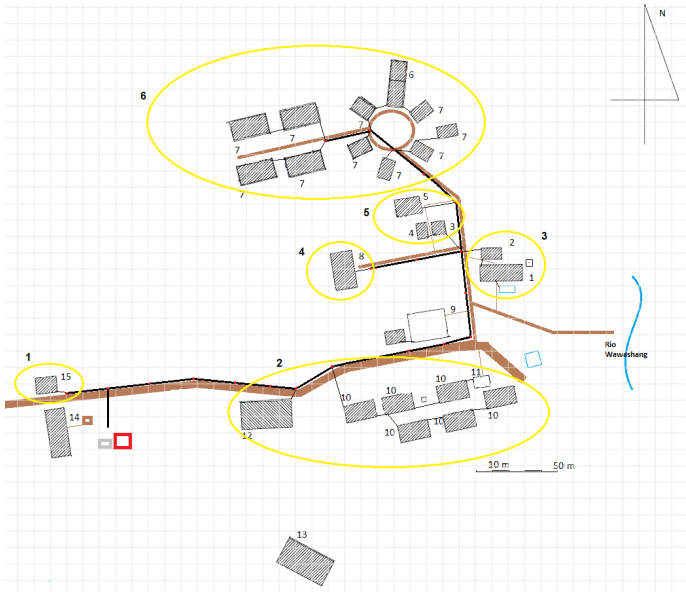

Figure 4.5: Map of Wawashang with Division of Loads

Table 4.1: Loads by Percentage and Location

Load (n)	**P**$_n$		**P**$_n$ **(7.5 peak)**	**L**$_n$	**P**$_n$**(7.5 peak)**×**L**$_n$
	$[kW]$	$[\%]$	$[kW]$	$[km]$	$[kW \times km]$
1	0.542	7.49	0.560	0.055	0.031
2	0.830	11.46	0.860	0.136	0.117
3	0.497	6.86	0.515	0.286	0.147
4	0.479	6.61	0.495	0.346	0.171
5	2.026	27.99	2.099	0.328	0.688
6	2.866	39.59	2.969	0.402	1.194
Total	7.240				2.384

The voltage drop and power loss is calculated for three different conductor sizes, AWG (American Wire Gauge) # 1, 2 and 3 (42.39 mm^2, 33.61 mm^2 and 26.65 mm^2) of which the optimal size will be chosen for the system.

In **Table 4.2**, the results for three different conductor sizes are presented. It is assumed that the load is perfectly balanced between the two phase-conductors and that the current in the neutral conductor is zero (and thereby no power loss or voltage drop in the return). Voltage drop and is calculated for each conductor with a peak load of 3.75 kW. The current listed in the table is the current in each conductor in the peak hour, and the power loss is the total loss in both conductors for the load in the peak hour (3.62 kW for each conductor).

Maximum voltage drop was set to 6 %, and although conductor AWG # 2 exceeds this by 0.07 percentage points, this is the conductor size chosen for the micro grid in Wawashang. The cost of increasing to AWG # 1 size is quite large and the power losses with the AWG # 2 conductor are not significantly large [39].

Table 4.2: Results, Conductor Sizing

AWG #	**A**	**r**	**x**	**VD**		**I**	**P_L**	
	[mm^2]	[Ω/km]	[Ω/km]	[V]	[%]	[A]	[kW]	[%]
1	42.39	0.434	0.394	6.11	5.09	26.10	0.237	3.2
2	**33.61**	**0.55**	**0.403**	**7.28**	**6.07**	**26.10**	**0.301**	**4.16**
3	26.65	0.69	0.411	8.7	7.25	26.10	0.375	5.18

4.5 Distribution Losses

Based on the results above, the distribution losses are calculated for each hour based on the load profiles presented in **Chapter 3**. Total losses are 2.75 kWh/day on weekdays and 0.68 kWh/day in weekends. Annual distribution loss is 896 kWh/year, or 2.4 % of the total demand.

In **Figure 4.6** the hourly distribution losses for the weekdays and weekends are shown, together with the load in the respective hour. For the purposes of the simulations of the production system for the micro grid, the distribution losses are added to the load. Exact values for the new hourly load can be found in **Appendix B**.

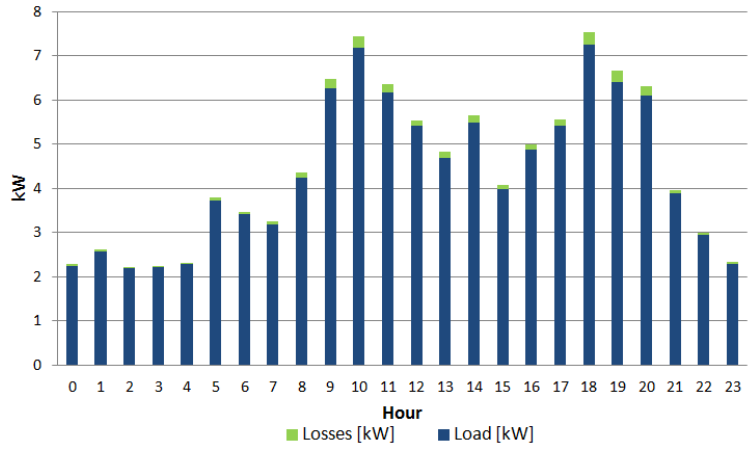

(a) Weekdays

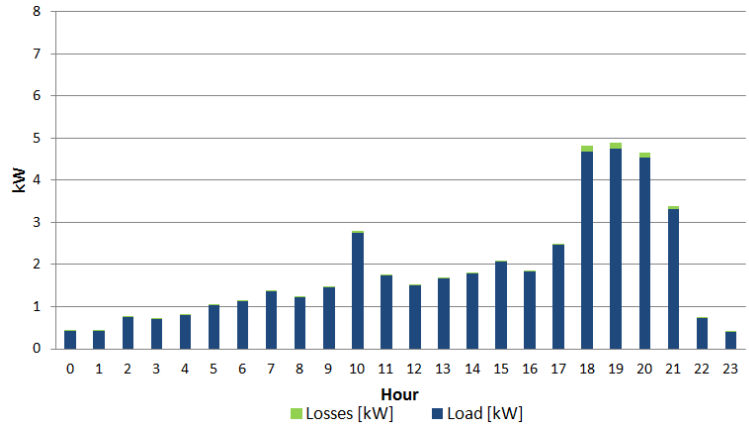

(b) Weekends

Figure 4.6: Load and Distribution Losses

Chapter 5

Electricity Production System

As mentioned, it has been concluded in previous work that a power supply with a mix of PV and biomass power and battery storage is the optimal solution for the Wawashang Complex. In this chapter the components of such production systems are presented and the simulation cases for evaluation of the production system are described.

5.1 System Components

5.1.1 PV system

Solar, or PV, cells convert the energy from sunlight (solar radiation) directly into electric energy. A PV cell consists of a semiconductor material, such as crystalline silicon (c-Si). Mono crystalline cells are typically more expensive and has a higher module efficiency than poly crystalline modules [41]. The challenges with integrating solar PV systems have been linked to the high cost of the technology. Over the last years, however, solar PV has experienced price reductions as can be seen in **Figure 5.1**. This is due to advances in technology, but also to a surplus in production of modules. The development has made solar power become more affordable also in developing countries. Rural use of renewable electricity and focus on micro grids has increased with the price reductions in solar power [6].

The PV module

In **Figure 5.2**, the structure of a PV array is shown. Due to the low voltage generation of one cell, several cells are connected in series (for increased voltage) and in parallel (for increased current) to create a PV module. One module usually consists of 36 to 72 cells.

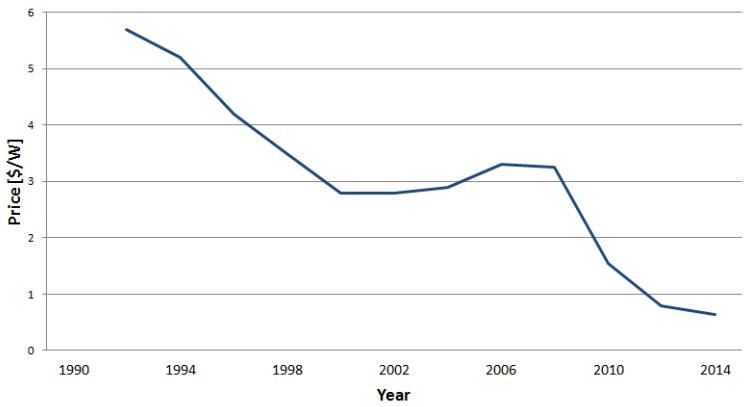

Figure 5.1: PV Module Price per Watt Development [42]

The PV modules are in turn connected in series and parallel into a PV array in order to achieve the desired voltage for the system. In a PV system consisting of multiple arrays, all arrays should have equal exposure to sunlight. If some modules are exposed to more shadow than others, unequal voltages will lead to some strings with unequal circulating current and internal heating producing power loss and lower efficiency [41].

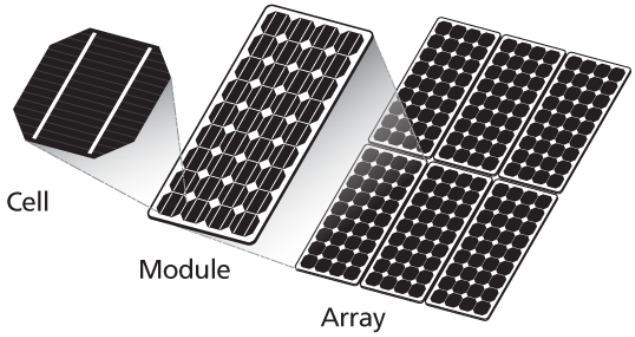

Figure 5.2: PV cell, module and array

The I-V characteristics of a PV cell is an important parameter for its performance. The amount of current and voltage available depend on the radiation that strikes the cell. The short-circuit current is the maximum current that can be drawn from the PV cell when the voltage is zero. The open-circuit voltage is the maximum voltage from a PV cell when the current through the cell is zero. These two parameters are shown as I_{SC} and V_{OC} in **Figure 5.3**. At both these operating points, the power from the PV cell is zero. The point on the I-V curve where the maximum power, P_{MPP}, can be extracted is found at current

I_{MPP} and voltage V_{MPP} [41].

$$P_{MPP} = V_{MP} \times I_{MP} \tag{5.1}$$

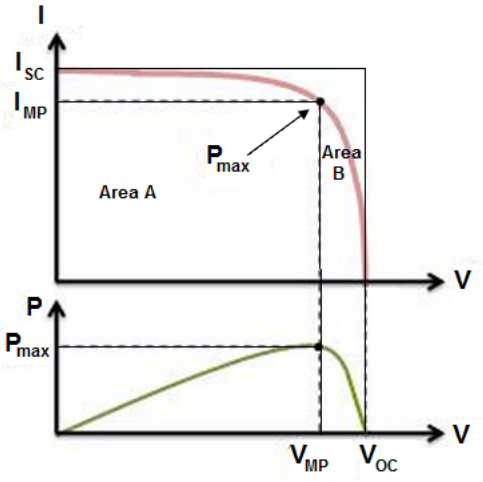

Figure 5.3: Current, Voltage and Power Characteristics for PV modules

Boost converter and MPPT

A PV module is a variable DC power source. Power output increases with increased exposure to solar irradiation. A DC-DC boost converter is a step-up converter that allows a wider range of DC power from the PV module to be captured by increasing the voltage to DC bus voltage that can be converted to AC power by a DC-AC inverter. The I-V characteristics of a PV cell varies with temperature, irradiation and load characteristics. It is therefore common to equip the boost converter with a maximum power point tracking (MPPT) control system. The MPPT control seeks to at all times operate the boost converter at the point on the I-V characteristics where the maximum power output is obtained at the given cell temperature, irradiation and load [41]. **Figure 5.4** shows the maximum power point of a typical PV modules is affected by increased temperature [37].

Efficiency and derating factor

The efficiency of a PV module defines the amount of solar energy that is converted into electricity at standard test condition (STC). STC for PV modules are a solar irradiance of 1000 W/m^2 at 25 °C and air mass AM1.5. For mono crystalline modules, the efficiency is typically 12-16 %, and for poly crystalline 11-15 %.

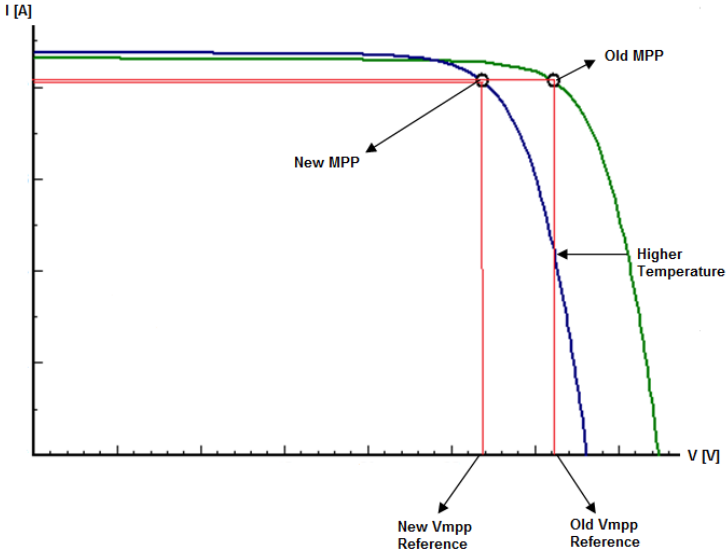

Figure 5.4: Maximum Power Point of a PV Module

The PV derating factor is a scaling factor for the PV array power output that account for reduced output in actual operating conditions compared to the STC under which the modules were rated. The derating factor accounts for factors such as mismatch, aging and soilng. In **Table 5.1** relevant components of the derating factor is listed [43].

Temperature and irradiation are also important factors for PV module efficiency. The higher the ambient temperature; the higher the cell temperature; the lower the efficiency. **Figure 5.5(a)** shows the relationship between cell temperature and efficiency for a typical PV module. Efficiency related to incident irradiation typically increases as the irradiation reaches a certain level, after which it flattens and decreases slightly with higher irradiation levels. In **Figure 5.5(b)**, the relationship between incident irradiation and efficiency for a typical PV module is shown [37].

5.1.2 Battery Bank

Battery energy storage systems (BESS) are the most common type of energy storage in micro grids and are essential for efficiently utilizing the energy produced by intermittent energy sources such as PV. Batteries convert electrical energy into chemical energy which is stored and converted back into electrical energy when needed. There is currently a significant development occurring in battery technology, but deep-cycle lead-acid batteries are still the most common due to its low cost and and high efficiency [44]. A bidirectional DC-DC charge controller controls the power flow to and from the battery. While deep-

Table 5.1: PV module derating factor [43]

PV module nameplate DC rating	Accounts for the accuracy of the manufacturers nameplate rating. Testing shows that the PV module power at STC will differ slightly from the nameplate rating.
Mismatch	Some PV modules yield slightly different current-voltage characteristics. When connected together electrically they therefore do not operate at their respective peak efficiencies.
DC wiring	Accounts for resistive losses in the wiring between the modules and the wiring connecting the PV array to the inverter
Soiling	Accounts for dirt or any other foreign matter that may appear on the front surface of the PV module and thereby reduce the amount of solar radiation that reaches the solar cells.
System Availability	Accounts for periods when the system is off due to maintenance and inverter and utility outages
Aging	Accounts for reduced performance of the PV modules over time
Charge Controller	Accounts for the efficiency of the charge controller of the batteries

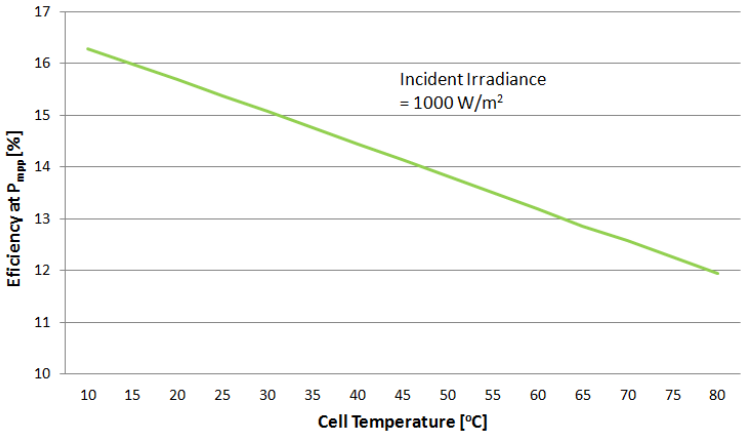

(a) Cell Temperature

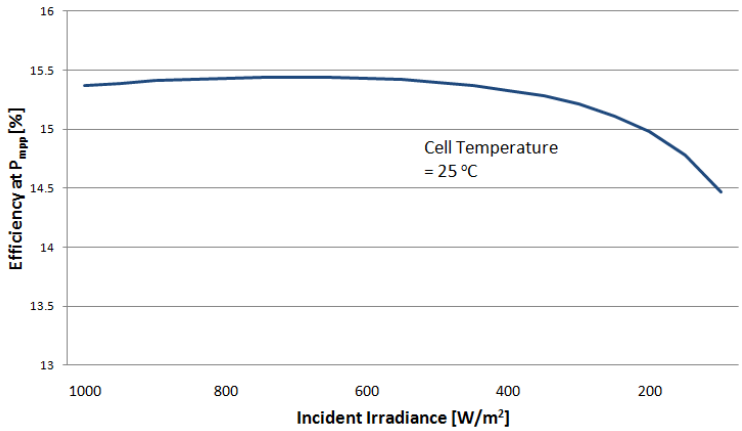

(b) Irradiation

Figure 5.5: Meteorological Effects on Efficiency of a Typical PV Module

cycle batteries are designed for deep discharges, the maximum discharge should still not exceed 75 % to avoid damaging the batteries [45].

5.1.3 Biomass Generator

Compared to other renewable energy sources such as PV and wind power, a clear advantage of biomass is that it can be stored in solid, liquid or gaseous form which allows for easy regulation and dispatch. Combustion of biomass is often used in large scale applications to run steam turbines that producte electricity or combined heat and power. The efficiency of power generation through steam turbines is highly dependent on the scale of the plant. Large-scale applications of biomass steam turbines are common, and efficiencies in steam turbines with power outputs of 10-50 MW range from 18-33 % [2]. Small-scale applications are still rare due to low efficiency. The use of biomass in stand-alone micro grids is increasing, and there are several case studies on rural electrification by bioenergy in India and Brazil. The technology of choice is normally biodigestion to produce biogas that can be used as fuel in a generator [46–49].

The company GreenTurbine has recently developed a new micro steam turbine with power outputs as low as 1-15 kW with relatively high efficiency. This technology is an interesting development for small-scale applications. GreenTurbine is a small steam-driven turbo generator which converts heat into electricity and promotes small size, silent operation and low costs. Depending on the type of power electronics used, the electric power type can be AC or DC, single- or three-phase, and various voltage and frequencies. The design speed of the turbine is 26 000 rmp. Estimated efficiency at maximum power output is 14 %. For operation, the turbine needs a condenser, vacuum pump, over-speed protector device and a rectifier (for DC-connection) or a rectifier+inverter/back-to-back converter (for AC-connection) [50, 51].

Figure 5.6, a typical configuration for connecting a micro turbine to a) the AC bus and b) the DC bus [52].

5.1.4 Inverter

A DC-AC power inverter converts power from DC to AC at system frequency and voltage and are necessary in systems with DC power or high-frequency AC power production supplying AC loads. The conversion efficiency of an inverter varies with the power output relative to its maximum rating. Every inverter has a point of maximum efficiency, which usually lies at between 20 and 30 percent of the maximum rating of the inverter. Typical peak efficiencies vary from about 92 % to 96 %. An inverter will normally have relatively low conversion efficiency at low power outputs, increasing until it reaches its peak efficiency point. At power outputs higher than this point, the efficiency normally remains relatively stable [53]. The efficiency curve of a given inverter will depend on its maximum power rating, rated efficiency and the no-load consumption of the inverter [54].

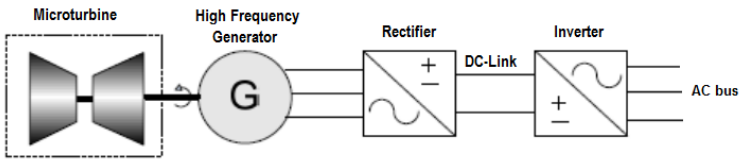

(a) Connected to AC bus

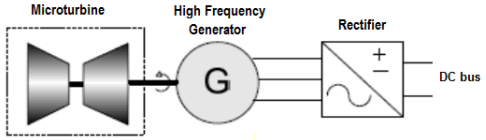

(b) Connected to DC bus

Figure 5.6: Power Electronic Coupling for Micro Turbine System

Inverter Loss Calculation

Although the efficiency curve of a specific inverter will be affected by other factors, a method for estimating an efficiency curve for any inverter based on theses parameters will be used in this thesis [54]. The efficiency curve at a given power output can be estimated as

$$\eta = \frac{P_{in}}{P_{out}} \tag{5.2}$$

Where

$$P_{in} = P_{out} \times B_{in} + P_{NL} \tag{5.3}$$

$$B_{in} = \frac{P_R - P_{NL}}{P_R \eta_R} \tag{5.4}$$

and

η	=	Efficiency at P_{in} and P_{out}
P_{in}	=	Input power [kW]
P_{out}	=	Output power [kW]

P_{NL} = No load power consumption [kW]
B_{in} = Constant relating output power to input power
η_R = Rated efficiency
P_R = Rated power [kW]

For the micro grid in Wawashang, the Sunnly Island 4548-US inverter is chosen to be used for the DC-AC conversion in the system. This inverter has a rated power of 4500 kW, so two inverters must be used in order to cover the peak load for Wawashang of 7.2 kW. The main properties of the inverter are shown in Table 5.2, and more detailed information can be found in the inverters data sheet [55].

Table 5.2: Sunny Island 4548-US parameters

Rated Power P_R [kW]	4500
Rated efficiency η_R [%]	0.96
No-load power consumption P_{NL} [kW]	0.025

Because the simulation tool, HOMER, that is used in this project does not allow for defining an efficiency curve for the inverter, but only applies one efficiency value independent of the load, the losses in the inverter are calculated prior to the simulations of the micro grid. For this purpose, the output power of the inverter is considered as equal to the loads at the complex at any specific hour, including the power loss in the distribution line, presented in **Chapter 4**. **Figure 5.7** shows the efficiency curve for the inverter, found by applying **Equations 5.2-5.3** for a different outputs from 0-4 500 kW. As can be seen, the maximum efficiency is about 96 % and the efficiency at low outputs can be as low as 30 %.

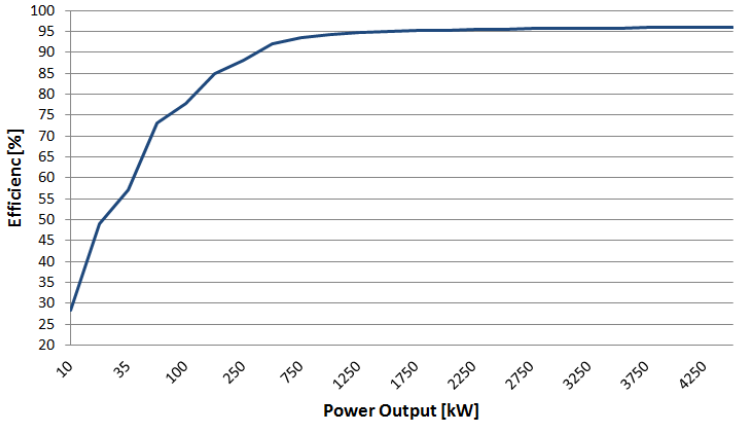

Figure 5.7: Inverter Efficiency

By applying **Equations 5.2-5.4** to each time step of the load for the micro grid, the corresponding efficiency, or conversely, the losses in the inverter for each time step can be found. **Figure 5.8** shows how the percentage of loss varies with the load of the micro grid. As can be seen, the highest loss occur during the weekends when the load is very low, with a peak of almost 14 %.

Total inverter losses on weekdays is 5.04 kWh/day in the weekdays 2.79 kWh/day. Annual inverter losses are 1722 kWh/year, or 4.6 % of total demand. The new load including inverter losses is presented in **Appendix B** together with the distribution losses.

5.2 Simulation Cases

5.2.1 Two simulation systems

In this thesis, the electricity demand in Wawashang is separated into two different systems for the purpose of the simulations of the production system. Because the load of the carpentry workshop constitutes over 50 % of the total expected future demand and 75-80 % of the load in peak hours, a PV-battery system needs to be very large to be able to cover both the total demand and the peak, if both are simulated in the same system. As mentioned, including the carpentry workshop in a PV-battery system had little support in Wawashang, and it was therefore determined to separate the carpentry workshop from the rest of the micro grid. The current electricity supply for the carpentry workshop consists of two diesel generators of 24 and 10 kW. The 10 kW generator is not functioning and must be replaced, as the 24 kW generator at the moment is operating alone and in some hours at very low efficiencies to cover low loads. The carpentry workshop is operating between 06:00 and 18:00. This is the about the same time of the day that the sun is up, as can be seen in **Table 5.3**.

Table 5.3: Sunrise and Sunset in Bluefields, Nicaragua

	Sunrise	**Sunset**
Longest Day (December 21^{th})	05:11	18:02
Shortest Day (June 20^{th})	05:50	17:16

The most critical time to have a backup generator for a PV-battery system is during the evening and night when there is no sun and when the batteries need charging. The idea therefore emerged to use the biomass generator in the carpentry workshop during the work day and in as backup for the micro grid during the evening and night. HOMER presents the possibility of defining separate loads, but not the option of specifying whether a specific load should be covered by a specific energy source. Therefore, the two systems have been simulated separately, yet simultaneously, in order to correct the amount of biomass available for the two systems based on reliability and the joined cost of the two systems. This process is further explained in **Chapter 6**. Two cases with different configurations for the micro grid system will be evaluated. The configuration for the carpentry workshop

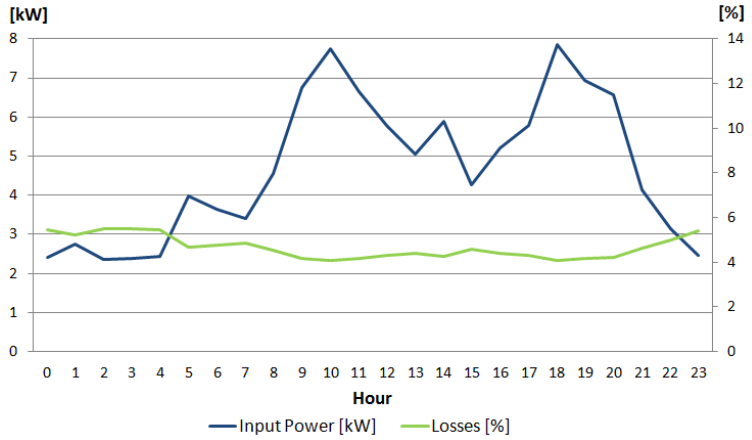

(a) Weekdays

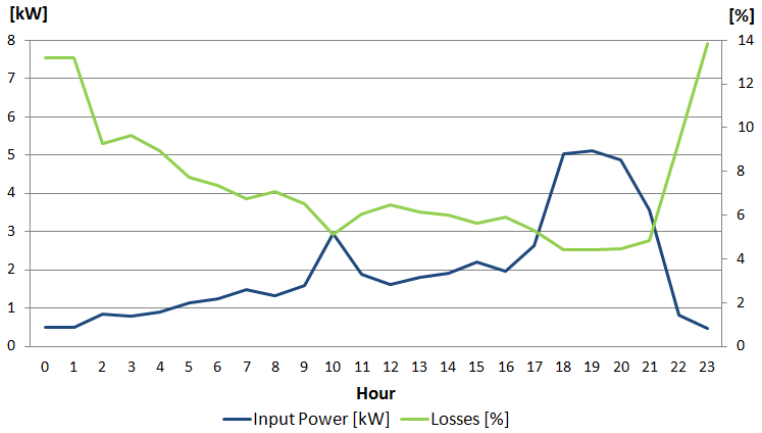

(b) Weekends

Figure 5.8: Inverter Loss and Input Power

is the same in both cases. In the the following sections, the simulation cases will be described.

5.2.2 Case I

In Case I, the micro grid system configuration is same as Case III in [24], the case with a biomass generator. In this system, the high-frequency output of the biomass generator is rectified to DC power before it is converted to AC power at the correct frequency and voltage and connected to the single-phase AC bus of the micro grid. This configuration is shown in **Figure 5.9**. This case requires an extra inverter, because the biomass generator is not connected through the common DC-bus with the PV-battery system, and might cause an increase in system cost. However, this system might be more flexible and provide extra security because the biomass generator can be operated at times when the PV-battery inverter is out of order. If a cycle charging strategy is applied for the generator in Case I, this will cause greater losses in the system, because the generator output will have to be rectified to the DC-bus voltage before it can charge the batteries, and be converted back to AC when the batteries are discharging. This would mean that the power generated by the biomass generator would have to go through four converter steps before the power reaches the load if it is used to charge the batteries.

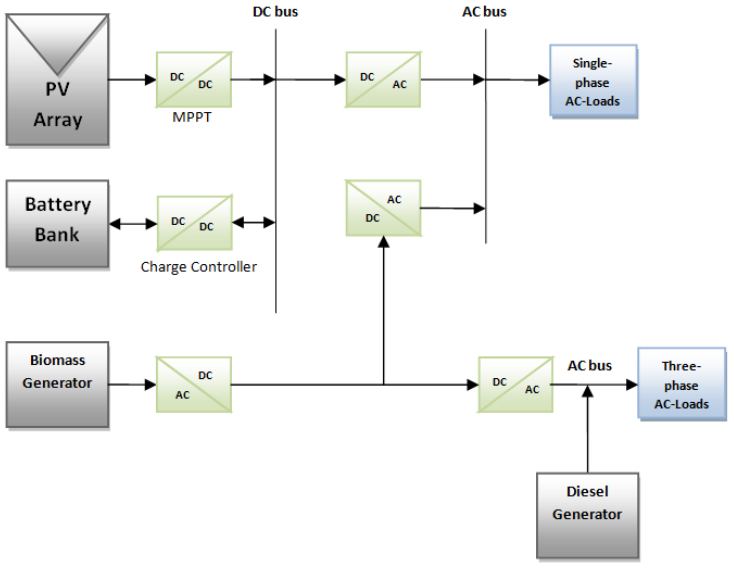

Figure 5.9: System Configuration, Case I

5.2.3 Case II

In the second case, the biomass generator is connected to the common DC-bus of the PV-battery system of the micro grid after the high-frequency output is rectified. This case requires one less power electronic component compared to Case I, and might consequently be the least expensive solution. In Case II it is more efficient to use the biomass generator to charge the batteries, because no extra conversion stage is necessary. However, should the DC-AC inverter be out of order for some reason, all three sources of energy will be unable to serve the load.

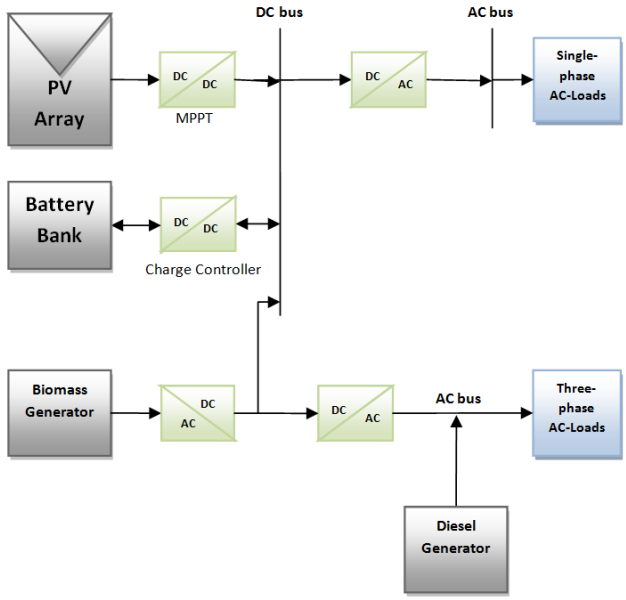

Figure 5.10: System Configuration, Case II

5.2.4 Carpentry Workshop

As can be seen in **Figures 5.9-5.10**, the biomass generator is connected to the three-phase loads at the carpentry workshop in the same way in both Case I and Case II. After the high-frequency output of the biomass generator is rectified, an inverter converts the power from DC to three-phase AC to supply the loads. The carpentry workshop is also supplied by a diesel generator.

Carpentry Workshop ”Business as Usual”

In the simulations, a subcase of the carpentry workshop called ”Business as Usual” will be included. In this case, the carpentry workshop is supplied only by the 24 kW diesel generator that allready exists, and this simulation scenario is run in order to get an idea of the cost of electricity if no changes are made.

Chapter 6

Simulation Methods and Settings

6.1 HOMER Simulation Software

HOMER (Hybrid Optimization Modelling software for Electric Renewable and fossil energy) is a simulation tool developed by the US National Renewable Energy Laboratory (NREL). The software is used for designing and analyzing hybrid power systems. For both off-grid and grid-connected systems, HOMER optimize power systems regarding both technical and economical aspects. HOMER allows for integration of renewable energy sources such as wind or PV power, generators with a variation of fuels and ESS such as battery or fuel cells. While optimizing the system HOMER determines economical feasibility, and therefore allows for both economical and technical analysis of the system [56]. In this theses, only off-grid solutions have been evaluated.

6.2 Data Retrieval

While doing simulations in HOMER, information about both type and price must be collected. In order to get the information as close to reality as possible, it has been attempted to choose equipment and prices that are available in and valid for Nicaragua. Components that are known to be available in Nicaragua have been used and information have been collected through contact with the companies that deliver them, particularly Ecami, and from blueEnergy [57, 58].

6.3 Simulation Method

HOMER allows the user to define different possible sizes of the PV system, battery bank, converter and generators. After each simulation, the optimal solution presented by HOMER is the system that, with the sizes and components available, can cover the load within the given technical contraints at minumum cost. HOMER also presents the sub-optimal solutions; solutions that is also capable of covering the load within the constraints, but at a higher cost. For each simulation, the optimal solution and the 3-4 first sub-optimal solutions have been considered, as the cost difference of these solutions normally is very small.

The simulations in HOMER were performed multiple times for each case. For each simulation, three evaluations of the results were made:

- In the beginning, a large step for the sizes of the PV array and battery bank (10 kW, 20 kW, 30kW etc.) were used. For each simulation, the sizes of were narrowed down, based on the results from the last simulation in order to obtain the exact optimal sizes.

- The two systems, the carpentry workshop and the micro grid, were simulated simultaneously for each case. In the first simulation, the biomass generator investment and replacement costs, the lifetime (hours of operation before needing replacement) and the amount of biomass available (total 326 kg/day average) were split equally between the two systems. After each simulation, the systems were evaluated based on the operation of the biomass generator. If the carpentry workshop used the biomass generator 2000 hours per year, while the micro grid used it 500 hours per year, in the next simulation its costs and lifetime would be split 80 % (workshop) and 20 % (micro grid). The amount of biomass available for each system was also corrected based on whether or not the system exploited all available biomass in the last simulation. This was done in a type of iteration process where, step after step, the correction necessary for the next simulation became smaller and smaller until the optimal total solution based on technical and economical aspects for both systems together was obtained.

- After the optimal operational regime of the biomass generator between the carpentry workshop and the micro grid was decided, the distribution of the biomass throughout the year was optimized. Multiple simulations were run, each time correcting the monthly distribution of biomass in the micro grid according to the unmet load, in order to obtain a system with a generator capable of balancing the PV production in the best way possible. After the optimal solution was found, the result was checked against the carpentry workshop to see if the results still were optimal for the system as a whole. If this was not the case, the process was repeated.

6.4 Simulation Settings, Micro Grid

6.4.1 Load Profiles

The load profiles used in the simulation of the micro grid are the ones calculated for future demand, explained in textbfChapter 3 with the added inverter and distribution losses, as explained in **Chapter 4** and **5**. The numerical values for these are presented in **Appendix B**. The load profiles are different for weekdays and weekends (1 day weekend), but otherwise equal throughout the year, giving a daily average demand of 103 kWh/day. The load was imported to HOMER in a file containing 8760 values, for every hour of the year.

6.4.2 Meteorological data

The meteorological data for temperature and irradiation was retrieved from the NASA-SSE database, and is described in Chapter 3 and displayed in **Table 3.4** on **Page 29**.

6.4.3 PV Modules

The PV modules chosen for the system are available from the company Ecami. The modules that were suggested were the ReneSola Virtus II JC250M-24. In HOMER, the specific PV module is not specified, however, all the technical and economical information used in HOMER correspond to the characteristics of the modules thought used for the real system. In **Table 6.1** the input parameters for the PV modules are given, and in the following sections the necessary explanations are made [37].

Table 6.1: PV Module Inputs

PV model		ReneSola Virtus II JC250M-24
Module size	[kW]	0.250
Sizes to Consider Case I	[kW]	28-32.5 (0.5 kW step)
Sizes to Consider Case II	[kW]	
Lifetime	[years]	20
Derating Factor	[%]	79
Tilt Angle	[°]	13
Azimuth	[°]	0
Albedo	[%]	25
Tracking System		No tracking
Temp. Coeff. of Power	[%/°C]	-0.4
Nom. Operating Cell Temp.	[°C]	45
Efficiency at STC	[%]	15.4
Investment Cost	[US$/module]	325

Derating Factor

In HOMER, a derating factor can be applied to the output of the PV array. This factor accounts for the different components explained in **Table 5.1** in **Chapter 5**. In the **Table 6.2**, the values for each component chosen for the simulations are stated. The values are, with some modifications, the same as the ones suggested as the default value in [43].

Table 6.2: PV module derating factor

PV module nameplate DC rating	0.95
Mismatch	0.98
DC wiring	0.98
Soiling	0.98
System availability	0.98
Aging	0.923
Charge controller	0.98
Total derate factor	**0.792**

The aging factor is based on the PV module performance information for the specific ReneSola module, which estimates that the PV module performance will be reduced to 85 % in 20 years [59]. This equals a reduction in performance of about 0.9915 % per year. On average over 20 years, the aging factor can therefore be expressed as shown in **Equation 6.1**.

$$\frac{1}{20} \times \sum_{i=0}^{19} 0.9915^i = \frac{1}{20} \times \frac{0.9915^{20} - 1}{0.9915 - 1} = 0.923 \tag{6.1}$$

Effect of Temperature

As explained in **Chapter 5**, temperature is an important factor when it comes to the efficiency of the PV modules. This effect can be modeled in HOMER based on the ambient temperature at the site and the temperature characteristics of the PV modules. The average monthly ambient temperatures were attained from the NASA-SSE database and are displayed in Table 3.4 in Chapter 3. Based on these temperatures, HOMER calculates the cell temperature in each time step. The temperature coefficient of power and the nominal operating cell temperature, stated in **Table 6.1**, are used to adjust the PV array power output [56].

Tilt Angle

The tilt angle, or slope, is the angle at which the PV array is placed relative to the horizontal with the goal to maximize the amount of irradiation that hits the PV cells. The PV array can be be placed in a fixed tilted plane, seasonal tilt adjustments (adjusting the angle

for summer and winter) or in different tracking modes [56]. In this thesis, a fixed tilted plane is chosen in order to reduce the amount of complex technology and operation and maintenance of the system. A simplified method of deciding the tilt angle is used; the tilt-at-latitude rule. The chosen angle is 13 °.

Azimuth

The azimuth is defined as the angle between the plane and the geographical south. Optimal angle is 0 °. As the PV-panels in Wawashang may be placed in any desired angle, the azimuth for the simulations is set to 0 °.

Albedo

The ground reflectance, or albedo, coefficient defines the fraction of global irradiation that is reflected by the ground in front of a tilted plane. The albedo varies with the type of ground the panels are placed upon, with between 0.12-0.22 for urban areas and up to 0.8 with snow-covered ground. The area intended for the PV-panels in Wawashang is a grass field. The albedo for grass varies from 0.15 to 0.26, and for the simulations a value of 0.25 is chosen [37].

Cost

One module costs US$ 325, and the cost information is provided by Ecami [58].

6.4.4 Batteries

The battery model thought used for the real system is the 6 V Trojan L16P batteries with a capacity of 420 Ah. In HOMER, these batteries are listed with a nominal capacity of 360 Ah. The main information for the batteries is presented in **Table 6.3**. The necessary parameters are explained in the following [56].

Minimum State of Charge

The minimum state of charge (SOC) parameter sets the limit for how low the batteries are allowed to be discharged. This setting is important because very low and frequent SOCs will damage the batteries and reduce their lifetime. For deep-cycle batteries a minimum SOC of 30 % is a common limit.

Table 6.3: Battery Inputs

Battery Type		Trojan L16P
Nominal Voltage	$[V]$	6
String Voltage	$[V]$	48
Numb. of Strings to Consider Case I		15-19
Numb. of Strings to Consider Case II		15-21
Nominal Capacity	$[Ah]$	360
Minimum State of Charge	$[\%]$	30
Initial State of Charge	$[\%]$	100
Minimum Battery Life	$[years]$	7
Investment Cost	$[US\$/unit]$	284

Cost

One battery costs US$ 284. Availability and price of the Trojan L16P is known from Ecami in Nicaragua [22].

6.4.5 Converter

The power converter chosen for the real system is the SunnyIsland 4548-US with the SMA Smartformer for Sunny Island Inverter Split-Phase 120/240 VAC. The main converter inputs in HOMER are stated in **Table 6.4** [55].

Table 6.4: Converter Inputs

Converter Type		SunnyIsland 4548-US
Sizes to consider	$[kW]$	9
Lifetime	$[years]$	10
Rectifier Relative Capacity	$[\%]$	95
Rectifier Efficiency	$[\%]$	95
Investment Cost	[US$kW]	711
Operation and Maintenance Cost	[US$/kW.year]	25

Cost

It has been confirmed that this converter is available from Ecami. The price, however, has not been confirmed. The cost, US$ 711 /kW, used in the simulations are the average power converter costs in 2013 [60].

6.4.6 Biomass Generator

The generator is a micro steam turbine that uses biomass as fuel, described in **Chapter 5**. As mentioned, the input information for the biomass generator was continuously changed during the process of the simulations. In **Table 6.5** the final input data for both cases of the micro grid is presented. In this section, the necessary data will be explained.

Table 6.5: Biomass Generator Input Micro Grid

		Micro Grid	
Input		**Case I**	**Case II**
Maximum Output (Size)	$[kW]$	7.5	7.5
Maximum Efficiency	$[\%]$	11	11
Lifetime	[h]	2 550	3300
Charging Strategies		CC/LF	CC/LF
Average Available Biomass	[kg/day]	60	60
Investment Cost	[US$]	9 582	5412
Replacement Cost	[US$]	4 486	4059

Charging Strategies

Two possible charging strategies can be applied to the generator in HOMER:

- The cycle charging strategy is a dispatch strategy where whenever a generator is operated to serve the load, it operates at maximum output power (as high as possible without resulting in excess electricity), in order to charge the batteries.
- The load following strategy is a dispatch strategy where the generator is only operated to serve the load. Charging the batteries is left to the PV power.

In this project, both options have been considered in the simulations, and HOMER chooses the optimal solution based on technical and economical aspects.

Maximum Output (size)

As explained, HOMER applies either a cycle charging strategy OR a load following strategy for the generator. When running the simulations, it became clear that the 15 kW generator was not optimal for the cycle charging strategy because the output of 15 kW is so high compared to the load and the size of the batteries, and the generator would have to be turned on and off a frequently. At the same time, the load following strategy was never considered, because running the generator at such low loads compared to the maximum output would not be considered efficient by HOMER. Therefore, it was decided to, for the purpose of the simulations, allow HOMER to choose a 7.5 generator instead, which in HOMER appears as the size of the generator, but is actually just the maximum output the

generator will use when producing for the micro grid. This allows the cycle charging strategy to be used without having to ”hold off” using the generator until it is necessary for it to produce 15 kW over a certain time period, and without the frequent start and stops.

Efficiency

According to GreenTurbine, the efficiency of the 15 kW micro turbine is approximately 14 % at maximum output [51]. The efficiency curve is corrected for the fact that the maximum output is 7.5 kW and not 15 kW, and maximum efficiency is set to 11 %.

Liftime

Lifetime is the number of hours the biomass generator can be operated before having to be replaced. The total lifetime hours of operation is 15 000 when the carpentry workshop is included for each case.

Cost

The cost of the 15 kW generator is still uncertain, but according to GreenTurbine, the estimated cost including all necessary components, will be about US$ 30 000. Exact price information for the 1.2 kW model of the GreenTurbine was presented, and this information is used as a guideline for deciding the price of the different components of the system. The price of the 1.2 kW generator with all components is presented in **Table 6.6** [51]. The price for the inverter in the 1.2 kW system is about 18 % of the total cost. Transferred to the 15 kW system, the inverter price is about US$ 5400, which corresponds well with the assumption of US$ 711 per kW that was made for the main power converter described previously. In Case II, the generator is connected through a rectifier to the DC bus and therefore the power is converted to AC power through the same DC-AC inverter as the PV-battery system, and the price of the system is therefore lower than in Case I. Because not all the components will need replacement at the same time, replacement costs are set as 75 % of the investment costs, and 25 % for the DC-AC inverter. The specific cost of the generator depends on the hours of operation in the micro grid compared to the carpentry workshop for the specific case. The final cost input for each case is presented in **Table 6.5**.

Biomass Resource

As mentioned, the biomass available for the micro grid is not distributed evenly throughout the year. This is because the amount of irradiation, and consequently the PV production, varies with season. In **Figure 6.1** shows how the biomass is distributed in each case together with the irradiation.

Table 6.6: 1.2 kW GreenTurbine Cost Information

Component	**Price** [US$]
1.2 kW Green Turbine	6124.5
Condenser	748.5
Vacuum Pump	544.4
Inverter	1 905
Speed Control	395.4
Steam Valve	113
Total	10 192

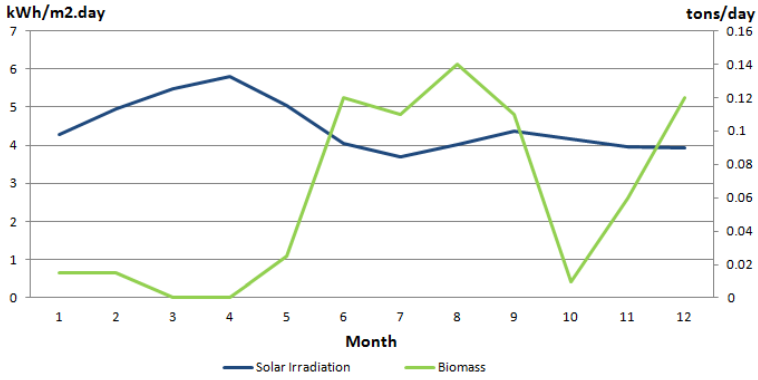

(a) Case I

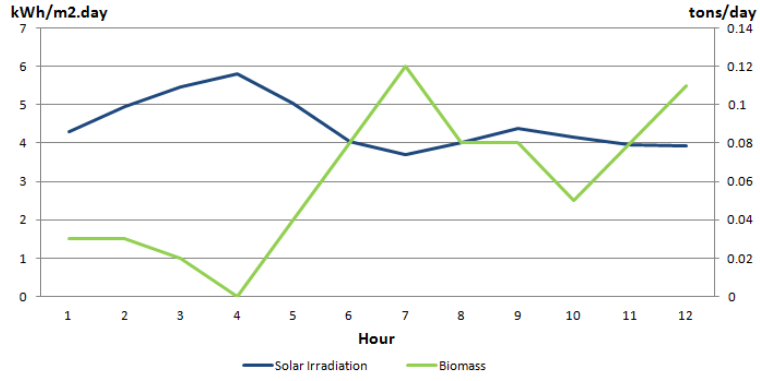

(b) Case II

Figure 6.1: Biomass Distribution

6.5 Simulation Settings, Carpentry Workshop

6.5.1 Load Profile

The load profiles for the carpentry workshop are also presented in **Chapter 3**. The carpentry workshop is closed in the weekends, in Easter and during Christmas. The load was imported to HOMER in a file containing 8760 values.

6.5.2 Biomass Generator

The input data for the biomass generator in the simulations for the carpentry workshop is presented in **Table 6.7**. The only size that has been considered is 15 kW.

Table 6.7: Biomass Generator Input - Carpentry Workshop

Input		Carpentry Workshop Case I	Carpentry Workshop Case II
Maximum Output (Size)	$[kW]$	15	15
Maximum Efficiency	$[\%]$	13	13
Lifetime	[h]		11 700
Average Available Biomass	[kg/day]	267	267
Investment Cost	[US$]	31 218	29 988
Replacement Cost	[US$]	18 013	17 091

Cost

Cost of the inverter is doubled compared to that of the micro grid, since the maximum output is doubled. Cost of the generator is calculated in the same manner as for the micro grid, and is dependent on how many hours per year it is operated in the carpentry workshop compared to in the micro grid for that specific case.

Biomass Resource

For the carpentry workshop, the biomass distribution is uniform throughout the year, 267 kg/day each month.

6.5.3 Diesel Generator in the Carpentry Workshop

The generator operating in the carpentry workshop today is a 24 kW diesel generator. In the simulations, the option of replacing the diesel generator with one of 15 or 20 kW is introduced. Efficiency at maximum output for the generator is 27 %. **Table 6.8** shows the input data for the diesel generator.

Table 6.8: Diesel Generator Carpentry Workshop

Size	$[kW]$	**15**	**20**	**24**
Maximum Efficiency	$[\%]$	27	27	27
Lifetime	[h]	15 000	15 000	15 000
Investment Cost	$[US\$]$	1 934	2 578	1 547
Replacement Cost	$[US\$]$	1 934	2 578	3 095
O&M	$[US\$/h]$	0.260	0.52	0.624
Diesel Price	$[US\$/L]$	1.4	1.4	1.4

Cost

Investment, replacement and operation and maintenance costs are retrieved from [61]. Investment cost of the 24 kW generator is half of the actual cost in order to account for the fact that there already is a generator present that has been assumed to have been in operation about 7 500 hours. The current diesel price in Nicaragua is US$ 1.2, and an extra US$ 0.2 is added to account for transportation costs to the complex [62]. These prices are also used for the carpentry workshop in the "Business as Usual" subcase.

6.6 Economics

The real interest rate in Nicaragua is changing rapidly. The last value reported from the World Bank was 2.9 % (2012), and this value is used in the simulations of both systems [63]. The lifetime of the project is 20 years, decided by the lifetime of the PV modules.

6.7 Contraints

6.7.1 Maximum Capacity Shortage

Maximum capacity shortage for the simulations of both the micro grid and the carpentry workshop is set to 1 %.

6.7.2 Schedule

Figure 6.2 shows how the biomass generator is operated between the micro grid and the carpentry workshop.

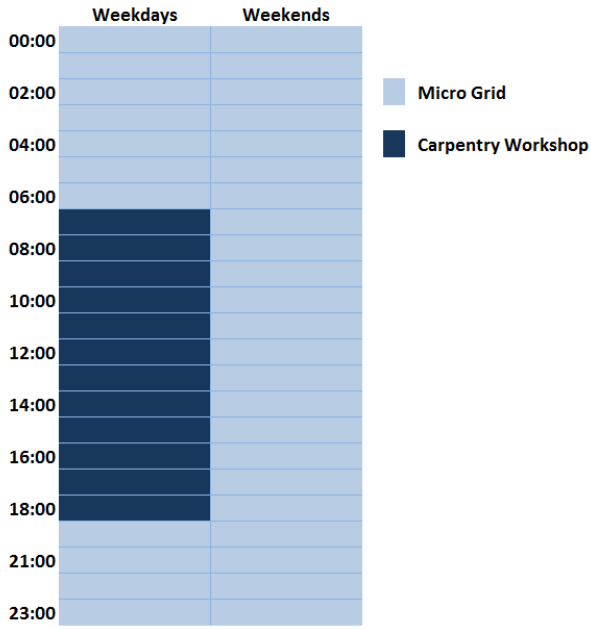

Figure 6.2: Biomass Generator Schedule

Chapter 7

Simulation Results

In the following sections, the main results from the HOMER simulations are presented. Full simulation reports can be found in **Appendix D-G**.

7.1 Micro Grid - Case I

7.1.1 System Design

In **Table 7.1**, the system design for the resulting optimal solution from the simulations in HOMER for Case I of the micro grid is presented. The system consists of a 34 kWp PV array, a 7.5 kW biomass generator and a battery bank with a capacity of 328 kWh. The converter size is 9 kW, corresponding with the peak load of the system. HOMER has evaluated the load following strategy to be the optimal solution in Case I. Hence, electricity is not transferred from the AC bus to the DC bus, and rectifier mode of the converter is consequently not considered.

7.1.2 Production and Consumption

Total yearly production of the system is 46 921 kWh/year, of which PV production consitutes 90 % and biomass production 10 %. Total demand is 37 595 kWh/year and consumption is 37 386 kWh/year. In other words, unmet load is very low, corresponding with the capacity shortage constraint of 1 % that was set for the simulations. **Table 7.2** presents a summary of the yearly production and consumption for Case I.

Figure 7.1 shows the average monthly production of biomass and PV for Case I. The PV production follows the irradiation trend, while the biomass production more or less follows the biomass distribution that was defined for the simulations.

Table 7.1: System Design, Micro Grid - Case I

PV Modules		
Total Amount		136
Total Global Power	$[kW]$	34
Biomass Generator		
Size	$[kW]$	7.5
Batteries		
Number of Strings		19
Total Amount		152
Total Nominal Capacity	$[kWh]$	328
Charging Strategy		LF
Inverter	$[kW]$	9
Rectifier	$[kW]$	0

Table 7.2: Production and Consumption, Micro Grid - Case I

	$[kWh/year]$	$[\%]$
Demand	37 595	
Total Production	46 921	
PV Array Production	42 221	90
Biomass Generator Production	4 710	10
Consumption	37 377	
Excess Electricity	6 224	13.3
Unmet load	218	0.6

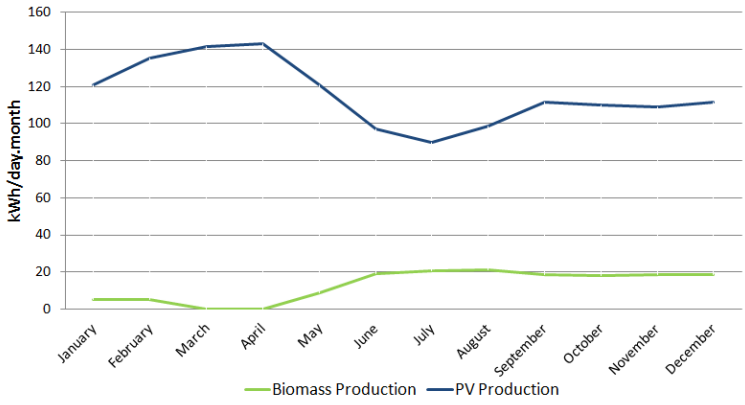

Figure 7.1: Electricity Production, Micro Grid - Case I

Unmet load is only 0.6 %, and is well within the acceptable limits. Nevertheless, it is relevant for the analysis of the behavior of the system to look at the distribution of unmet

load throughout the year. As can be seen in **Figure 7.2**, the occurrence of unmet load is to a great extent concentrated in July and August, which coincidences with the months with lowest PV production.

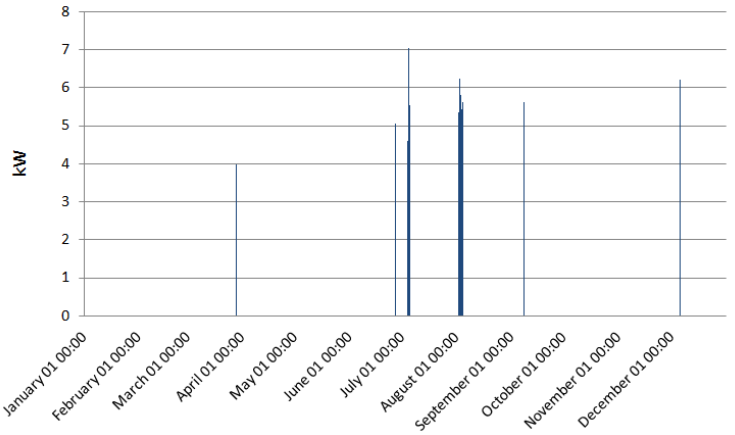

Figure 7.2: Unmet Load, Micro Grid - Case I

Figure 7.3 shows that also excess electricity is affected by seasonal variations in PV production. Excess electricity is very low in the months with low irradiation and high in the months with high irradiation.

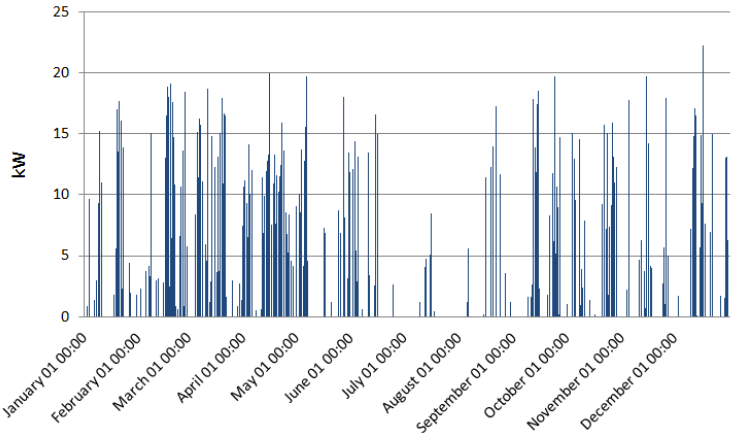

Figure 7.3: Excess Electricity, Micro Grid - Case I

7.1.3 Component Details

Table 7.3 gives an indication of how the different components of the system are operated throughout the year. The capacity factor of the PV array is only 14.2 % (4.8 kW mean electrical output). Hours of operation is a little lower that 50 % of the hours of the year, corresponding well with the average length of the day in Nicaragua. The biomass generator is only operated 727 hours of the year. Minimum power output is as low as 1.5 kW and average output is 6.48 kW, 86 % of the maximum output. Mean electrical efficiency of the generator is 10.8 %. Autonomy of the batteries is a little over two days. Expected life is high, 9.7 years. Minimum electrical output of the inverter is 0 kW, suggesting that there are some hours where the either the biomass generator supplies the load without help from the batteries or the PV array, or no load is covered.

Table 7.3: Component Details, Micro Grid - Case I

PV Array		
Mean Electrical Output	$[kW]$	4.8
	$[kWh/day]$	116
Hours of Operation	$[h]$	4 442
Capacity Factor	$[\%]$	14.2
Biomass Generator		
Mean Electrical Output	$[kW]$	6.46
Hours of Operation	$[h]$	727
Biomass feedstock consumption	$[tons/year]$	13.7
Mean electrical efficiency	$[\%]$	10.8
Battery Bank		
Annual Throughput	$[kWh/year]$	16 853
Battery Losses	$[kWh/year]$	2 618
Autonomy	$[h]$	53.6
Expected Life	$[years]$	9.7
Inverter		
Mean Electrical Output	$[kW]$	3.73
Hours of Operation	$[h]$	8274

Low state of charge is not significantly frequent for Case I, as can be seen in **Figure 7.4**, corresponding with the high life expectancy of the batteries.

7.1.4 System Cost

Table 7.4 the system cost information for Case I. Total net present cost (NPC) is US$ 162 226 and the levelized cost of energy (COE) is US$ 0.289 /kWh.

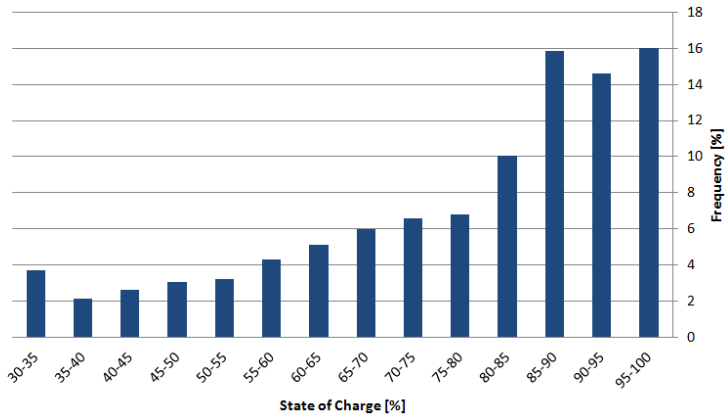

Figure 7.4: Battery State of Charge Frequency, Micro Grid - Case I

Table 7.4: System Cost, Micro Grid - Case I

Capital	$[US\$]$	103 349
Replacement	$[US\$]$	79 094
O&M	$[US\$]$	3 379
Salvage	$[US\$]$	-23 595
Total NPC	$[US\$]$	**162 226**
Annulized Total Cost	$[US\$/year]$	10 804
Lev. COE	$[US\$/kWh]$	0.289

7.2 Micro Grid - Case II

In the optimal solution from the simulations in HOMER for Case II of the micro grid, both the size of the battery bank and the PV array is reduced to a capacity of 294 kWh and 30 kWp, respectively, compared to Case I. Maximum output of the biomass generator is 7.5 kW. The converter size the same as in Case I, 9 kW. In this case, HOMER has evaluated the cycle charging strategy to be the optimal solution, but because all the production components are connected to the DC bus, there is still no electricity being transferred from the AC bus to the DC bus, and rectifier mode of the converter is not applied. In **Table 7.5** a summary of the system design is given.

Table 7.5: System Design, Micro Grid - Case II

PV Modules		
Total Amount		120
Total Global Power	$[kW]$	30
Biomass Generator		
Size	$[kW]$	7.5
Batteries		
Number of Strings		17
Total Amount		136
Total Nominal Capacity	$[kWh]$	294
Charging Strategy		CC
Inverter	$[kW]$	9
Rectifier	$[kW]$	0

7.2.1 Production and Consumption

In **Table 7.6**, the production and consumption data for Case II is presented. Total production is 44 734 kWh/year, 83 % PV production and 17 % biomass production. Demand is 37 595 kWh/year and total consumption is 37 443 kWh/year, even higher than in Case I.

Table 7.6: Production and Consumption, Micro Grid - Case II

	$[kWh/year]$	$[\%]$
Demand	37 595	
Total Production	44 734	
PV Array production	37 254	83
Biomass Generator Production	7 480	17
Consumption	37 437	
Excess Electricity	3 992	8.92
Unmet load	152	0.4

Figure 7.5 shows the monthly average electricity production from biomass and PV. Both sources are again following the trends of the inputs for the simulations. In this case, it is quite clear how the biomass production complements the PV production.

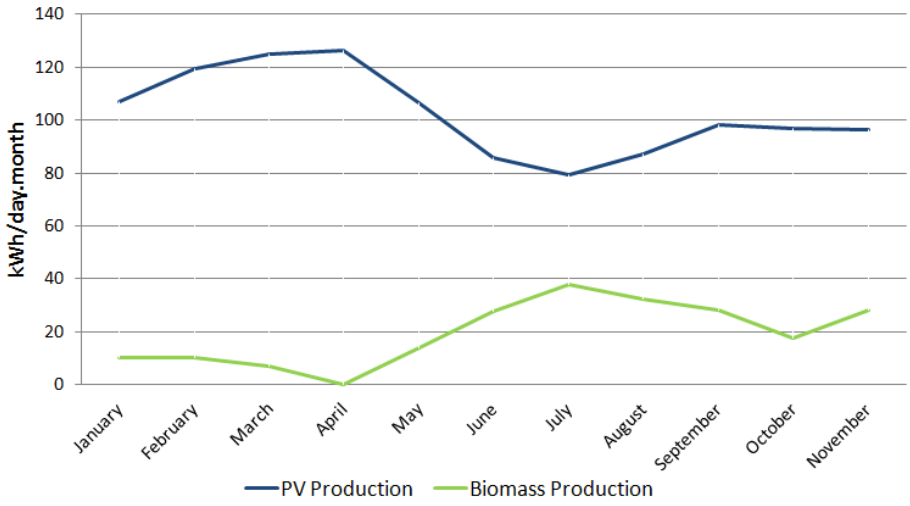

Figure 7.5: Electricity Production, Micro Grid - Case II

Unmet load is as low as 0.42 %, and **Figure 7.6** shows that although there is still a small overweight in July, the unmet load is otherwise occurring in both rainy and dry season.

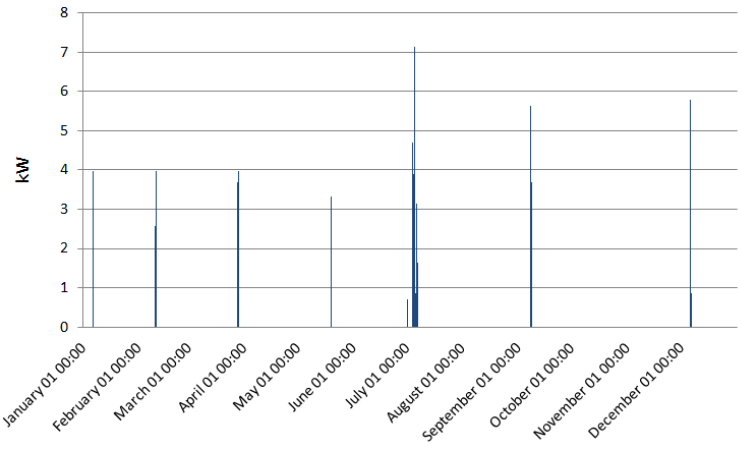

Figure 7.6: Unmet Load, Micro Grid - Case II

Excess electricity is lower in Case II than in Case I, only 8.94 %, and, as can be seen in

Figure 7.7, not as affected by seasonal variations as the first case.

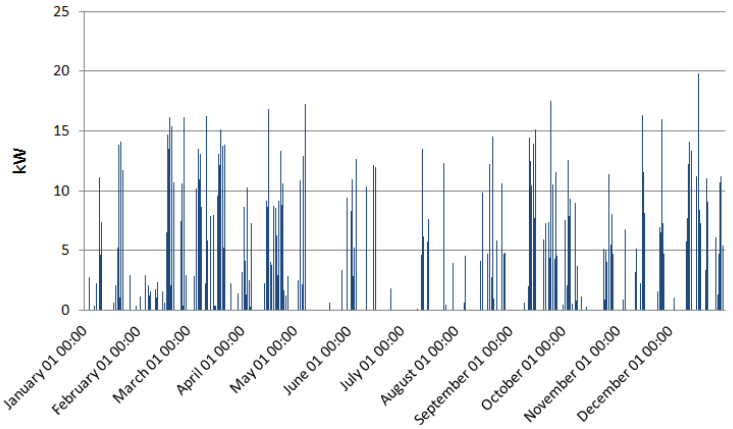

Figure 7.7: Excess Electricity, Micro Grid - Case II

7.2.2 Component Details

In Case II the capacity factor of the PV array is 14.3 & (4.3 kW mean electrical output). Hours of operation is naturally the same as in Case I. The mean output of the generator is 7.44 kW, 99 % of maximum output in Case II, and the electrical efficiency (11 %) confirms that the generator is operated at maximum load most of the time. The generator is operated 1 005 hours of the year and 21.3 tons of biomass is consumed per year. The autonomy of the battery bank is two days. Expected life is lower than in Case I, 9.16 years, but still high. Minimum electrical output of the inverter is 0 kW also in this case, which suggests that there are times where no load is covered since there is no electricity production on the AC-bus. In **Table 7.7** the most important component details are listed.

State of charge frequency for Case II is shown in **Figure 7.8**. Low state of charge is not frequent.

7.2.3 System Cost

The total NPC of the system in Case II is US$ 148 125 and levlized COE is US$ 0.263 /kWh. More details on cost of the system is found in **Table 7.8**

Table 7.7: Component Details, Micro Grid - Case II

PV Array		
Mean Electrical Output	$[kW]$	4.3
	$[kWh/day]$	102
Hours of Operation	$[h]$	4 442
Capacity Factor	$[\%]$	14.3
Biomass Generator		
Mean Electrical Output	$[kW]$	7.44
Hours of Operation	$[h]$	1 005
Biomass feedstock consumption	$[tons/year]$	21.3
Mean electrical efficiency	$[\%]$	11
Battery Bank		
Annual Throughput	$[kWh/year]$	15 968
Battery Losses	$[kWh/year]$	2501
Autonomy	$[h]$	47.9
Expected Life	$[years]$	9.16
Inverter		
Mean Electrical Output	$[kW]$	4.27
Inverter Losses	$[kWh/year]$	764
Hours of Operation	$[h]$	8 745

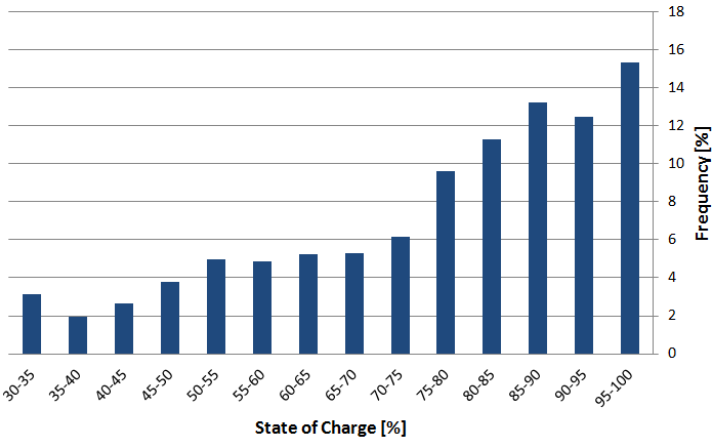

Figure 7.8: Battery State of Charge Frequency, Micro Grid Case II

7.3 Carpentry Workshop

For the carpentry workshop, the two cases ended up with the same operating strategy and only slightly different costs. As explained in the previous chapter, the simulation settings were exactly the same for diesel price and the generator, but the biomass generator costs

Table 7.8: System Cost, Micro Grid Case II

Capital	$[US\$]$	89 724
Replacement	$[US\$]$	75 180
O&M	$[US\$]$	3 373
Salvage	$[US\$]$	-19 868
Total NPC	$[US\$]$	**148 125**
Annualized Total Cost	$[US\$/year]$	9 865
Lev. COE	$[US\$/kWh]$	0.263

were different. Nevertheless, the operation strategies turned out equal, and are therefore presented together as one case.

7.3.1 System Design

The optimal solution from the simulations of the carpentry workshop in HOMER resulted to be replacing the current 24 kW generator with a smaller 15 kW generator, which together with the biomass generator is able to cover the full load at the carpentry workshop.

Table 7.9: System Design, Carpentry Workshop

Diesel Generator	$[kW]$	15
Biomass Generator	$[kW]$	15

7.3.2 Production and Operation

Table 7.10 shows that the biomass generator production is 85 % of the total power in the carpentry workshop. Excess electricity is very low, and the full load is covered.

Table 7.10: Production and Consumption, Carpentry Workshop

	$[kWh/year]$	$[\%]$
Demand	35 296	
Total Production	36 397	
Diesel Production	5 400	15
Biomass Production	30 997	85
Consumption	35 296	
Excess Electricity	1 101	3.03
Unmet load	0	0

Because the load is constant and the energy sources are controllable, the production throughout the year is more or less constant every day in the carpentry workshop. **Figure 7.9**

shows the typical daily production. The exceptions are the Easter and Christmas holidays and weekends when the carpentry is closed.

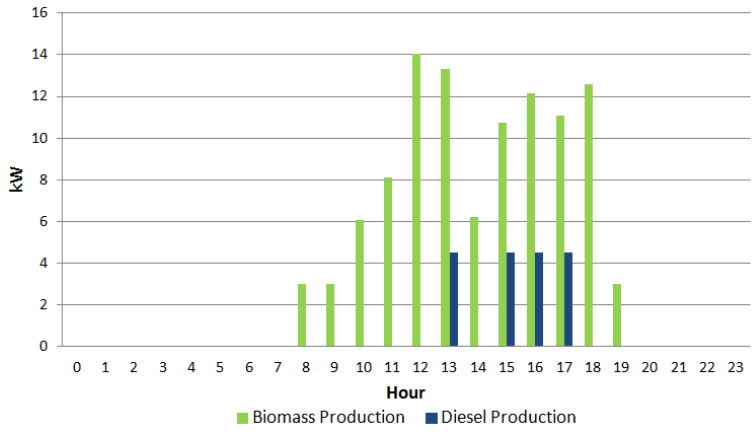

Figure 7.9: Typical Daily Production, Carpentry Workshop

Excess electricity is constant every day, and occurs at 06:00-8:00 and 17:00-18:00. This is when the load is lower than the minimum output that was set for the generators (20 % of maximum output for the biomass generator and 30 % for the diesel generator). The excess electricity is shown in **Figure 7.10**.

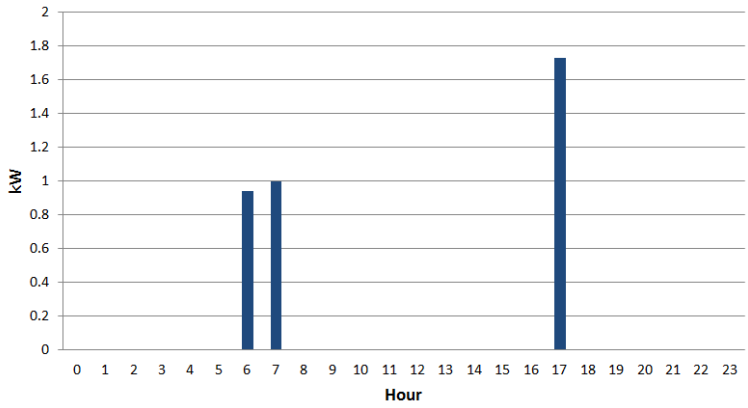

Figure 7.10: Excess Electricity, Carpentry Workshop

7.3.3 Component Details

Table 7.11 shows that the biomass feedstock consumption and hours of operation of the biomass generator are very high, its mean electrical output is 8.2 kW and mean efficiency of 10 %. Mean efficiency of the diesel generator is 20.5%, and mean electrical output is 4.5 kW, which is also the minimum output.

Table 7.11: Component Details, Carpentry Workshop

Diesel Generator		
Mean Electrical Output	$[kW]$	4.5
Hours of Operation	$[h]$	1 200
Diesel Consumption	$[L/year]$	2 682
Mean Electrical Efficiency	$[\%]$	20.5
Biomass Generator		
Mean Electrical Output	$[kW]$	8.61
Hours of Operation	$[h]$	3 600
Biomass feedstock consumption	$[tons/year]$	97.2
Mean electrical efficiency	$[\%]$	10

7.3.4 Cost

The total cost of the carpentry workshop is US$ 221 higher in Case II than in Case I. Fuel costs are significant, about 35 % of the total costs of both systems. More details on the system cost of the carpentry workshop are presented in **Table 7.12**.

Table 7.12: System Cost, Carpentry Workshop

		Case I	**Case II**
Capital	$[US\$]$	33 152	31 922
Replacement	$[US\$]$	68 958	76 368
O&M	$[US\$]$	7 027	7 027
Fuel	$[US\$]$	56 382	56 382
Salvage	$[US\$]$	-2 642	- 8 601
Total Cost	$[US\$]$	**162 878**	**163 099**
Total Annualized Cost	$[US\$/year]$	10 847	10 862
Lev. COE	$[US\$/kWh]$	0.307	0.308

7.4 Total System Data

In **Table 7.13**, the accumulated data for the micro grid and the carpentry workshop is presented for both cases. It can be mentioned that overall excess electricity and unmet

load are low in both cases. Total biomass feedstock consumption is highest in Case II. Although diesel consumption is the same in both cases, the diesel generator constitutes a larger percentage of production in Case II, because there is overall less electricity produced in this case.

Table 7.13: Total System Information

		Case I	**Case II**
Total Demand	$[kWh/year]$	72 891	72 891
Demand Micro Grid	$[kWh/year]$	37 595	37 595
Demand Carpentry Workshop	$[kWh/year]$	35 296	35 296
Total Production	$[kWh/year]$	83 318	81 131
Total PV Production	$[kWh/year]$	42 221	37 254
	$[\%]$	45.8	45.9
Total Biomass Production	$[kWh/year]$	35 707	38 477
	$[\%]$	42.9	47.4
Total Diesel Production	$[kWh/year]$	5 400	5 400
	$[\%]$	6.5	6.7
Total Consumption	$[kWh/year]$	72 682	72 733
Total Excess Electricity	$[kWh/year]$	7 428	5 093
	$[\%]$	8.9	6.3
Total Unmet Load	$[kWh/year]$	209	152
	$[\%]$	0.27	0.21
Biomass Generator			
Total Feedstock Consumption	$[tons/year]$	110	118.5
Total Hours of Operation	$[h]$	4327	4605
Total Cost	$[US\$]$	**325 104**	**311 224**
Total Annualized Cost	$[US\$/year]$	21 651	20 727
Total Lev. COE	$[US\$/kWh]$	0.298	0.285

7.5 Carpentry Workshop "Business as Usual"

Table 7.14 shows the main data from the simulation in HOMER of the carpentry workshop "Business as Usual" system. Total NPC is as high as US$ 418 159, of which fuel costs constitutes 89 %. Levelized COE is US$ 0.789/kWh.

Table 7.14: Carpentry Workshop "Business as Usual"

Demand	$[kWh/year]$	35 296
Diesel Production	$[kWh/year]$	40 813
Consumption	$[kWh/year]$	35 296
Excess Electricity	$[kWh/year]$	5 518
	$[\%]$	13.5
Unmet Load	$[kWh/year]$	0
	$[\%]$	0
Diesel Consumption	$[L/year]$	17 789
Fuel Cost	$[US\$]$	373 956
Total Cost	$[US\$]$	**418 159**
Annualized Cost	$[US\$/year]$	27 848
Lev. COE	$[US\$/kWh]$	0.789

Chapter 8

Discussion

8.1 Distribution System Design

The decisions made for the distribution system design were based on a desire to obtain the lowest possible power loss and voltage drop for the system at a low cost. The single-phase/three-wire (split-phase) solution was chosen because, in addition to being a common configuration in Nicaragua, reduces necessary size of the conductors used. In this project it is assumed that the future load profiles are the correct load profiles for scaling the system. It was considered at one point to scale the conductors for a peak load 25-30 % higher than the actual load. Similarly, it was considered to choose a single-phase/two-wire option, which inhabits the advantage of being possible to transform into a three-wire 120-0-120 system should the load increase. Both of these options were disregarded because if the case is that the conductors will need a 25-30 % higher capacity in the future, the scaling of the future load profiles should reflect this to begin with.

Power losses in the resulting distribution system constitute 2.4 % of the demand and, compared to inverter losses, are not very significant.

8.2 Production System Simulations

In the discussion of the production system simulations it is assumed that the estimations that were made prior to the simulations, such as the available biomass and the future load profiles, are correct and final. It would, for example, be possible to argue that Case I is more flexible in case the load should increase because not all of the available biomass was exploited in this case. Similarly, it could be argued that at a place like the Wawashang complex with a such big plantation, it will always be possible to find more sources of biomass if necessary, allowing the biomass generator to produce more electricity in both

cases. However, such arguments opens up a vast amount of uncertainties that, for the sake of being able to say something concrete about the simulation results, are omitted.

8.2.1 Micro Grid

Technical Aspects

Both simulation cases for the micro grid have low unmet load, relatively low excess electricity and a high life expectancy of the batteries. What separates the two cases the most, and what might be causing the biggest variations in the results, is the choice of charging strategy for the biomass generator. In Case I, where the biomass generator is connected to the AC bus, the load following strategy is applied for the generator. This means that the generator is never used to charge the batteries but only operated to cover the load. In Case II on the other hand, the cycle charging strategy is applied and as long as the batteries are not full, the generator is used at full power output each time it is called upon to cover the load. The consequence of this is that the generator in Case II is operated at higher efficiencies, produces more electricity per hour of operation and consumes more biomass. The results show that the generator in Case I in general is operated less frequent, suggesting that it is not considered as efficient to operate the generator at low output compared to increasing the PV array and battery bank. The generator in Case I only exploits 13.7 of the 22 tons biomass available compared to 21.2 in Case II.

With the load following strategy in Case I, the avoids extra losses due to transmission of electricity from AC to DC to charge the batteries and back to AC when the batteries are discharged. Total losses for the two systems (as percentage of total delivered electricity) are consequently almost equal. It also serves as an extra security; if the power converter for the PV-battery system is disconnected for any reason, the biomass generator can still supply the loads.

Although the generator is not available to charge the batteries, the capacity of the battery bank is higher in Case I. This suggest that the extra 4 kW capacity of the PV array is enough to keep the state of charge of the batteries at an acceptable level, also in the rainy season. Low state of charge is only slightly less frequent in Case II than in Case I. Low SOC may damage the batteries and lower their life expectancy. However, the results show that life expectancy is actually longer in Case I. Looking closer to the battery details reveals that the capacity of the battery bank in Case I is 11.5 % higher than in Case II, while annual throughput is only 5.3 % higher. This suggests fewer charge/discharge cycles of the battery bank, which will cause less damage to the batteries. In this case, fewer charge/discharge cycles have a stronger positive effect on the battery life expectancy than low state of charge has a negative effect. Autonomy is calculated based on number of hours the battery bank can supply the load at initial full state of charge, and is therefore naturally longest in Case I, 5.7 hours longer than in Case II. The overall operation of the batteries is better in Case I, and also provides longer security in case the PV array is disconnected due to errors or maintenance.

As mentioned, unmet load is low in both cases and this is due to the low capacity shortage

constraint (1 %) that was defined for the simulations. Still, the problem that was the focus of previous work on this project - lower reliability in the rainy season without the presence of a backup generator - is evident particularly in Case I. Biomass production is only 10 % of total production, compared to 17 % in Case II, which seems to be inadequate to balance the seasonal variations of solar power although the biomass was distributed throughout the year in order to complement irradiation. Also the distribution of excess electricity shows evidence of this. Excess electricity is highest in Case I, 13.5 % against 8.9 % in Case II, and in this case, excess electricity is high in the months with high irradiation and low in the months with low irradiation. Even though total electricity production is higher in Case I than in Case II, the system fails to deliver more electricity to the consumer. With values as low as the ones presented for unmet load and excess electricity in this project, this unbalance does not have great consequences, but it says something about how well the system is operated as a whole. It can be expected that if a higher capacity shortage constraint (3 or 5 %) was set, the unbalance would be very clear.

Overall, both cases present positive and negative results. Case II is, at first glance, the most reliable. However, should a reduction of 32 kWh/year unmet load in Case II have a greater significance than the higher autonomy of the batteries in Case I? The probability of the system having to rely solely on the batteries over a time period longer than 48 hours several times per year is not considered as very likely, so the answer in this project would be yes, and it is considered that Case II is the optimal system for the micro grid based on technical aspects.

Economical Aspects

Figure 8.1 shows the net present cost divided by component for the two cases, where light colors on the left represent Case I, and dark colors on the right represent Case II. This figure shows that what separates the two systems is the increased cost of the biomass generator in Case I due to the extra AC-DC inverter, and the larger PV array and battery bank necessary in due to lower production from the generator. In Case II the generator itself costs more than in Case I due to a higher percentage of the hours of operation available between the micro grid and the carpentry workshop. Comparing **Table 7.4** and **Table 7.8** in **Chapter 7**, it can be seen that the differences in total cost of the systems are US$ 14 101 in NPC for the whole project life of 20 years, US$ 939 in annualized costs and US$ 0.024 /kWh in levelized COE. These are relatively low and should alone play a small role when deciding which system is the optimal for Wawashang.

8.2.2 Carpentry Workshop

Technical aspects

As mentioned in **Chapter 7**, the optimal solution from the simulations of the carpentry workshop were almost identical for the two cases. While running the simulations, not surprisingly it became clear that the optimal solution would not matter what be to operate

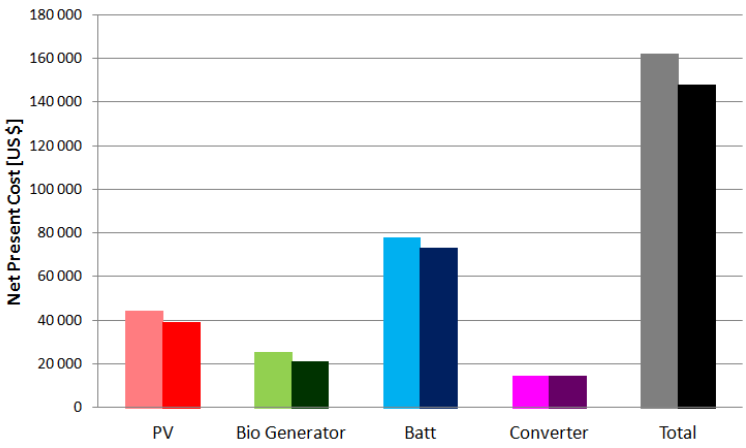

Figure 8.1: Net Present Cost by Component, Micro Grid Case I (left) and Case II (right)

the biomass generator as much as possible due to the high cost of diesel. Hence, the biomass generator is operated to the fullest in both cases, and the diesel generator covers the peaks in hours with a higher load than 15 kW. This can be seen in **Figure 7.9** in **Chapter 7**. Consequently, the diesel generator is never operated higher than 4.5 kW, which is its minimum possible output. It might be argued that the diesel generator should be replaced with an even smaller generator of 5-10 kW, but it is also a desire for Wawashang to have a decent sized generator present both as a security backup for the complex, and also to be able to supply most of the load in the carpentry should the biomass generator be out of order.

Economical aspects

The two cases for the carpentry workshop are similar also in cost, with only US$ 221 separating the two. Case I is the least expensive, for the same reason that the generator is most expensive for this case in the micro grid. Although the hours of operation per year of the biomass generator is the same in both cases, the percentage of total hours of operation per year is less in Case I.

8.2.3 Combining the Two Systems

When looking at the micro grid and the carpentry workshop together as one system, both cases present a well functioning system with high reliability and acceptable cost. Unmet load and excess electricity is slightly less in Case II but low in both cases. Total cost is lowest in Case II, but the difference is smaller than for the micro grid cases alone. Levelized COE for the whole system is US$ 0.298 in Case I and 0.285 in Case II.

Since the systems were simulated completely separate from each other, it might be interesting to investigate whether some of the unmet load in the micro grid could have been covered by the excess electricity from the carpentry workshop or if it could have been used to charge the batteries in Case II. Analyzing the hourly data for each case reveals that there in fact are some hours in each case where the unmet load could have been reduced or completely covered by the excess electricity from the carpentry workshop. **Figure 8.2** shows the hours in each case where there is excess electricity in the carpentry workshop at the same time as there is unmet load in the micro grid. As can be seen, unmet load is considerably higher than the excess electricity for most of the relevant hours, and the number of hours that coincide are few compared to the number of hours that suffer from either unmet load or excess electricity (12 in Case I and 10 in Case II).

At the same time, it can be seen in **Figure 8.3** that the batteries in both cases of the micro grid are discharging in many of the hours when there are excess electricity in the carpentry workshop. The discharge, and consequently the load that must be covered, is still considerably higher than the excess electricity, but if the two systems were combined, this electricity could have been used instead of going to waste.

Also as with the two systems combined, Case II presents the lowest excess electricity, unmet load and total cost, and this system is evaluated to be the optimal solution for the Wawashang Complex.

Carpentry Workshop, "Business as Usual"

The subcase, carpentry workshop "Business as Usual", shows that if a new micro grid is not implemented, and nothing is done with the currently high diesel consumption of the carpentry workshop, the result will be even more expensive over the next 20 years than it would be to invest in a PV-battery system and a biomass generator. Total cost difference is US$ 93 055 between the carpentry workshop "Business as Usual" and the most expensive case from the simulations (Case I), including both the carpentry and the micro grid.

8.2.4 Comparison to Previous Work

Compared to previous work on the Wawashang-project, the demand is more than halved. Additionally, the carpentry workshop, which constitutes half of the future demand and 75-80 % of the load in peak hours, has been taken out of the equation when it comes to scaling the PV-battery system. It was still considered as reasonable to assume that the optimal mix of energy sources would be the same as in [24]. This because in [24], the results show that the main advantage of including a biomass generator in the system is that it reduces the impact seasonal variations in PV production have on reliability of the system while reducing the need for fossil fuels. This is valid regardless of the size of the load what size the load is.

Compared to the results in [24], the system is more reliable, and has a lower percentage of excess electricity, as can be seen in **Table 8.1**. Levelized COE is higher in this project,

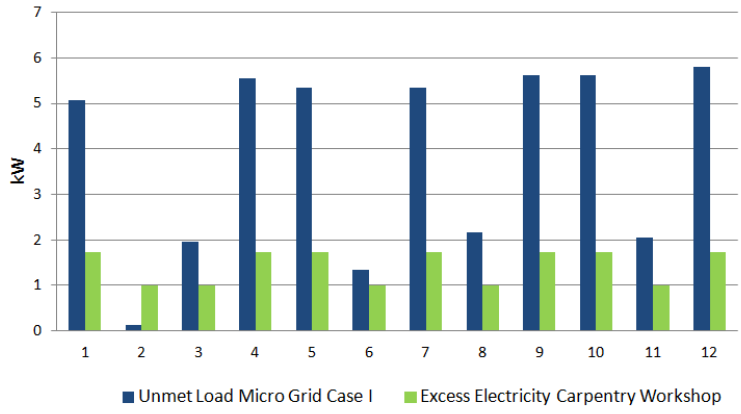

(a) Case I

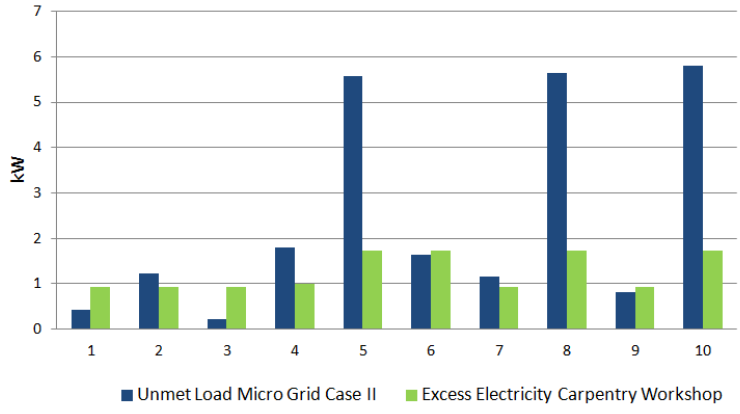

(b) Case II

Figure 8.2: Unmet Load in Micro Grid and Excess Electricity in Carpentry Workshop

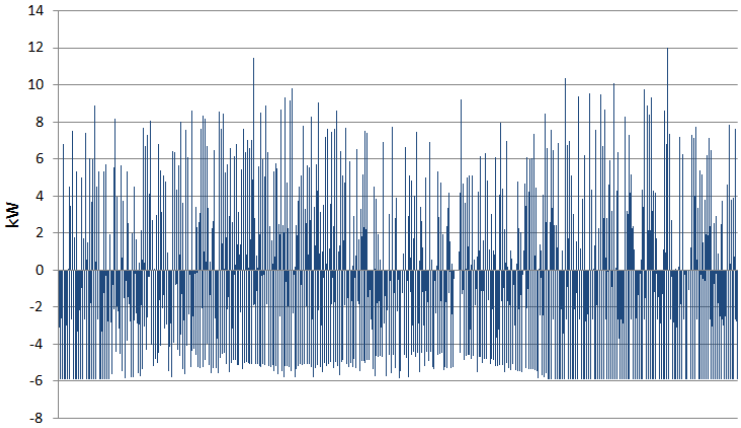

(a) Case I

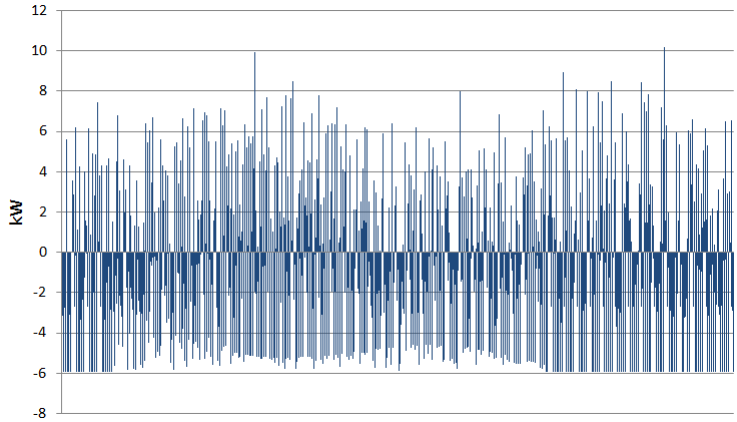

(b) Case II

Figure 8.3: Battery Input in Micro Grid in Hours with Excess Electricity in Carpentry Workshop

which is not surprising because the diesel fuel adds a cost that didn't exist in the system from [24]. However, in the optimal result from [24], 1.28 kWh is produced for every kWh that is consumed while in the new system this ratio is only 1.14 for Case I and 1.12 for Case II. Although a bit more expensive, the results from this project presents a system with overall higher reliability and higher efficiency.

Table 8.1: Comparison to Previous Results

		New System		
		Case I	**Case II**	**System from [24]**
Total Demand	$[kWh/year]$	72 891	72 891	158 406
Total Production	$[kWh/year]$	83 318	81 131	201 355
Unmet Load	$[\%]$	0.27	0.21	0.8
Excess Electricity	$[\%]$	8.9	6.3	14.9
Lev. COE	$[US\$/kWh]$	0.289	0.285	0.274

Chapter 9

Conclusion

In this thesis, an evaluation of a stand-alone hybrid micro grid for the Wawashang Complex in rural Nicaragua has been presented. A solution for a new electricity supply and distribution system for the complex has been proposed with a focus on optimal configuration of the system. Scaling of the distribution system and simulations of the production system have been made based on expected future demand with a 5 year time horizon. The future load profiles have been scaled based on information obtained during a field trip to Wawashang in April 2014 and with help from engineers in blueEnergy who works in the area and are familiar to the area. The demand to be covered has been divided into two systems; the micro grid, which denotes all buildings excluding the carpentry workshop and is the system for which the distribution system is designed, and the carpentry workshop which is isolated from the micro grid and supplied directly from a biomass based generator and a diesel generator. A single-phase/three-wire (split-phase) solution for the distribution system configuration have been chosen, presenting the advantage of considerably smaller conductor size requirements than single-phase/two-wire systems for the same voltage drop and power loss. The required conductor size for a maximum 6 % voltage drop is 2 AWG (33.6 mm^2) and the conductor type that has been chosen is a copper THHN/THWN wire. The total power loss of the distribution system is 896 kWh/year, or 2.4 % of the demand.

The production system that has been evaluated consists of a PV array and a battery bank for the micro grid and a diesel generator for the carpentry workshop, in addition to a biomass based generator available for both systems according to a defined schedule. The simulation software HOMER has been used to run simulations for the two systems simultaneously, with the intention of obtaining optimal operation of the biomass generator. Two cases have been evaluated. In Case I the high frequency AC power output from the biomass generator is rectified to DC power and then connected to the single-phase AC bus of the micro grid through a DC-AC converter and similarly to the three-phase AC loads of the carpentry workshop. In Case II the output from the biomass generator is connected to

the DC bus of the micro grid after rectification. The simulation results have shown that the optimal solution in both cases is to operate the biomass generator as much as possible in the carpentry workshop with the diesel generator available as peak power. In Case I, the biomass generator is operated with a load following strategy and is not used to charge the batteries, while in Case II a cycle charging strategy is applied resulting in a higher exploitation of the available biomass resource in the latter. Both cases present advantages and disadvantages and are similar in reliability and cost. The main argument for choosing Case I would have been that the system would allow the biomass generator to cover the loads of the micro grid in a situation where the DC-AC inverter for the PV-battery system is out of operation due to failure or maintenance. However, although differences in economical aspects have been considered as too small to play a big role in choosing the optimal system, Case II has been evaluated as the optimal solution for the Wawashang Complex, as is overall the least expensive, most reliable and least unbalanced system when it comes to seasonal variations. The system consists of a 9 kW converter, a 30 kWp PV array, producing a total of 37 254 kWh/year and a battery bank with a nominal capacity of 294 kWh (for the micro grid), a 15 kW biomass generator producing a total of 38 477 kWh/year divided between the micro grid (19.4 %) and the carpentry workshop (80.6 %) and a 15 kW diesel generator producing 5 400 kWh/year. Total excess electricity is 6.3 % and unmet load is 0.21 %. Total NPC is US$ 311 224 and levelized COE is US$ 0.285/kWh.

For further work, the distribution system should be further investigated, obtaining system cost information valid for Nicaragua and a more thorough design of the system including poles and service drops. For optimal balancing of the split-phase system, the location of the loads should be mapped in greater detail, together with an assessment of where the increase in demand most likely will take place. The possible grid connection for the Wawashang Complex should be confirmed or disproved, and may open up for the option of evaluating a grid-connected system in the future. Regarding the use of the biomass resource, a solution for storing the biomass should be suggested. Hopefully, a close relationship and cooperation between IUG and FADCANIC and also blueEnergy will continue. Improving the electricity supply for the Wawashang Complex is essential for school and agricultural center to be able to continue growing and executing the important and inspirational work they do for the community of the South Atlantic Region in Nicaragua.

Bibliography

[1] Christian E Casillas and Daniel M Kammen. The delivery of low-cost, low-carbon rural energy services. *Energy Policy*, 2011.

[2] InternationalEnergyAgency. Technology Roadmap: Bioenergy for Heat and Power. 2012.

[3] Swiss Agency for Development and Cooperation. Small hydroelectric power plants in nicaragua, 2013.

[4] WorldBank. Nicaragua - offgrid rural electrification for development report. 2002.

[5] Christian E Casillas and Daniel M Kammen. The energy-poverty-climate nexus. *Renewable energy*, 2010.

[6] Gregoire Lena. Rural electrification with pv hybrid systems. Technical report, InternationEnergyAgency, 2013.

[7] InternationalEnergyAgency. Bioenergy - a sustainable and reliable energy source. 2009.

[8] Khalid Malik. Human development report 2013. the rise of the south: Human progress in a diverse world. 2013.

[9] Central Intelligence Agency. The world factbook, 2013.

[10] Vidiani, maps of all countries in one place, administrative and road maps, physical and topographical maps, gps maps and other maps of the world, 2014.

[11] Vianica. About Nicaragua: Climate. http://vianica.com/nicaragua, 2013.

[12] Encyclopaedia Britannica Online. Nicaragua, 2013.

[13] European Union Election Observation Mission. Nicaragua final report: General elections and parlacen elections 2011, 2011.

[14] FADCANIC. Fadcanic, fundacin para la autonoma y el desarollo de la costa atlntica de nicaragua. http://www.fadcanic.org.ni/, 2014.

[15] Trading Economics. Nicaragua: Access to electricity. http://www.tradingeconomics.com/nicaragua/access-to-electricity-percent-of-population-wb-data.html, 2013.

[16] Rebublica de Nicaragua Ministerio de Energia y Minuas. Plan incicativo de expansion de la generacion electrica 2013-2017. 2013.

[17] Clean energy info portal - reegle. http://www.reegle.info/countries/nicaragua-energy-profile/NI, 2014.

[18] Claire McGuigan and Christian Aid. The impact of world bank and imf conditionality: An investigation into electricity privatisation in nicaragua. *Christian Aid, July*, 2007.

[19] Randall S Wood. The nicaraguan energy sector: Characteristics and policy recommendations. 2005.

[20] Ingenirer uten Grenser. www.iug.no, 2014.

[21] blueenergy. http://www.blueenergygroup.org/, 2013.

[22] Linn Solheim. Scaling an optimized pv-cluster as part of a microgrid in wawashang, nicaragua. master's thesis, Institute of Electric Power Engineering, NTNU, 2013.

[23] Marco Boninella. Off-grid energy system for wawashang, east nicaragua: analysis of the energy potential and design of a micro hydropower installation. master's thesis, Institute of Electric Power Engineering, NTNU, 2013.

[24] Marte Wiig Loetveit. Introducing biomass as part of a pv micro grid in the village of wawashang, nicaragua. specialization project, Institute of Electric Power Engineering, NTNU, 2013.

[25] Marte Loetveit, Jon Are Suul, Elisabetta Tedeschi, and Marta Molinas. A study of biomass in a hybrid stand-alone micro-grid for the rural village of wawashang, nicaragua. In *Ecological Vehicles and Renewable Energies (EVER), 2014 Ninth International Conference on*. IEEE, 2014.

[26] NASA, POWER. Surface meteorology and solar energy. https://eosweb.larc.nasa.gov/sse/, 2013.

[27] A Borchgrevink. Evaluation of saihs support for fadcanics wawashang environmental and agroforestry educational centre. 2009.

[28] SImetric. Density of materials. http://www.simetric.co.uk, 2013.

[29] Gilles Charlier. Perfil de proyecto para national geographic. 2012.

[30] Instituto Nacional de Tecnologia Industrial. Densidad de maderas ordenadas por nombre comun. http://www.inti.gob.ar/maderaymuebles/pdf/, 2013.

[31] Tallas en madera Castor. La madera de caoba. http://www.castor.es/caoba.html, 2013.

[32] Biomass Energy Center. Typical calorific values of fuel. http://www.biomassenergycentre.org.uk, 2013.

[33] Typical calorific values. http://www.biofuelsb2b.com/, 2013.

[34] Rena Perez. *Feeding Pigs in the Tropic*. Food and Agriculture Organization of the United Nations, 2013.

[35] Pyromex. Waste to energy. http://www.sludgefacts.org/.

[36] Meteonorm. Measurement Stations. http://meteonorm.com/products/meteonorm/stations/, 2013.

[37] PVsyst SA. Pvsyst 6 help. http://files.pvsyst.com/help/.

[38] L Marandin, M Craig, C Casillas, and J Sumanik-Leary. Small-scale wind power in nicaragua: Market analysis 2012-2013. *Green Empowerment*, 2013.

[39] Allan R. Inversin. Mini-grid design manual. 2000.

[40] Thhn: Understanding the thhn wire. www.distributorwire.com, 2014.

[41] Ali Keyhani. *Smart Power Grid Renewable Energy Systems*. John Wiley and Sons Inc., 2011.

[42] Solar cell central, solar markets. http://solarcellcentral.com, 2014.

[43] National Renewable Energy Laboratory (NREL). Pv watts changing system parameters. http://rredc.nrel.gov/solar/calculators/pvwatts/version1/derate.cgi/, 2014.

[44] E Koutroulis and K Kalaitzakis. Novel battery charging regulation system for photovoltaic applications. In *Electric Power Applications, IEE Proceedings-*, volume 151. IET, 2004.

[45] Jerry Ventre Roger A. Messenger. *Photovoltaic Systems Engineering*. Taylor and Francis Group, 2010.

[46] Diego Silva Herran and Toshihiko Nakata. Optimization of decentralized energy systems using biomass resources for rural electrification in developing countries. In *Proceedings of the 32nd IAAE international conference, San Francisco*, volume 23, 2010.

[47] SK Singal, RP Singh, et al. Rural electrification of a remote island by renewable energy sources. *Renewable Energy*, 32, 2007.

[48] Biomass gasification for decentralized power generation: The indian perspective. *Renewable and Sustainable Energy Reviews*, 14, 2010.

[49] Biogas/photovoltaic hybrid power system for decentralized energy supply of rural areas. *Energy Policy*, 38, 2010.

[50] GreenTurbineBV. Green turbine, the worlds smallest micro steam turbine. 2013.

[51] Magda Post and GreenTurbine. Private Communication, 2013.

[52] Marta Molinas. The role of power electronics in distributed energy systems. In *The 5th AIST Symposium on Distributed Energy Systems, Tokyo, Japan*, volume 9, 2008.

[53] Richard Perez. Off-grid inverter efficiency. www.homepower.com, 2006.

[54] JF Manwell, A Rogers, G Hayman, CT Avelar, JG McGowan, U Abdulwahid, and K Wu. *Hybrid2: A Hybrid System Simulation Model: Theory Manual*. National Renewable Energy Laboratory, 1998.

[55] Sunny island 4548-us - the efficient offgrid manager. www.sma-america.com.

[56] Homer software. http://homerenergy.com/software.html, 2013.

[57] Ecami. http://ecami.com.ni/, 2014.

[58] Ecami. Private Communication, 2014.

[59] ReneSola. http://www.renesola.com/, 2014.

[60] SolarBuzz. Inverter prices. http://www.solarbuzz.com/facts-and-figures/retail-price-environment/inverter-prices, 2014.

[61] Hybrid systems for decentralized power generation in bangladesh. *Energy for Sustainable Development*.

[62] World Bank. Diesel price, 2014.

[63] WorldBank. Real interest rate, 2013.

Appendix A: Article Presented at the EVER Conference 2014

Title: ”A Study of Biomass in a Hybrid Stand-Alone Micro-Grid for the Rural Village of Wawashang, Nicaragua”

2014 Ninth International Conference on Ecological Vehicles and Renewable Energies (EVER)

A Study of Biomass in a Hybrid Stand-Alone Micro-Grid for the Rural Village of Wawashang, Nicaragua

Marte Løtveit[1] Jon Are Suul[1,2,3] Elisabetta Tedeschi[1,2,3] Marta Molinas[1,3]

[1]Norwegian Univ. of Science and Technology
O. S. Bragstads Plass 2E
7491 Trondheim
martewii@stud.ntnu.no Jon.A.Suul@sintef.no

[2]SINTEF Energy Research
Sem Sælands vei 11
7465 Trondheim, Norway
tedeschi@ieee.org

[3]ren-PEACE
Jakob Kjeviks vei 6D
7020 Trondheim, Norway
marta.molinas@ntnu.no

***Abstract*— Stand-alone MicroGrids based on renewable energy sources have emerged as a suitable way of ensuring reliable energy supply in rural areas without access to electricity grids. Planning of such stand-alone grids should ensure systems that provide electricity with high security, reliability and an acceptable impact on the environment, all at a minimum cost. Transition away from traditional use of biomass for cooking and heating in developing countries, to more efficient, modern uses with less negative impacts on the local environment, is also an important measure on the way towards sustainable use of energy. This paper presents technical and economical investigations of the potential for using biomass for electricity generation in a micro-grid for the village of Wawashang, Nicaragua. The simulation tool HOMER is used to evaluate a reference case based on only photovoltaic (PV) power generation with battery energy storage compared to a case including a biomass steam turbine based on local biomass resources. The results show how the use of biomass in combination with PV reduces the impacts of seasonal variations and results in a more reliable and cost-effective system.**

Keywords*— *MicroGrids, hybrid system, rural electrification, solid biomass, micro steam turbine

I. INTRODUCTION

About 70 % of the world's extremely poor people live in rural areas [1]. For improving their situation it is essential to improve the access to goods, services and information, all of which are linked with a reliable access to energy [2]. For many rural areas, construction of transmission lines needed for connection to large scale power grids is not an economically viable solution for providing electricity supply. In Nicaragua, where the rural areas along the east coast are situated at long distances from the existing main grid, stand-alone MicroGrids therefore stands out as the preferred solution [3]. Due to low initial costs, accessibility and simple operation, diesel generators have been the technology of choice for initial electrification of such rural areas. However, increasing fuel costs, together with additional cost of transportation into isolated areas, makes diesel generators too expensive for providing reliable electricity supply in the long run. Considering the need for sustainable long term energy supply, electric power should also be provided on basis of local renewable sources in ways that are cost-effective, with the goal to mitigate rural poverty while transitioning away from fossil fuel dependence [4].

On a world-wide basis, biomass is the largest single renewable energy source today, accounting for 10 % of the total primary energy supply [5]. In developing countries, most of the biomass is consumed through inefficient traditional ways for cooking and heating, with negative local impacts such as pollution and deforestation. Although the numbers are steadily increasing, modern use of bioenergy is small in comparison. Only about 1.5 % of the global electricity generation in 2010 came from bioenergy. Compared to other easily available renewable sources like photovoltaic (PV) or wind power, a significant advantage of biomass is that the available energy can be stored in solid, liquid or gaseous form, allowing for easy regulation and dispatchability [6]. Thus, it is expected that sustainably produced bioenergy will play an increasingly important role in achieving significant reductions in greenhouse gas emissions from the energy sector [5]. This also implies that off-grid electricity supply from biomass can become a key measure to improve electricity access in developing countries and achieving the goals of universal access to clean energy by 2030 [5].

Today, electricity from biomass is mainly produced through combustion, with power generation through steam turbines, in large scale thermal power plants. The overall efficiency of such plants is dependent on the power range, and the potential for utilizing surplus heat. Efficiencies of electricity generation through steam turbines with power outputs between 10 to 50 MW are usually in the range from 18 to 33 % [5]. However, the potential for small scale electricity generation has led to the recent development of integrated steam turbine units with power output as low as 1.2 kW [7]. With a claimed electrical

978-1-4799-3787-5/14/$31.00 ©2014 IEEE

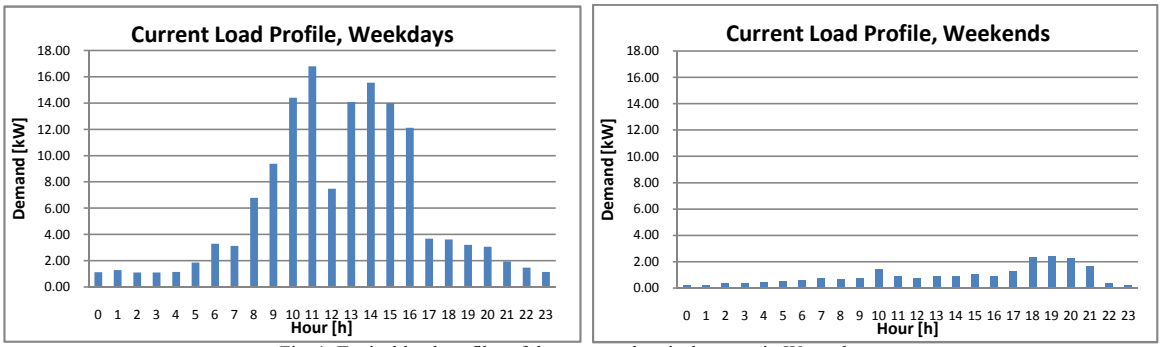

Fig. 1. Typical load profiles of the current electrical system in Wawashang

efficiency of 14 %, silent operation, competitive prices and applicability for a variety of purposes, such products are expected to be very suitable for small-scale electricity generation based on biomass [7], [8]. Combined with an appropriate boiler, such units can be easily used for electricity generation from solid biomass. However, since such products have not previously been available, there is a lack of reference studies of small-scale applications of solid biomass for electricity production with steam turbines. Instead, most previous studies on the use of biomass as a power source in MicroGrids, have considered gasification of solid biomass or biodigestion of wet biomass to make biogas for running gas turbines or combustion engines [9]-[12].

In this article a MicroGrid for the village of Wawashang, Nicaragua, is evaluated based on expected electricity demand in 2032. The simulation tool HOMER is used to find a technically and economically optimal system that ensures a reliable energy supply to the village. Two cases are evaluated; a reference case with a PV-cluster and battery energy storage, and a second case that in addition includes a small-scale steam turbine based on solid biomass combustion from local resources. In the following, the investigated site, its energy need, the available energy resources and the required technology are described. On this basis, results from simulations of the system energy balance are presented, and technical and economical evaluations of the results are discussed.

II. Study Area and Input Data

Wawashang is a village located in the rural areas of the South Atlantic Autonomous Region (RAAS) of Nicaragua, which is characterized by limited infrastructure and high poverty rates. The Center of Agroforestry Development in Wawashang is a complex constructed with support from the Foundation for the Autonomy and Development of the Atlantic Coast of Nicaragua (FADCANIC). FADCANIC is a non-profit, non-partisan, civil society organization based in the Autonomous Regions of Nicaragua [13]. The organization works for improving the quality of life of the peoples of the Caribbean Coast. It ensures funding for innovative projects, and the Wawashang Complex is one of their greatest achievements, consisting of a boarding school with a large plantation and a carpentry workshop, and an Agricultural Center [13]. There is no road access to the Wawashang village, and the main transport route is by boat, but the Wawashang Complex is one of the few villages in the area with access to electricity.

A. The Current Electrical System in Wawashang

The current energy system of the Wawashang complex consists of rooftop PV-panels, batteries for energy storage and a set of diesel and gasoline generators [14]-[16]. The current system configuration is inefficient with respect to the location of the PV-panels and maintenance of the PV-modules and batteries, and there is no distribution system enabling electricity to be shared between the different buildings. Some of the existing PV panels are also partially shaded by trees. All transport of gasoline to the complex is made by boat, and is therefore inconvenient and expensive. There is a need for enhancing or completely renewing the current electrical system to improve the performance and to cover an expected increase in demand due to expansion of the complex.

B. Load Profiles

Estimates of load profiles representing the current demand in the Wawashang complex were established through measurements at the different buildings of the complex during a field trip in March 2013 [14], [15]. The measurements gave per-minute-values, and a maximization approach was used to derive the hourly profiles shown in Fig. 1, by using the peak power for each hour. Although this resulted in an over-dimensioned demand, it has been considered important to account for the peak loads of the various installations. At the time of the field trip it was, however, not possible to measure the electricity consumption of all the buildings, and only a limited time period was available for the measurements. Thus, so some uncertainty must be accepted in the load data, and the results shown in Fig. 1 are considered to represent the current system with a reasonable accuracy. Expected load profiles for 2032 have also been estimated

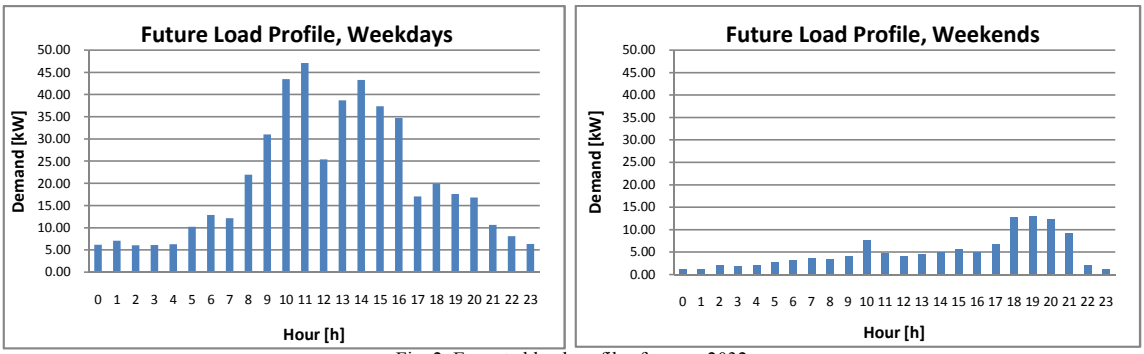

Fig. 2. Expected load profiles for year 2032

through evaluation of the planned expansion of the complex and discussions with representatives from FADCANIC and blueEnergy [14], [15], [17]. The most electricity-consuming activity at the complex is the carpentry workshop, using high power equipment during the weekdays. The rest of the buildings need electricity mainly for lighting, fans and charging of computers and cell-phones. It was determined that the future demand for the carpentry workshop should be calculated using a multiplication factor of 2 compared to the current load profiles, while a multiplication factor of 5 has been assumed for the rest of the buildings. These multiplication factors were chosen while keeping in mind the maximization approach used to determine the current load profiles. Additionally, a few new buildings are planned for the expansion of the complex. The resulting total estimated future load profiles are displayed in Fig. 2, showing that the peak demand is expected to increase with about 30 kW, from about 17 kW today and up to about 47 kW in 2032.

In previous studies of the Wawashang complex, a new MicroGrid based on a PV-cluster and batteries has been evaluated with or without a diesel backup [14]. The conclusion of this work was that a system without backup generators was the most relevant solution for the Wawashang complex, even though the reliability was significantly better with backup. This conclusion was partly based on the consideration that use of fossil fuels should be avoided and that in the future it might be possible to exploit the biomass potential of the complex. This article will compare the option of increasing the rating of the PV-cluster and battery storage to get a more reliable system with the possibility of integrating a biomass generator in the system, making it a fully renewable hybrid MicroGrid. Most of the assumptions and parameters used in [14] will be used for the scaling of the PV-system in the simulations, whereof the most important parameters are presented in Table 1.

TABLE 1 INPUT PARAMETERS FOR SIMULATIONS IN HOMER

Batteries	Type of Batteries	Trojan L16P
	Capital cost [14]	284 $
	Battery voltage	6 V
	String voltage	48 V
	Nominal Capacity	360 Ah
	Minimum state of charge	30 %
	Minimum Battery Lifetime	7 years
PV Modules	Size	0.215 kW
	Capital cost [14]	520 $
	Lifetime	20 years
	Tilt	13°
	Azimuth	0°
	Albedo	25 %
Converter	Capital cost	711 $/kW
	Lifetime [17]	10 years
	Inverter efficiency [17]	95 %
	Rectifier efficiency [17]	85 %
Generator	Size	15 kW
	Capital cost (all components)	30000 $
	Lifetime (operating hours)	15000 h
	Efficiency [8]	14 %
Economics	Annual Real Interest Rate [19]	2.9 %
	Project lifetime	20 years
Constraints	Maximum Capacity Shortage	5 % or 1.5 %

TABLE 2 AVERAGE HORIZONTAL GLOBAL IRRADIATION AND TEMPERATURE IN WAWASHANG

Month	**Irradiation** [kWh/m^2/mth.]	**Temperature** [°C]
January	133.0	24.8
February	138.9	25.1
March	169.6	25.8
April	1734.3	26.7
May	156.9	26.6
June	121.2	26.4
July	115.0	26.2
August	124.6	26.3
September	131.4	26.2
October	128.6	26.0
November	118.5	25.7
December	121.8	25.2
Year	1633.8	25.9

C. Solar Potential

In Table 2, the monthly averaged horizontal global irradiation for Wawashang is presented, together with the monthly average temperatures. This meteorological data is imported from the NASA-SSE database by entering the latitude 12.65° and longitude −83.75° [21].

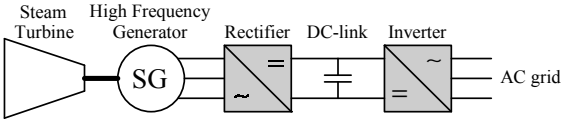

Fig. 3. Typical power electronics coupling for micro turbine system

TABLE 3 TOTAL SOLID BIOMASS POTENTIAL

Source	Amount [kg/day]	Thermal Energy Potential [kWh_{th}/day]
Sawdust	176.4	397
Wood pieces	13.0	45
Coconut shells	13.2	62
Bagasse	96	241
Year	298.6	745

D. Biomass Potential

To evaluate the possibility of utilizing electricity generated from biomass in the MicroGrid, both the potential of manure for biogas production and the potential for utilizing solid biomass have been investigated. It was found that the potential of solid biomass is the highest. Estimation of the thermal energy potential of available solid biomass in Wawashang was based on numbers from [22] and information obtained during the field trip in March 2013 [15]. The results are presented in Table 3.

E. Technology: Green Turbine

The 15 kW steam turbine unit under development by Green Turbine is a small turbo generator that converts heat into electricity [7]. Combined with an appropriate burner, the turbine is compatible with a variation of fuels such as biogas, fossil fuels and solid biomass. The design speed is 26.000 rpm and the power output of the generator integrated with the turbine is 3 phase AC at 1000 Hz that is rectified to DC [7]. Thus, depending on the type of power electronics interface used together with the turbine unit, the electrical power can be delivered as DC or AC, in the latter case with single-phase or three-phase at specified voltage and frequency. Fig. 3 shows a typical generic configuration for connecting a micro turbine to an AC power system [23].

F. MicroGrid configuration

Fig. 4 shows a general outline of the system planned for Wawashang, including the steam turbine generator. A DC-DC boost converter with a maximum power point tracking (MPPT) algorithm is used to boost the voltage from the PV array to the voltage of the common DC-bus for the PV converter and the battery storage [24]. A bidirectional DC-DC converter is used to control the charge and discharge of the batteries. Finally, an inverter is used to integrate the DC system of the PV and battery with the AC system providing power to the loads. It is assumed that it should be possible to operate the biomass generator and supply the AC loads even if the DC-bus or inverter of

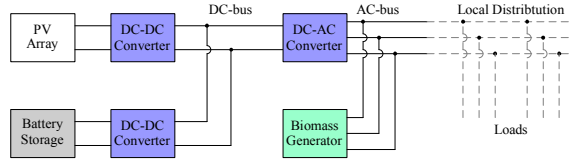

Fig. 4. General configuration of the MicroGrid

TABLE 4 BIOMASS DISTRIBUTION

Month	Biomass [kg/day]
January	100
February	80
March	100
April	0
May	100
June	450
July	700
August	700
September	120
October	200
November	600
December	400
Year	296

the PV and battery systems are out of operation. Thus, the biomass generator is connected to the AC bus of the system through a separate inverter according to the structure from Fig. 3.

III. SIMULATIONS

In the following sections, the two cases simulated in HOMER are further described.

A. Case I: PV + Battery

In the first case, the initial system from [14] based on a PV-cluster and a battery with a maximum capacity shortage of 5 % is used as a starting point. For the same system, an attempt of improving the reliability by reducing the maximum capacity shortage to 1.5 % is also presented.

B. Case II: PV + Battery + Biomass generator

In the second case, a biomass generator is added to the system, based on the available local resources presented in Table 3. The solid biomass is burnt in a boiler and used to run a 15 kW steam turbine when needed. The biomass generator can be operated to supply load directly, but can also be used to charge the batteries when this will improve the utilization and efficiency of the overall system. To ensure that the two energy sources complement each other the best way possible, the biomass resource is distributed to the months with lowest irradiation, as shown in Table 4.

IV. RESULTS

A. Case I: Initial System with PV and Battery

1) Initial System Design

Table 5 shows the system architecture for the initial system suggested by HOMER, with 666 PV modules and 640 batteries. The corresponding results for yearly

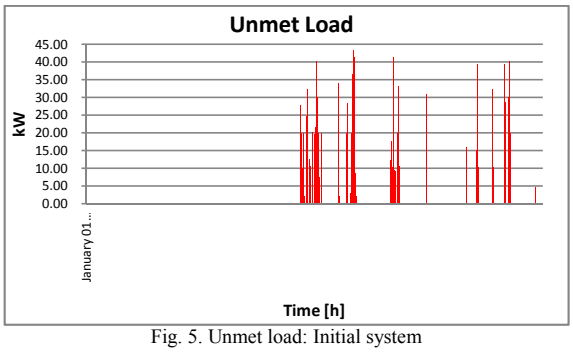

Fig. 5. Unmet load: Initial system

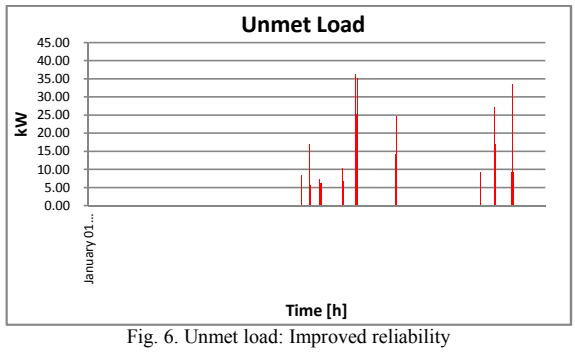

Fig. 6. Unmet load: Improved reliability

TABLE 5 SYSTEM ARCHITECTURE: INITIAL SYSTEM

PV modules	Number of Modules	666
	Global Array Power	143 kW
Batteries	Number of Batteries	640
	Total Capacity	1 382 kWh
DC-AC Converter	Rating	53 kW

TABLE 6 PRODUCTION AND CONSUMPTION: INITIAL SYSTEM

	[MWh/year]	%
Production	202.74	
Demand	158.4	
Consumption	151.83	
Excess Electricity	32.37	16
Unmet Load	6.6	4.2

production and consumption of the system are listed in Table 6. This case reveals a high amount of excess electricity of 32.37 MWh/year which is about 1/6 of the total yearly production. The amount of unmet load is 6.6 MWh/year and equals 4.2 %, which is as expected since the maximum capacity shortage is predefined at 5 %. The optimal case presented by HOMER is the cheapest solution within the technical constraints.

The unmet load of the system is shown in Fig. 5, and from this figure it is clear that the unmet load is concentrated in June-September, November and December. This is the rainy season in Nicaragua, and the solar irradiation is lower than the rest of the year. Comparing the maximum unmet load in Fig. 5 with the maximum power of the load profiles in Fig. 2, it can be seen that there are some hours and days where almost no load is covered. For a reliable system, this should not be acceptable.

2) Improved Reliability

The results from HOMER with a maximum capacity shortage of 1.5 % are listed in Table 7, showing how the number of PV modules has increased while the battery pack is smaller. This is due to the economical optimization of HOMER when the capacity shortage constraint is leading to a larger PV installation. Table 8 shows that the unmet load is reduced to only 1 %, and is still occurring only during the rainy season, as can be seen in Fig. 6. Due to the large PV array, excess electricity has increased

TABLE 7 SYSTEM ARCHITECTURE: INITIAL SYSTEM WITH IMPROVED RELIABILITY

PV modules	Number of Modules	861
	Global Array Power	185 kW
Batteries	Number of Batteries	560
	Total Capacity	1 209 kWh
DC-AC Converter	Rating	45 kW

TABLE 8 PRODUCTION AND CONSUMPTION: INITIAL SYSTEM WITH IMPROVED RELIABILITY

	[MWh/year]	%
Production	262.1	
Demand	158.4	
Consumption	156.75	
Excess Electricity	86.94	33.2
Unmet Load	1.66	1

TABLE 9 SYSTEM ARCHITECTURE: WITH BIOMASS GENERATOR

PV modules	Number of Modules	582
	Global Array Power	125 kW
Biomass Generator	Size	15 kW
	Mean Electrical Efficiency	14.7 %
Batteries	Number of Batteries	480
	Total Capacity	1 036 kWh
DC-AC Converter	Rating	50 kW

TABLE 10 PRODUCTION AND CONSUMPTION: WITH BIOMASS GENERATOR

	[MWh/year]	%
Production PV	177.09	
Production Generator	25.55	
Total Production	202.64	
Demand	158.4	
Consumption	156.5	
Excess Electricity	29.93	14.8
Unmet Load	1.32	0.8

significantly, to 86.94 MWh/year, which is 1/3 of the produced electricity, and a highly undesirable amount of spillage. It is therefore clear that an alternative energy source that can supply power during the rainy season will significantly improve the possibilities for optimizing the system design.

B. Case II: System with PV, Battery and Biomass

Table 9 shows the system architecture for the system with biomass generator. The amount of PV modules

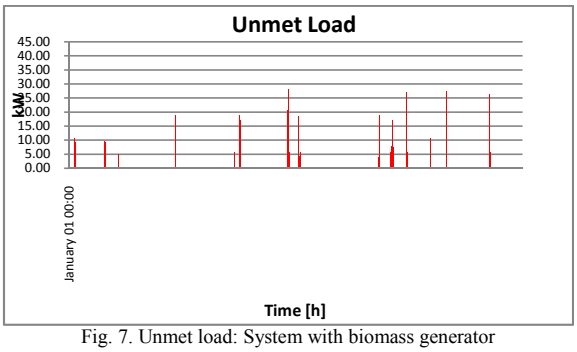

Fig. 7. Unmet load: System with biomass generator

needed is 582, and the number of batteries is 480. The size of the generator is 15 kW with average output efficiency of 14.7 %. As expected, the presence of the biomass generator has significantly reduced the overall size of the PV-battery system.

Table 10 shows that although the PV array is reduced with more than 80 modules compared to the initial system, the total electricity production is only slightly reduced. The biomass generator produces 25.55 MWh/year of the total 202.64 MWh/year. Excess electricity is reduced to 29.93 MWh/year and unmet load is as low as 0.8 %. The unmet load is now spread out throughout the year, as shown in Fig. 7, due to the complementary properties of the biomass resource and the solar resource.

V. Discussion and Comparison of Cases

The amount of excess energy and the distribution of unmet load in the initial optimized system design resulting from HOMER simulations implies that the PV panels are over-sized for the dry season with high irradiation, resulting in spillage, and under-sized for the rainy season, resulting in large share of unmet load. This is a problem when trying to scale a stand-alone system using only resources that are sensitive to daily and seasonal climatic variations. The daily variations can be solved by using energy storage like batteries, where excess electricity produced during the day can be stored and used after sundown. However, energy storage is not an economically viable option for seasonal variation. In order to make the PV-battery system reliable for the whole year without adding new renewable energy sources or conventional backup generators, the system must be dimensioned to cover the months with lowest irradiation, as shown when designing the system from Case I for improved reliability. This results in a high amount of excess electricity and an inefficient system. Additionally, the small amount of unmet load is still concentrated in the months with low irradiation, resulting in an actual unmet load higher than 1.5 % for these months, and 0 % during the dry season.

Table 11 Cost Summary: Initial System

Component	Capital [$]	Replacement [$]	O&M [$]	Salvage [$]	Total [$]
PV	345 860	0	0	0	345 860
Battery	181 760	136 567	0	0	318 327
Converter	37 683	28 313	19 896	0	85 893
System	560 304	164 880	19 896	0	**750 080**

Table 12 Cost Summary: Improved Reliability without Generator

Component	Capital [$]	Replacement [$]	O&M [$]	Salvage [$]	Total [$]
PV	447 442	0	0	0	447 442
Battery	159 040	215 030	0	-77 045	297 025
Converter	31 995	20 838	16 893	-12 042	57 684
System	638 477	235 868	16 893	-89 086	**802 151**

Table 13 Cost Summary: with Generator

Component	Capital [$]	Replacement [$]	O&M [$]	Salvage [$]	Total [$]
PV	302 326	0	0	0	302 326
Generator	30 000	41 799	0	-11 449	60 350
Battery	136 320	102 425	0	0	238 745
Converter	35 550	23 153	18 770	-13 380	64 093
System	504 196	167 377	18 770	-24 828	**665 514**

Adding a biomass generator and at the same time distributing the biomass resources to complement the solar irradiation, solves the problems with seasonal variations in production to a large extent. The overall size of the PV-battery system is reduced, as is the amount of excess electricity and unmet load. In case II, the unmet load is not only distributed over the whole year, the peak values are also lower than for the initial system and for the improved system without generator. However, since the burner of the biomass generator is flexible with respect to the type of fuel, additional biomass can most likely be gathered and stored locally to be used during the days with unmet load shown in Fig. 7. In that case, this system might be kept in operation without any unmet load by limited additional efforts from the local community. It can, however, be seen from Fig. 7 that the unmet load in some few hours is higher than the 15 kW rating of the biomass generator. To be able to cover this load, the biomass generator should therefore be used to charge the batteries and ensure a minimum state of charge before the hours of the day with the highest loads.

The results listed in Table 11, Table 12 and Table 13 show the lifetime cost summaries for all three system designs that have been evaluated. This shows that adding a biomass generator is a cost saving option compared to the system with only PV and batteries, with a difference of almost 85 000 $ between the initial system in case I and the system in case II. Compared to the system with improved reliability in case I, the cost difference is more than 130 000 $. This is to a large extent due to the assumption that the biomass resource is locally available at the complex at no cost. Having to pay for the biomass would increase the price of the system in case II

significantly. The negative cost of salvage present in Table 11, Table 12 and Table 13 is due to a lifetime slightly lower than 10 years for some of the components in these systems. As the lifetime of the project is set to 20 years, there is some payback of remaining value at the end of this period since not all of the components have reached their end of life.

VI. Conclusion

In this article, the potential for introducing electricity generation from solid biomass in a stand-alone MicroGrid for the rural village of Wawashang has been investigated. Two cases have been studied; one reference case based solely on PV and batteries, and an alternative case including a biomass generator with a micro steam turbine. Simulations in HOMER based on expected future demand in 2032 have shown that including the generator and distributing the available local biomass resource throughout the year in a manner that complements the solar irradiation decreases the size of the PV-battery system needed to ensure a reliable energy supply to the village. The lifetime cost of the MicroGrid, and thus the cost of a reliable electricity supply for the investigated village, can therefore be significantly reduced by the utilization of locally available solid biomass.

Acknowledgment

Engineers Without Borders, (IUG) Norway, FADCANIC and blueEnergy, Nicaragua are acknowledged for supporting the Master project of Marte Løtveit at the Norwegian University of Science and Technology and for providing information needed for this study.

References

[1] The World Bank ,"*World Development Report 2010: Development and Climate Change*," Washington DC., 2010

[2] C. E. Casillas, D. M. Kammen, "The energy-powerty-climate nexus," in *Science*, Vol. 330, No. 6008, 26 November 2010, pp. 1181-1182

[3] The World Bank, "Nicaragua – Offgrid Rural Electrification for Development Project," http://documents.worldbank.org/curated/en/2002/07/1976186/nicaragua-offgrid-rural-electrification-development-project-supplemental-credit

[4] C. E. Casillas, D. M. Kammen, "The delivery of low-cost, low-carbon rural energy services," in *Energy Policy*, vol. 39, no. 8, August 2011, pp. 4520-2528

[5] International Energy Agency, IEA, "*Technology Roadmap: Bioenergy for Heat and Power*," Paris, France, 2012

[6] A. Bauen, G. Berndes, M. Junginger, M. Londo, F. Vuille, "*Bioenergy – a Sustainable and Reliable Energy Source*," report prepared for IEA Bioenergy, June 2009

[7] GreenTurbine BV, The Netherlands, information available from http://www.greenturbine.com

[8] M. Post, GreenTrubine BV, Private communication with M, Løtveit, 2013

[9] D. S. Herran, T. Nakata, "Optimization of decentralized energy systems using biomass resources for rural electrification in developing countries," in *Proceedings of the 32nd IAAE International Conference – Energy, Economy, Environment: The Global View*, San Francisco, California, USA, 21-24 June 2009, 19 pp., available from http://www.usaee.org/usaee2009/submissions/OnlineProceedings/Silva-Nakata-Proceeding.pdf

[10] S. Singal, Varun, R. Singh, "Rural electrification of a remote island by renewable energy source," in *Renewable Energy*, Vo. 32, no. 15, December 2007, pp. 2492-2501

[11] B. Buragohain, P. Mahanta, V. S. Moholkar, "Biomass gasification for decentralized power generation: The Indian perspective," in *Renewable and Sustainable Energy Reviews*, vol. 14, no.1, January 2010, pp. 73-92

[12] M. B. Neto, P. Carvalho, J. Carioca. F. Canafistula, "Biogas/photovoltaic hybrid power system for decentralized energy supply of rural areas," in *Energy Policy*, vol. 38, no 8, August 2010, pp. 4497-4506

[13] FADCANIC, Fundación para la autonomía y el desarollo de la costa Atlántica de Nicaragua, (Foundation for the autonomy and development of the Atlantic coast of Nicaragua), http://www.fadcanic.org.ni

[14] L. Solheim, "*Scaling an optimized PV-cluster as part of a microgrid in Wawashang, Nicaragua*," Master Thesis, Norwegian University of Science and Technology, Trondheim, Norway, June 2013

[15] M. Boninella, "*Off-grid energy system for Wawashang, East Nicaragua: Analysis of the energy potential and design of a micro hydropower installation*," Master Thesis, Norwegian University of Science and Technology, Trondheim, Norway, June 2013

[16] M. Boninella, L. Solheim, M. Molinas, "Hybrid Micro Grid Feasibility study for the Wawashang Complex in Nicaragua," in *Proceedings of the 4th International Youth Conference on Energy*, IYCE 2013, Siokok., Hungary, 6-8 June 2013, 8 pp.

[17] blueEnergy, information available from: http://www.blueenergygroup.org/

[18] C. P. Cameron, A. C. Goodrich, "The Levelized Cost of Energy for Distributed PV: A Parametric Study," in *Conference Rectord of the 35th IEEE Photovoltaic Specialists Conference*, PVSC 2010, Honolulu, Hawaii, USA, 20-25 June 2010, pp. 529-534

[19] A. H. Mondal, M. Denich, "Hybrid Systems for decentralized power generation in Bangladesh," in *Energy for Sustainable Development*, vol. 14, no. 1, March 2010, pp. 48-55

[20] The World Bank, Real Interest Rate, available from: http://data.worldbank.org/indicator/FR.INR.RINR/countries/NI?display=graph

[21] NASA Atmospheric Science Data Center, "*Surface Meteorology and Solar Energy – A Renewable Energy Resource web site (releasae 6.0)*," available from: https://eosweb.larc.nasa.gov/sse/

[22] G. Charlier, "Perfil de proyecto para National Geographic," 2012

[23] M. Molinas, "The role of power electronics in distributed energy systems," in *Proceedings of the 5th AIST Symposium on Distributed Energy Systems*, Tokyo, Japan 9th of December 2008, 7 pp.

[24] A. Keyhani, "*Design of smart power grid renewable energy systems*," Hoboken, New Jersey, John Wiley & Sons, 2011

Appendix B: Current and Future Load Profiles

Current Load Profiles [kW]

	Micro Grid		Carpentry Workshop
Hour	**Weekdays**	**Weekends**	**Weekdays**
0	1.13	0.22	0
1	1.28	0.22	0
2	1.10	0.38	0
3	1.11	0.35	0
4	1.14	0.39	0
5	1.86	0.52	0
6	1.71	0.58	1.59
7	1.59	0.68	1.54
8	2.12	0.62	4.66
9	3.14	0.74	6.25
10	3.58	1.38	10.8
11	3.09	0.88	13.7
12	2.71	0.75	4.78
13	2.35	0.84	11.72
14	2.75	0.89	12.81
15	1.99	1.04	11.99
16	2.44	0.91	9.67
17	2.71	1.23	0.98
18	3.62	2.34	0
19	3.20	2.38	0
20	3.06	2.26	0
21	1.94	1.66	0
22	1.48	0.37	0
23	1.15	0.20	0

Future Load Profiles [kW]

	Micro Grid		Carpentry Workshop
Hour	**Weekdays**	**Weekends**	**Weekdays**
0	2.25	0.43	0
1	2.57	0.43	0
2	2.20	0.75	0
3	2.22	0.70	0
4	2.28	0.79	0
5	3.72	1.04	0
6	3.42	1.14	2.06
7	3.19	1.37	1.99
8	4.25	1.23	6.06
9	6.27	1.47	8.13
10	7.17	2.75	14.06
11	6.18	1.75	17.81
12	5.41	1.50	6.22
13	4.69	1.68	15.24
14	5.49	1.78	16.65
15	3.99	2.07	15.59
16	4.88	1.83	12.58
17	5.41	2.46	1.27
18	7.24	4.68	0
19	6.40	4.76	0
20	6.11	4.53	0
21	3.88	3.32	0
22	2.95	0.74	0
23	2.29	0.40	0

Future Load Profiles Micro Grid, Including Distribution and Converter Losses [kW]

	Including Distribution Losses		Including Converter Losses	
Hour	**Weekdays**	**Weekends**	**Weekdays**	**Weekends**
0	2.28	0.43	2.41	0.49
1	2.61	0.43	2.75	0.49
2	2.23	0.75	2.36	0.83
3	2.25	0.70	2.38	0.78
4	2.31	0.80	2.44	0.88
5	3.79	1.05	3.98	1.13
6	3.48	1.15	3.65	1.24
7	3.25	1.38	3.41	1.48
8	4.35	1.24	4.56	1.33
9	6.47	1.48	6.75	1.58
10	7.44	2.80	7.76	2.96
11	6.36	1.77	6.64	1.88
12	5.54	1.51	5.79	1.61
13	4.82	1.69	5.05	1.81
14	5.65	1.79	5.90	1.91
15	4.08	2.09	4.28	2.21
16	4.99	1.84	5.22	1.96
17	5.55	2.49	5.79	2.63
18	7.54	4.81	7.86	5.04
19	6.66	4.89	6.95	5.12
20	6.30	4.65	6.58	4.87
21	3.96	3.38	4.15	3.55
22	2.99	0.74	3.15	0.82
23	2.33	0.40	2.47	0.47

Appendix C: Equations for Calculating Conductor Size

Resistance of a conductor

$$r = \frac{18.4 \times k}{A}$$

where

r	=	resistance [Ω/km]
A	=	cross-sectional area of conductor [mm^2]
k	=	1 for copper 1.6 for aluminum 10 for steel

Reactance of a conductor

$$x = 2\pi f \left[19 + 46 \times log(\frac{s}{d})\right] \times 10^{-5}$$

where

f	=	line frequency, 60 Hz
s	=	equivalent spacing of conductors [m]
d	=	overall physical diameter of the conductor [m]

Magnitude of Current

$$I = \frac{P(kW)}{cos(\phi)V} 10^3$$

where
P(kW) = power [kW]
V = Voltage [V]
I = Current [A]
cos(ϕ) = power factor
VI = *P(kVA)* = apparent power [kVA]

Voltage drop for each conductor in a single-phase/three-wire configuration

$$VD \approx L\big(rcos(\phi) + xsin(\phi)\big)I = L\big(rcos(\phi) + xsin(\phi)\big)\frac{P(kW)}{2Vcos(\phi)}10^3$$

where
VD = voltage drop [V]
I = current in the line [A]
L = length of line [km]
cos(ϕ) = power factor at beginning of line $\approx$ power factor at load
P(kW) = total load suppplied by both phase-conductors [kW]

Voltage drop percentage in each conductor

$$\%VD \approx 100\frac{VD}{V}$$

Power loss along the line in each conductor in a single-phase/three-wire configuration

$$P_l = I^2 rL10^{-3}$$

where
P_l = power loss in each conductor [kW]

Equivalent load at the end of the line with N loads distributed at different locations on the line

$$P_T = \frac{\sum_{n=1}^{N} L_n \times P_n}{L}$$

where

P_T	=	Equivalent load at end of the line [kW]
L_n	=	distance from power supply for load n [km]
P_n	=	load n [km]
L	=	total distance from power supply to end of line [km]

Percentage of voltage drop for each conductor at the end of a single-phase/three-wire with load distributed at different locations on the line

$$\%VD \approx \big(rcos(\phi) + xsin(\phi)\big) \frac{\sum_{n=1}^{N} L_n \times P_n}{V^2 cos(\phi)} 10^5$$

Appendix D: HOMER Full System Report Micro Grid Case I

System Report - MicroGridAC

System architecture

PV Array	34 kW
Biomass Generator	7.5 kW
Battery	152 Trojan L16P
Inverter	9 kW
Rectifier	8.55 kW
Dispatch strategy	Load Following

Cost summary

Total net present cost	$ 162,226
Levelized cost of energy	$ 0.289/kWh
Operating cost	$ 3,921/yr

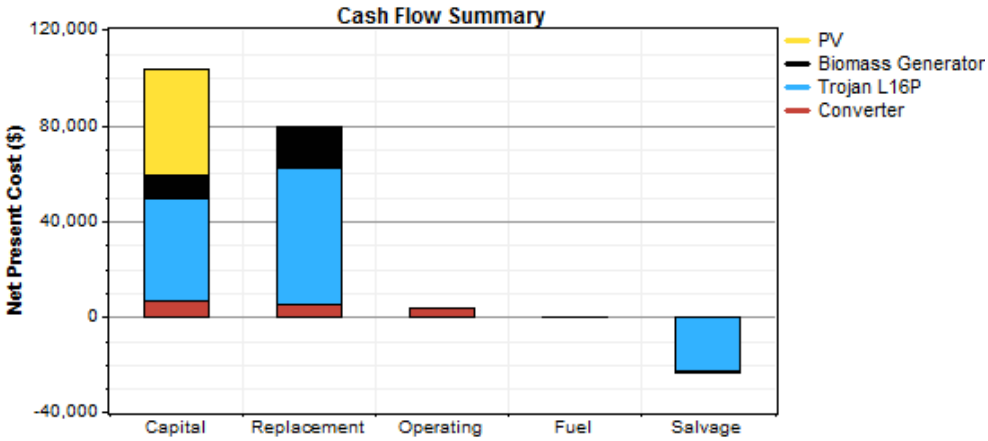

Net Present Costs

Component	Capital	Replacement	O&M	Fuel	Salvage	Total
	($)	($)	($)	($)	($)	($)
PV	44,200	0	0	0	0	44,200
Biomass Generator	9,582	16,770	0	0	-755	25,598
Trojan L16P	43,168	57,515	0	0	-22,841	77,843
Converter	6,399	4,808	3,379	0	0	14,586
System	103,349	79,094	3,379	0	-23,595	162,226

Annualized Costs

Component	Capital	Replacement	O&M	Fuel	Salvage	Total
	($/yr)	($/yr)	($/yr)	($/yr)	($/yr)	($/yr)
PV	2,944	0	0	0	0	2,944
Biomass Generator	638	1,117	0	0	-50	1,705
Trojan L16P	2,875	3,830	0	0	-1,521	5,184

Converter	426	320	225	0	0	971
System	6,883	5,267	225	0	-1,571	10,804

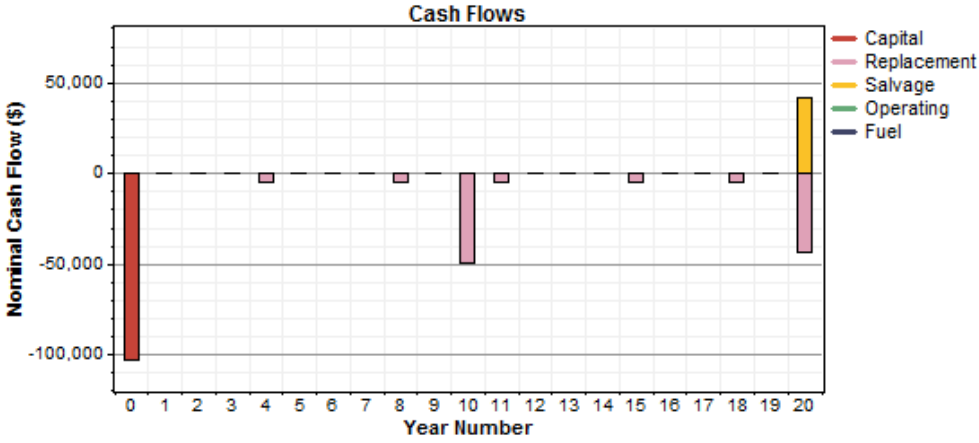

Electrical

Component	Production (kWh/yr)	Fraction
PV array	42,221	90%
Biomass Generator	4,710	10%
Total	46,931	100%

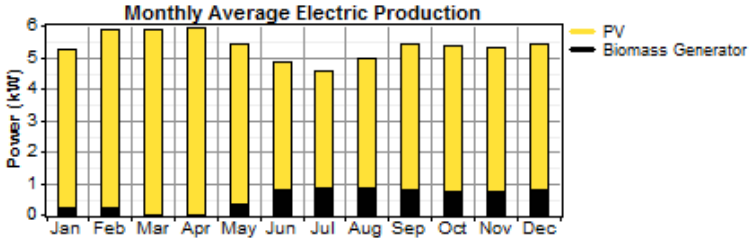

Load	Consumption (kWh/yr)	Fraction
AC primary load	37,377	100%
Total	37,377	100%

Quantity	Value	Units
Excess electricity	6,224	kWh/yr
Unmet load	218	kWh/yr
Capacity shortage	218	kWh/yr
Renewable fraction	1.000	

PV

Quantity	Value	Units

Rated capacity	34.0	kW
Mean output	4.82	kW
Mean output	116	kWh/d
Capacity factor	14.2	%
Total production	42,221	kWh/yr

Quantity	Value	Units
Minimum output	0.00	kW
Maximum output	29.1	kW
PV penetration	112	%
Hours of operation	4,442	hr/yr
Levelized cost	0.0697	$/kWh

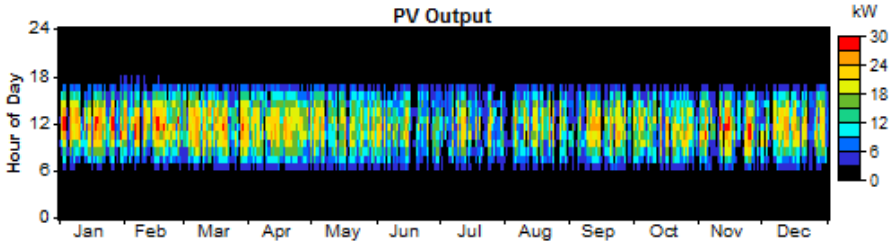

Biomass Generator

Quantity	Value	Units
Hours of operation	727	hr/yr
Number of starts	259	starts/yr
Operational life	3.51	yr
Capacity factor	7.17	%
Fixed generation cost	1.76	$/hr
Marginal generation cost	0.00	$/kWhyr

Quantity	Value	Units
Electrical production	4,710	kWh/yr
Mean electrical output	6.48	kW
Min. electrical output	1.50	kW
Max. electrical output	7.50	kW

Quantity	Value	Units
Bio. feedstock consump.	13.7	t/yr
Specific fuel consumption	2.903	kg/kWh
Fuel energy input	43,679	kWh/yr
Mean electrical efficiency	10.8	%

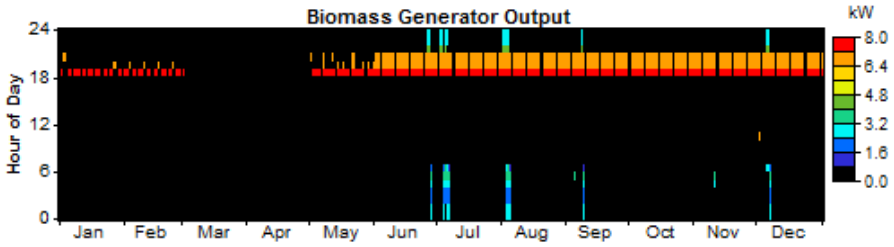

Battery

Quantity	Value
String size	8
Strings in parallel	19
Batteries	152
Bus voltage (V)	48

Quantity	Value	Units
Nominal capacity	328	kWh
Usable nominal capacity	230	kWh
Autonomy	53.6	hr
Lifetime throughput	163,400	kWh
Battery wear cost	0.287	$/kWh
Average energy cost	0.000	$/kWh

Quantity	Value	Units
Energy in	18,201	kWh/yr
Energy out	15,538	kWh/yr
Storage depletion	45.2	kWh/yr
Losses	2,618	kWh/yr
Annual throughput	16,853	kWh/yr
Expected life	9.70	yr

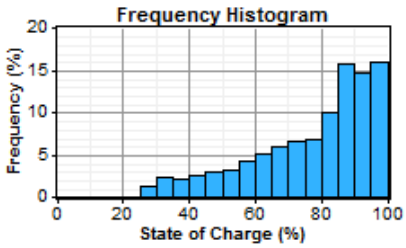

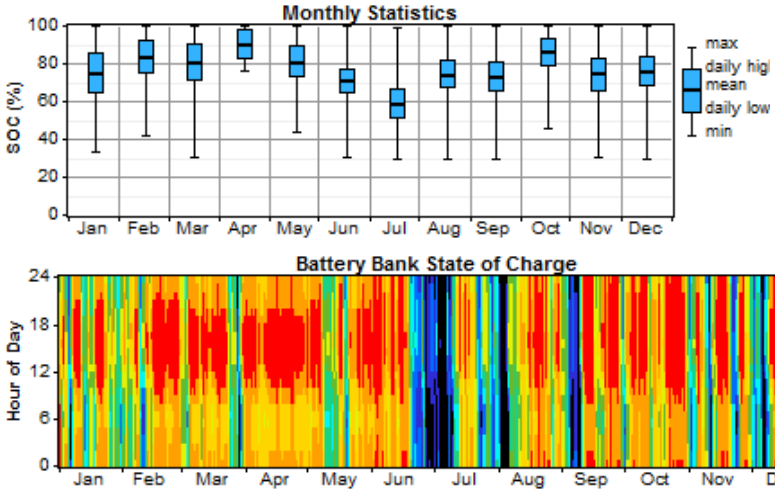

Converter

Quantity	Inverter	Rectifier	Units
Capacity	9.00	8.55	kW
Mean output	3.73	0.00	kW
Minimum output	0.00	0.00	kW
Maximum output	7.86	0.00	kW
Capacity factor	41.4	0.0	%

Quantity	Inverter	Rectifier	Units
Hours of operation	8,292	0	hrs/yr
Energy in	33,335	0	kWh/yr
Energy out	32,667	0	kWh/yr
Losses	668	0	kWh/yr

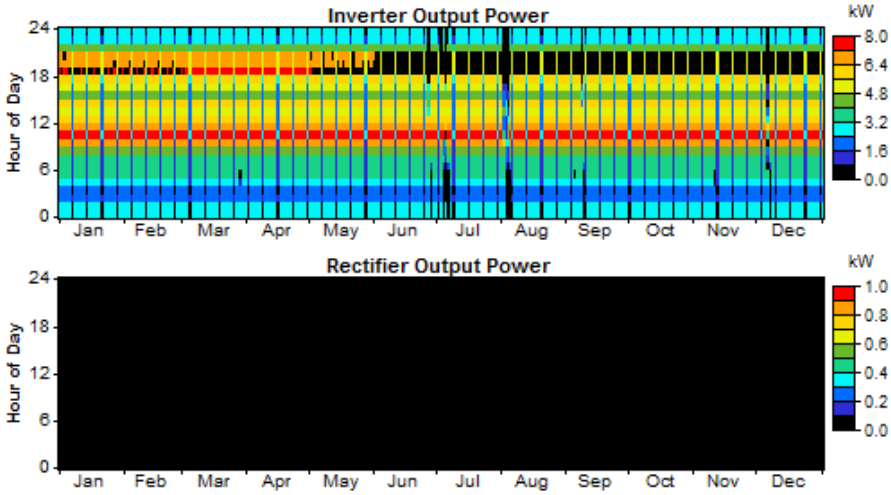

Appendix E: HOMER Full System Report Micro Grid Case II

System Report - MicroGridDC

System architecture

PV Array	30 kW
Biomass Generator	7.5 kW
Battery	136 Trojan L16P
Inverter	9 kW
Dispatch strategy	Cycle Charging

Cost summary

Total net present cost	$ 148,125
Levelized cost of energy	$ 0.263/kWh
Operating cost	$ 3,909/yr

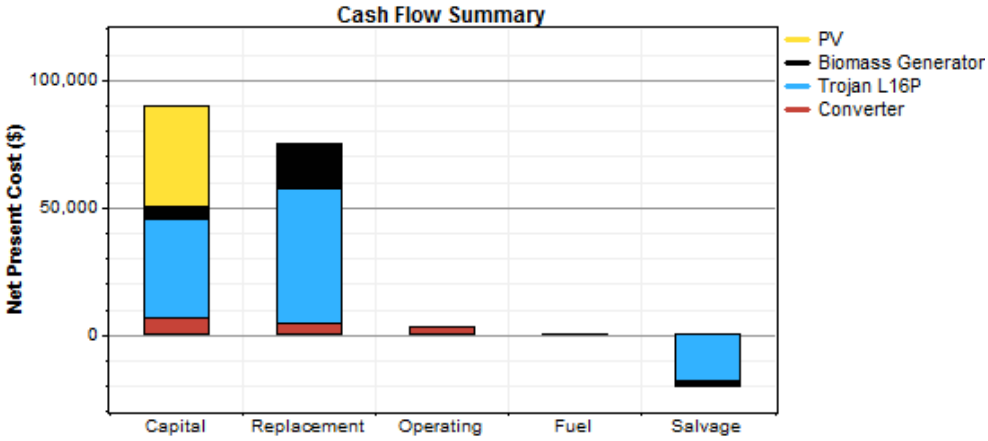

Net Present Costs

Component	Capital	Replacement	O&M	Fuel	Salvage	Total
	($)	($)	($)	($)	($)	($)
PV	39,000	0	0	0	0	39,000
Biomass Generator	5,412	17,760	0	0	-2,083	21,089
Trojan L16P	38,624	52,612	0	0	-17,785	73,450
Converter	6,399	4,808	3,379	0	0	14,586
System	89,435	75,180	3,379	0	-19,868	148,125

Annualized Costs

Component	Capital	Replacement	O&M	Fuel	Salvage	Total
	($/yr)	($/yr)	($/yr)	($/yr)	($/yr)	($/yr)
PV	2,597	0	0	0	0	2,597
Biomass Generator	360	1,183	0	0	-139	1,404
Trojan L16P	2,572	3,504	0	0	-1,184	4,891
Converter	426	320	225	0	0	971

System	5,956	5,007	225	0	-1,323	9,865

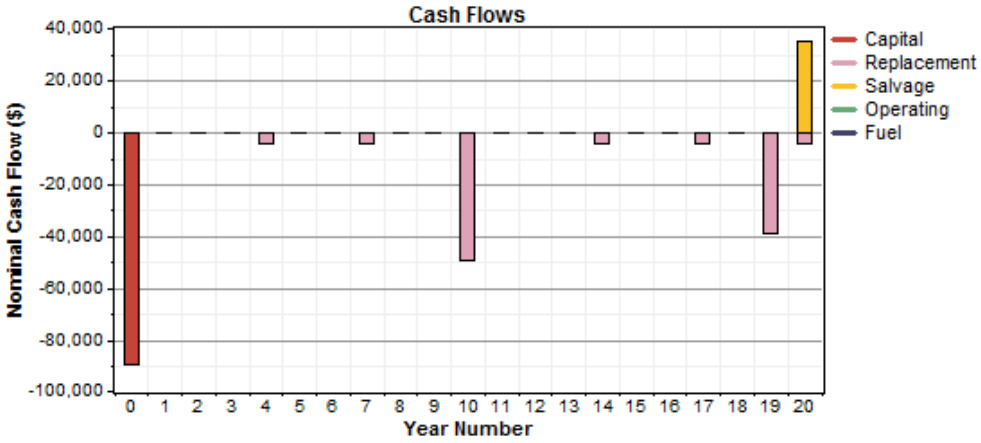

Electrical

Component	Production (kWh/yr)	Fraction
PV array	37,254	83%
Biomass Generator	7,480	17%
Total	44,734	100%

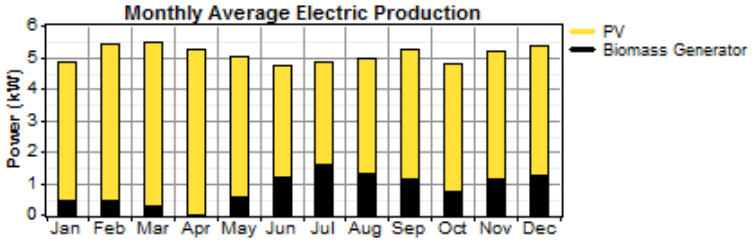

Load	Consumption (kWh/yr)	Fraction
AC primary load	37,443	100%
Total	37,443	100%

Quantity	Value	Units
Excess electricity	3,992	kWh/yr
Unmet load	152	kWh/yr
Capacity shortage	152	kWh/yr
Renewable fraction	1.000	

PV

Quantity	Value	Units
Rated capacity	30.0	kW

Mean output	4.25	kW
Mean output	102	kWh/d
Capacity factor	14.2	%
Total production	37,254	kWh/yr

Quantity	Value	Units
Minimum output	0.00	kW
Maximum output	25.6	kW
PV penetration	99.1	%
Hours of operation	4,442	hr/yr
Levelized cost	0.0697	$/kWh

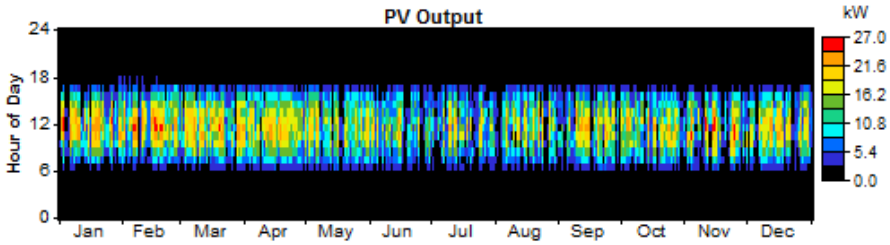

Biomass Generator

Quantity	Value	Units
Hours of operation	1,005	hr/yr
Number of starts	365	starts/yr
Operational life	3.28	yr
Capacity factor	11.4	%
Fixed generation cost	1.23	$/hr
Marginal generation cost	0.00	$/kWhyr

Quantity	Value	Units
Electrical production	7,480	kWh/yr
Mean electrical output	7.44	kW
Min. electrical output	5.33	kW
Max. electrical output	7.50	kW

Quantity	Value	Units
Bio. feedstock consump.	21.3	t/yr
Specific fuel consumption	2.843	kg/kWh
Fuel energy input	67,935	kWh/yr
Mean electrical efficiency	11.0	%

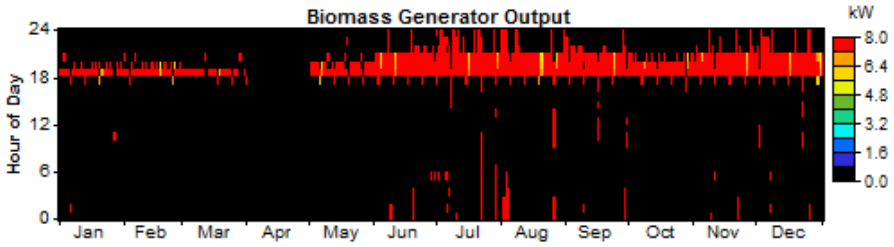

Battery

Quantity	Value
String size	8
Strings in parallel	17
Batteries	136
Bus voltage (V)	48

Quantity	Value	Units
Nominal capacity	294	kWh
Usable nominal capacity	206	kWh
Autonomy	47.9	hr
Lifetime throughput	146,200	kWh
Battery wear cost	0.287	$/kWh
Average energy cost	0.000	$/kWh

Quantity	Value	Units
Energy in	17,256	kWh/yr
Energy out	14,721	kWh/yr
Storage depletion	33.9	kWh/yr
Losses	2,501	kWh/yr
Annual throughput	15,968	kWh/yr
Expected life	9.16	yr

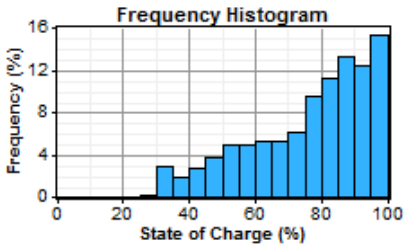

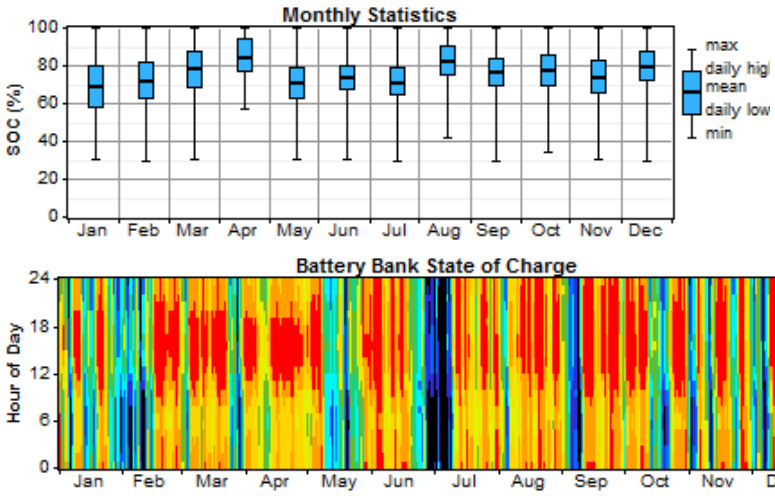

Converter

Quantity	Inverter	Rectifier	Units
Capacity	9.00	0.00	kW
Mean output	4.27	0.00	kW
Minimum output	0.00	0.00	kW
Maximum output	7.86	0.00	kW
Capacity factor	47.5	0.0	%

Quantity	Inverter	Rectifier	Units
Hours of operation	8,745	0	hrs/yr
Energy in	38,207	0	kWh/yr
Energy out	37,443	0	kWh/yr
Losses	764	0	kWh/yr

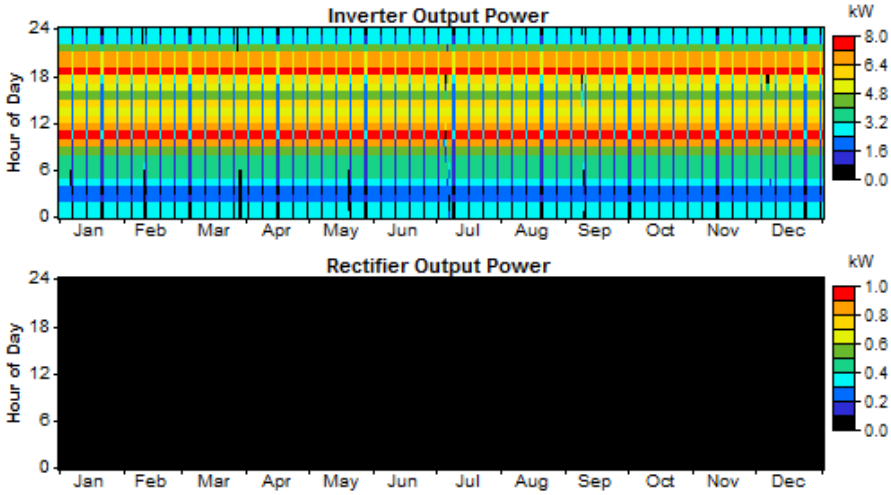

Appendix F: HOMER Full System Report Carpentry Workshop Case I

System Report - CarpentryAC

System architecture

Biomass Generator	15 kW
Generator 2	15 kW

Cost summary

Total net present cost	$ 162,878
Levelized cost of energy	$ 0.307/kWh
Operating cost	$ 8,639/yr

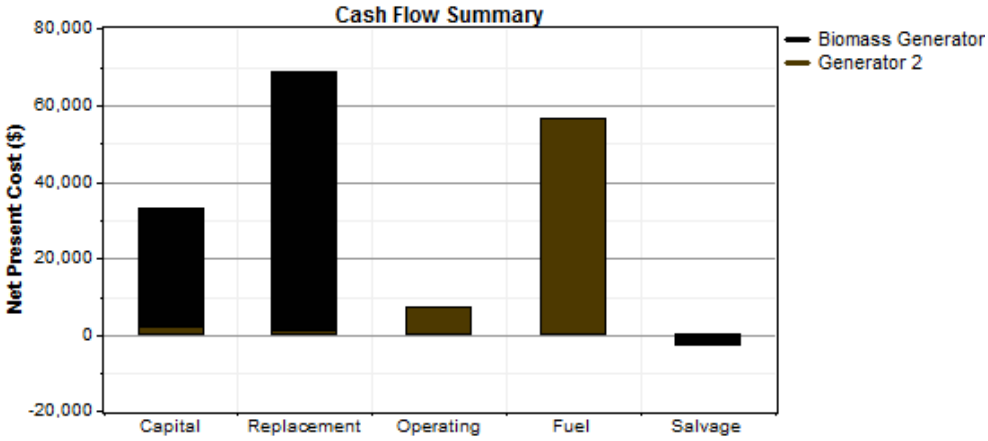

Net Present Costs

Component	Capital	Replacement	O&M	Fuel	Salvage	Total
	($)	($)	($)	($)	($)	($)
Biomass Generator	31,218	67,606	0	0	-2,205	96,618
Generator 2	1,934	1,353	7,027	56,382	-437	66,260
System	33,152	68,958	7,027	56,382	-2,642	162,878

Annualized Costs

Component	Capital	Replacement	O&M	Fuel	Salvage	Total
	($/yr)	($/yr)	($/yr)	($/yr)	($/yr)	($/yr)
Biomass Generator	2,079	4,502	0	0	-147	6,434
Generator 2	129	90	468	3,755	-29	4,413
System	2,208	4,592	468	3,755	-176	10,847

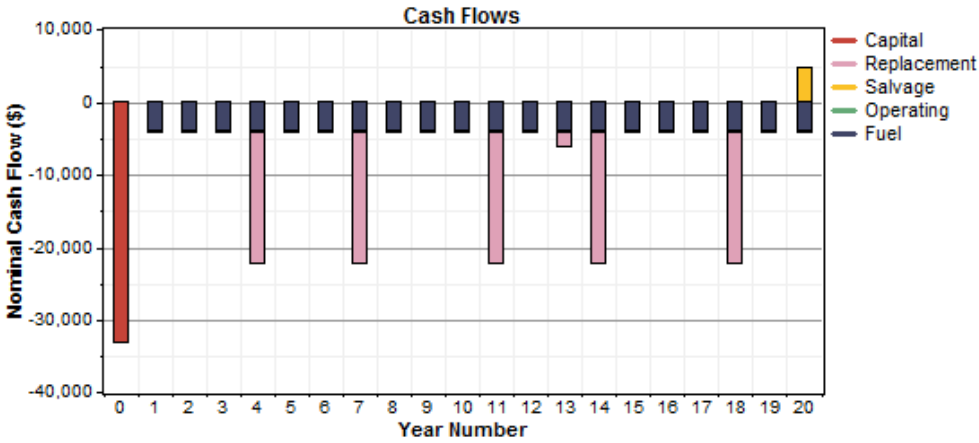

Electrical

Component	Production (kWh/yr)	Fraction
Biomass Generator	30,997	85%
Generator 2	5,400	15%
Total	36,397	100%

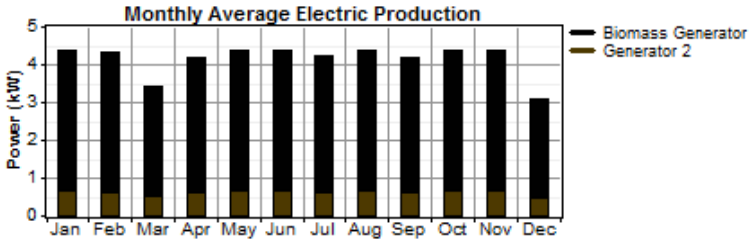

Load	Consumption (kWh/yr)	Fraction
AC primary load	35,296	100%
Total	35,296	100%

Quantity	Value	Units
Excess electricity	1,101	kWh/yr
Unmet load	0.00	kWh/yr
Capacity shortage	0.00	kWh/yr
Renewable fraction	0.847	

Biomass Generator

Quantity	Value	Units
Hours of operation	3,600	hr/yr
Number of starts	300	starts/yr

Operational life	3.46	yr
Capacity factor	23.6	%
Fixed generation cost	1.45	$/hr
Marginal generation cost	0.00	$/kWhyr

Quantity	Value	Units
Electrical production	30,997	kWh/yr
Mean electrical output	8.61	kW
Min. electrical output	3.00	kW
Max. electrical output	14.1	kW

Quantity	Value	Units
Bio. feedstock consump.	97.2	t/yr
Specific fuel consumption	3.137	kg/kWh
Fuel energy input	310,604	kWh/yr
Mean electrical efficiency	10.0	%

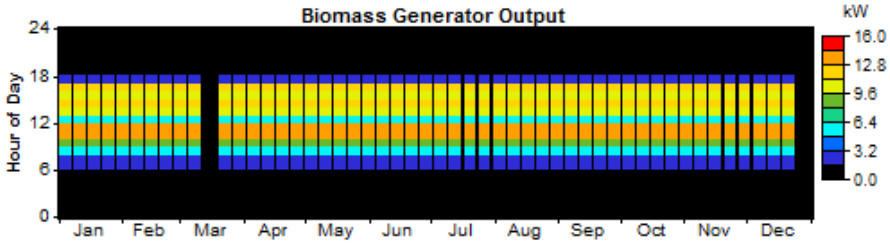

Generator 2

Quantity	Value	Units
Hours of operation	1,200	hr/yr
Number of starts	600	starts/yr
Operational life	12.5	yr
Capacity factor	4.11	%
Fixed generation cost	1.57	$/hr
Marginal generation cost	0.462	$/kWhyr

Quantity	Value	Units
Electrical production	5,400	kWh/yr
Mean electrical output	4.50	kW
Min. electrical output	4.50	kW
Max. electrical output	4.50	kW

Quantity	Value	Units
Fuel consumption	2,682	L/yr
Specific fuel consumption	0.497	L/kWh
Fuel energy input	26,391	kWh/yr

Mean electrical efficiency	20.5	%

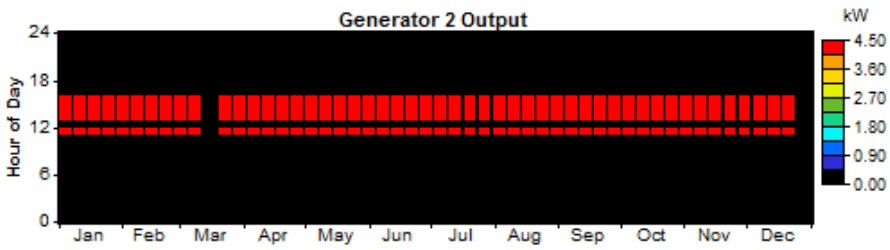

Emissions

Pollutant	Emissions (kg/yr)
Carbon dioxide	7,079
Carbon monoxide	18.1
Unburned hydocarbons	2
Particulate matter	1.36
Sulfur dioxide	14.2
Nitrogen oxides	161

Appendix G: HOMER Full System Report Carpentry Workshop Case II

System Report - CarpentryWorkshopDC

System architecture

Biomass Generator	15 kW
Generator 2	15 kW

Cost summary

Total net present cost	$ 163,099
Levelized cost of energy	$ 0.308/kWh
Operating cost	$ 8,736/yr

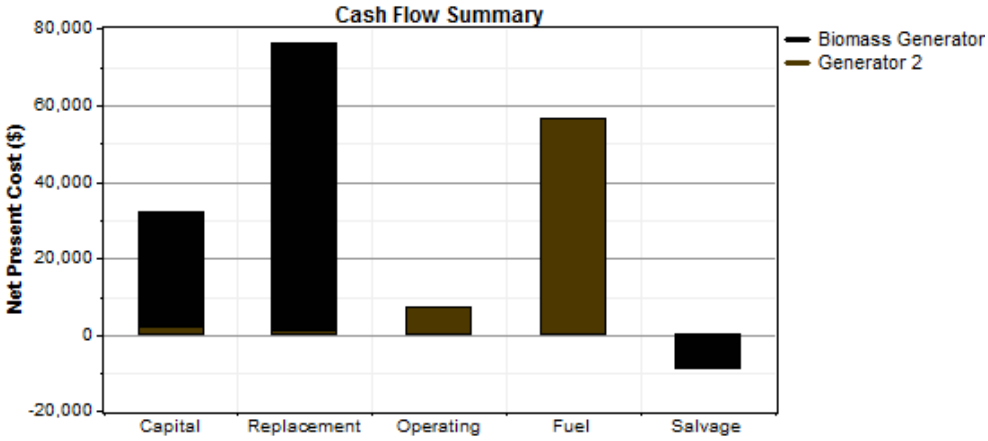

Net Present Costs

Component	Capital	Replacement	O&M	Fuel	Salvage	Total
	($)	($)	($)	($)	($)	($)
Biomass Generator	29,988	75,015	0	0	-8,164	96,839
Generator 2	1,934	1,353	7,027	56,382	-437	66,260
System	31,922	76,368	7,027	56,382	-8,601	163,099

Annualized Costs

Component	Capital	Replacement	O&M	Fuel	Salvage	Total
	($/yr)	($/yr)	($/yr)	($/yr)	($/yr)	($/yr)
Biomass Generator	1,997	4,996	0	0	-544	6,449
Generator 2	129	90	468	3,755	-29	4,413
System	2,126	5,086	468	3,755	-573	10,862

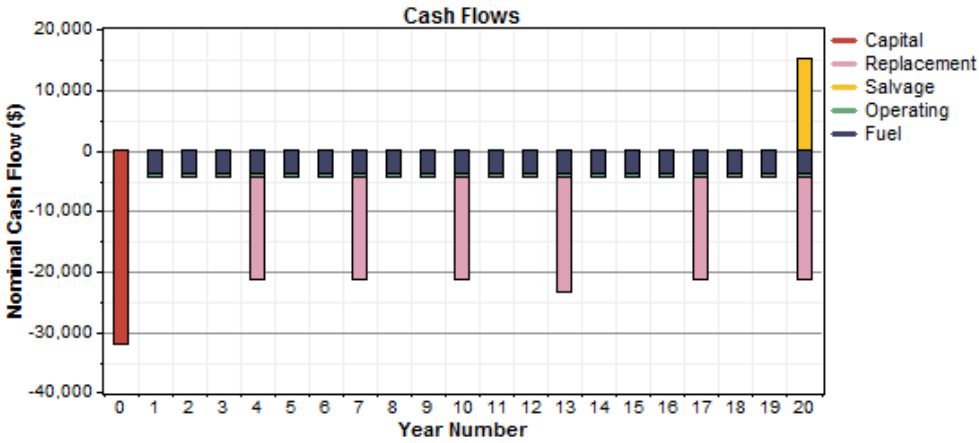

Electrical

Component	Production (kWh/yr)	Fraction
Biomass Generator	30,997	85%
Generator 2	5,400	15%
Total	36,397	100%

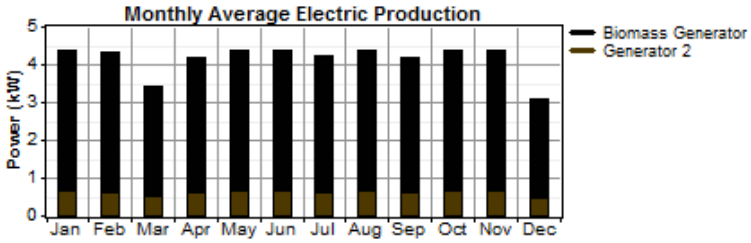

Load	Consumption (kWh/yr)	Fraction
AC primary load	35,296	100%
Total	35,296	100%

Quantity	Value	Units
Excess electricity	1,101	kWh/yr
Unmet load	0.00	kWh/yr
Capacity shortage	0.00	kWh/yr
Renewable fraction	0.847	

Biomass Generator

Quantity	Value	Units
Hours of operation	3,600	hr/yr
Number of starts	300	starts/yr

Operational life	3.25	yr
Capacity factor	23.6	%
Fixed generation cost	1.46	$/hr
Marginal generation cost	0.00	$/kWhyr

Quantity	Value	Units
Electrical production	30,997	kWh/yr
Mean electrical output	8.61	kW
Min. electrical output	3.00	kW
Max. electrical output	14.1	kW

Quantity	Value	Units
Bio. feedstock consump.	97.2	t/yr
Specific fuel consumption	3.137	kg/kWh
Fuel energy input	310,604	kWh/yr
Mean electrical efficiency	10.0	%

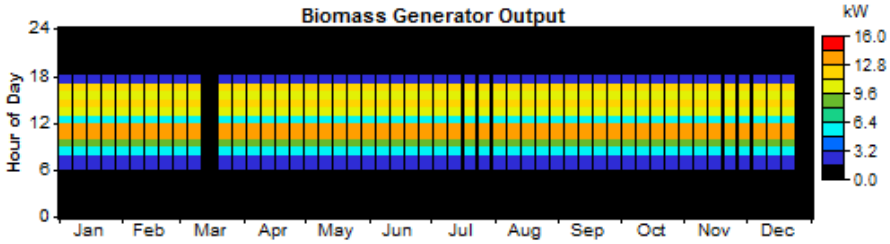

Generator 2

Quantity	Value	Units
Hours of operation	1,200	hr/yr
Number of starts	600	starts/yr
Operational life	12.5	yr
Capacity factor	4.11	%
Fixed generation cost	1.57	$/hr
Marginal generation cost	0.462	$/kWhyr

Quantity	Value	Units
Electrical production	5,400	kWh/yr
Mean electrical output	4.50	kW
Min. electrical output	4.50	kW
Max. electrical output	4.50	kW

Quantity	Value	Units
Fuel consumption	2,682	L/yr
Specific fuel consumption	0.497	L/kWh
Fuel energy input	26,391	kWh/yr

Mean electrical efficiency	20.5	%

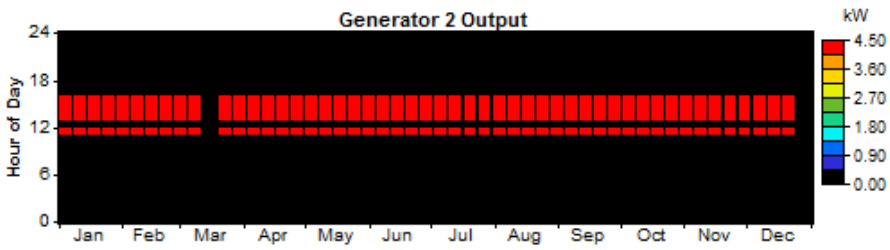

Emissions

Pollutant	Emissions (kg/yr)
Carbon dioxide	7,079
Carbon monoxide	18.1
Unburned hydocarbons	2
Particulate matter	1.36
Sulfur dioxide	14.2
Nitrogen oxides	161